



Universitat Autònoma de Barcelona
DEPARTMENT OF BIOCHEMISTRY AND MOLECULAR BIOLOGY
SCHOOL OF VETERINARY MEDICINE
CENTER OF ANIMAL BIOTECHNOLOGY AND GENE THERAPY

**GENETIC ENGINEERING OF THE
SKELETAL MUSCLE TO
COUNTERACT INSULIN
RESISTANCE AND OBESITY**

CARLES ROCA LECHA

This PhD thesis has been carried out under the direction of Dr. Fàtima Bosch i Tubert at the Biochemistry and Molecular Biology Department of the Veterinary School of Medicine and at the Center of Animal Biotechnology and Gene Therapy (CBATEG).

CARLES ROCA LECHA
BOSCH I TUBERT

FÀTIMA

JANUARY 2014
BELLATERRA

A vosaltres família

Són moltes les persones a les quals haig de donar les meves gràcies més sinceres. Per més paraules que escrigui no podré expressar la gratitud personal que us dec.

En primer lloc vull donar les gràcies a la Dra. Fàtima Bosch i Tubert per haver-me donat l'oportunitat de realitzar aquesta tesi doctoral en el seu grup d'investigació. Gràcies per la teva energia, empenya i bon cor que et caracteritzen i que han fet possible aquest treball.

Vull agrair també a totes les persones que durant tots aquests anys han anat passant per la meva vida científica al laboratori i amb qui he treballat més a prop.

Vull donar unes gràcies especials a la Dra. Anna Pujol i a l'Anna Arboç per haver-me donat confiança i guiar-me durant els meus primers dies en el món del laboratori, sense vosaltres no seria on sóc. A la Tura per agafar el seu relleu i ensenyar-me tantes tècniques que després m'han servit per créixer. A la Mònica George per ensenyar-me les primeres pinzellades de com funciona la ciència. A tu Sabrina, en pau descansis, per la teva bona voluntat i dedicació per volguer fer el meu treball millor.

Gràcies Iveta per estar al meu costat cada un d'aquests anys d'ençà que vam començar al laboratori. Moltíssimes gràcies per la teva dedicació i paciència, sobretot durant l'etapa final. Gràcies als "pardis", Albert, Sergio i Xavier. Treballar al vostre costat ho ha fet tot més fàcil. Gràcies David per tantes hores compartides de feina. Gràcies Chris, Edu i Miquel, ha estat un plaer discutir i aprendre de mil qüestions amb vosaltres. Gràcies Laia per la teva ajuda quan la he necessitat. Gràcies Maria Molas, Xavier León i Luca per ser-hi sempre amb els vostres consells tècnics i bon companyerisme. Gràcies a la resta de companys del laboratori amb els que he compartit tants i tants moments. La vostra companyia tant en el camp professional com en el personal és impagable. A tu Estefania, Pilar, Sara, Albert Rivera, Sandra, Alba, Vicky, Cristina, Vero, Claudia, Meritxell, Joan, Sylvie i Efrén. Als que ja no hi son, a tu Iris, Judith, Tami, Albert, Joel, Mercé, Marc, Ricardo, Ariana i Antonio. Als més nous, Marisa, Cristian, Jordi, Víctor MPS, Víctor Adipós i Ivàn, ja ens anirem

coneixent. Gràcies Jeny i Lúdia per tota la feina que feu. A la Marta per tota la histologia. Thank you Malcolm and Judy.

Moltes gràcies a tot l'equip del SER-CBATEG. Gràcies Pedro per dirigir el servei. Gràcies Mireia per la teva ajuda sempre que l'he necessitat. Gràcies a la Unitat d'Animals Transgènics. Gràcies Sandra per completar una tant bona feina. Gràcies a l'equip d'anàlisi morfològica, amb el Doctor Jesús Ruberte al capdavant. Gràcies als que formeu un tant bon equip. Gràcies Carles Ros per tots aquests anys i per tants consells.

Gràcies als companys de la cinquena planta. Gràcies Miguel i Assumpció. Al personal de l'SLIPI i seguretat.

Finalment agrair als meus pares, germana, avis i a tota la família per no deixar mai de creure amb mi, donar-me suport i confiança durant tots aquests anys. Per fer-me la persona que sóc, gràcies. A tots els amics de Badalona i Barcelona per ser-hi.

Aquesta tesi ha estat possible gràcies al finançament rebut del Plan Nacional I+D+I (SAF2005-01262, SAF2008-00962 i SAF2011-24698), de la Gestió d'Ajuts Universitaris i de Recerca (ajuts per a grups de recerca consolidats 2009SGR 224) i dels projectes europeus: Network of Excellence LIFESCIHEALTH (EUGENE2, Network of Functional Genomics of Type 2 Diabetes- LSHM-CT-2004-512013), European Network for the Advancement of Clinical Gene Transfer and Therapy (CLINIGENE, LSHB-CT-2006-018933).

ABBREVIATIONS

AACE	American Association of Clinical
Endocrinologists	
AAV1	Adeno-associated vector serotype 1
AAV <i>Gck</i>	Adeno-associated vector serotype 1 carrying
the	rat glucokinase gene
AAVPGC	Adeno-associated vector serotype 1 carrying
the	<i>Pgc1α</i> gene
AAVPPAR	Adeno-associated vector serotype 1 carrying
the	<i>Pparδ</i> gene
AAVPGC/ <i>Gck</i>	Mixture of an adeno-associated vector 1
carrying	the <i>Pgc1α</i> gene and an adeno-
associated vector	1 carrying the rat
glucokinase gene	
AAVPGC/PPAR	Mixture of an adeno-associated vector 1
carrying	the <i>Pgc1α</i> gene and an adeno-
associated vector	1 carrying the <i>Pparδ</i> gene
ADA	American Diabetes Association
ADA	Adenosine diphosphate
AKT	Protein kinase B
AKT-P	Phosphorylated AKT
AKT-T	Total AKT
AMPK	Adenosine Monophosphate-activated
Protein	Kinase
ATP	Adenosine triphosphate
BMI	Body Mass Index
BSA	Bovin Serum Albumin
CaN	Calcineurin
CaMK	Ca-calmodulin dependent kinase
Cap	Capsid proteins
CAT	Carnitine translocase
CD36	Fatty acid translocase
cDNA	Complementary Deoxyribonucleic Acid
CMV	Cytomegalovirus
CPT1	Carnitine palmitoyltransferase I
CPT2	Carnitine palmitoyltransferase II
CREB	cAMP response element-binding protein
CsCl	Cesium Chloride
DAG	Diacylglycerol
DNA	Deoxyribonucleic Acid
DTT	Dithiothreitol
ETC	Electron transport chain
F-1-P	Fructose-1-phosphate
F-6-P	Fructose-6-phosphate
FABPpm	Plasma membrane-bound fatty acid binding
	protein
FADH ₂	Flavin Adenine dinucleotide

FATP	Fatty acid transport protein
FFA	Free Fatty Acids
G-6-P	Glucose 6-phosphate
GCK	Human glucokinase
<i>Gck</i>	Murine glucokinase
GDM	Gestational Diabetes Mellitus
GFP	Green fluorescence protein
GIP	Gastric inhibitory peptide
GLP	Glucagon-like peptide-1
GLUT1	Glucose transporter 1
GLUT4	Glucose transporter 4
GWAS	Genome Wide Association Studies
H ⁺	Protons
HFD	High Fat Diet
HK	Hexokinase
IgG	Immunoglobulin G
ITR	Inverted Terminal Repeat
ITT	Insulin Tolerance Test
LCACoA	Long Chain Acil Coa
M	Molar
MCAD	Medium-chain acyl-coenzyme A
dehydrogenase	
MEF2C	Myocyte-specific enhancer factor 2C
MHC	Myosin heavy chain
mM	milimolar
MOPS	3-(N-morpholino)propanesulfonic acid
NADH	Nicotinamide adenine dinucleotide
NRF-1	Nuclear Respiratory Factor 1
NRF-2	Nuclear Respiratory Factor 2
ORF	Open reading frame
PBS	Phosphate Buffered Saline
PCR	Polymerase Chain Reaction
PGC1 α	Peroxisome proliferator-activated receptor-
gamma	coactivator 1 alpha
Poly A	Simian Virus 40 Polyadenylation Signal
PKC	Protein kinase C
PPAR α	Peroxisome proliferator activated receptor-alpha
PPAR δ	Peroxisome proliferator activated receptor-
delta	
PPAR γ	Peroxisome proliferator activated receptor-
gamma	
RB	Roller Bottle
Rep	Replication proteins
RIA	Radio immunoassay
RNA	Ribonucleic Acid
ROS	Reactive oxygen species
SDS	Sodium Dodecyl Sulphate
SDS-PAGE	Sodium Dodecyl Sulphate Polyacrylamide Gel
	Electroforesis
UCP3	Uncoupling Protein 3
WAT	White adipose tissue
WHO	World Health Organization
T2DM	Type 2 Diabetes Mellitus
TBS	Triss-buffered Saline
TBS-T	Triss Buffered Saline-Tween

TCA
Tfam
TG
TZD

Tricarboxylic acid cycle
Mitochondrial transcription factor A
Triglycerides
Thiazolidinediones

5. ROLE OF THE PEROXISOME PROLIFERATOR-ACTIVATED RECEPTOR-GAMMA COACTIVATOR 1 ALPHA IN THE SKELETAL MUSCLE	35
5.1. Regulation of PGC1 α transcription in the skeletal muscle.....	36

5.2. PGC1 α and skeletal muscle fibre type conversion	37
5.3. PGC1 α , respiration and mitochondrial biogenesis	37
5.4. PGC1 α and lipid metabolism.....	38
5.5. PGC1 α and muscular glucose uptake	39
5.6. PGC1 α and type 2 diabetes	39
6. ROLE OF THE PEROXISOME PROLIFERATOR-ACTIVATED RECEPTOR-DELTA IN THE SKELETAL MUSCLE	41
6.1. PPAR δ transcription in the skeletal muscle	43
6.2. PPAR δ and fibre type conversion	43
6.3. PPAR δ , lipid metabolism and oxidation.....	44
6.4. PPAR δ and type 2 diabetes	44
7. GENE THERAPY	46
7.1. Introduction to gene therapy.....	46
7.2. Non-Viral vectors	47
7.3. Viral vectors.....	48
7.4. Adeno-associated vectors (AAV)	49
7.4.1. Biology of wild-type adeno-associated viruses.....	49
7.4.2. Recombinant adeno-associated viral vectors	50
III. OBJECTIVES	53
IV. RESULTS.....	54
1. GENETIC MODIFICATION OF THE SKELETAL MUSCLE AND EXPERIMENTAL DESIGN	54
1.1. Transduction of the skeletal muscle with AAV vectors.....	54
1.2. Experimental design	55
2. GENETIC MODIFICATION OF THE SKELETAL MUSCLE TO OVEREXPRESS GLUCOKINASE	57
2.1. Design of an AAV1 vector carrying the <i>Gck</i> gene	57
2.2. Metabolic effects of the <i>Gck</i> expression in the skeletal muscle of High-fat fed mice.....	58
2.2.1. Glucokinase expression in the skeletal muscle.....	58
2.2.2. Body weight gain and adiposity.....	59
2.2.3. Hepatic triglyceride content.....	60
2.2.4. Study of glucose homeostasis.....	61
2.2.5. Insulin signalling in the skeletal muscle.....	63
2.2.6. Determination of circulating metabolites	65

2.3. Metabolic effects of the expression of high levels of <i>Gck</i> in the skeletal muscle	66
2.3.1. Glucokinase expression in the skeletal muscle.....	66
2.3.2. Body weight gain and adiposity	67
2.3.3. Hepatic triglyceride content	68
2.3.4. Triglyceride content and fatty acid oxidation in the skeletal muscle	70
2.3.5. Study of glucose homeostasis.....	71
2.3.6. Insulin signalling in the skeletal muscle.....	72
2.3.7. Determination of circulating metabolite	73
3. GENETIC MODIFICATION OF THE SKELETAL MUSCLE TO OVEREXPRESS <i>Gck</i> AND <i>Pgc1α</i>	75
3.1. Design of an AAV1 with the <i>Pgc1α</i> gene.....	75
3.2. Metabolic effects of the <i>Pgc1α</i> expression in the skeletal muscle of high-fat fed mice.....	76
3.2.1. <i>Pgc1α</i> expression in the skeletal muscle	76
3.2.2. Body weight gain and adiposity	77
3.2.3. Hepatic triglyceride content	78
3.2.4. Triglyceride content and fatty acid oxidation in the skeletal muscle	80
3.2.5. Study of glucose homeostasis.....	81
3.2.6. Insulin signalling in the skeletal muscle.....	82
3.2.7. Determination of circulating metabolites	83
3.3. Metabolic effects of <i>Gck</i> and <i>Pgc1α</i> overexpression in the skeletal muscle of high-fat fed mice.....	85
3.3.1. <i>Pgc1α</i> and <i>Gck</i> expression in the skeletal muscle	85
3.3.2. Body weight gain and adiposity	86
3.3.3. Hepatic triglyceride content	87
3.3.4. Triglyceride content and fatty acid oxidation in the skeletal muscle	89
3.3.5. Study of glucose homeostasis.....	90
3.3.7. Determination of circulating metabolites	91
4. GENETIC MODIFICATION OF THE SKELETAL MUSCLE TO OVEREXPRESS <i>Pgc1α</i> AND <i>Pparδ</i>.....	93
4.1. Design of an AAV1 with the <i>Pparδ</i> gene	93

4.2. Metabolic effects of <i>Pparδ</i> overexpression in the skeletal muscle of high-fat fed mice.....	94
4.2.1. <i>Pparδ</i> expression in the skeletal muscle.....	94
4.2.2. Body weight gain and adiposity.....	95
4.2.3. Hepatic triglyceride content.....	96
4.2.4. Triglyceride content and fatty acid oxidation in the skeletal muscle.....	98
4.2.5. Study of glucose homeostasis.....	99
4.2.6. Insulin signalling in the skeletal muscle.....	100
4.2.7. Determination of circulating metabolites.....	101
4.3. Metabolic effects of <i>Pparδ</i> and <i>Pgc1α</i> overexpression in the skeletal muscle of high-fat fed mice.....	102
4.3.1. <i>Pparδ</i> and <i>Pgc1α</i> expression in the skeletal muscle.....	102
4.3.2. Body weight gain and adiposity.....	103
4.3.3. Hepatic triglyceride content.....	104
4.3.4. Triglyceride content and fatty acid oxidation in the skeletal muscle.....	106
4.3.5. Study of glucose homeostasis.....	107
4.3.6. Insulin signalling in the skeletal muscle.....	108
4.3.7. Determination of circulating metabolites.....	109
V. DISCUSSION.....	111
VI. CONCLUSIONS.....	124
VII. MATERIALS AND METHODS.....	125
1. MATERIALS.....	126
1.1. Bacterial Strains.....	126
1.2. Animals.....	126
1.3. Anaesthetics.....	126
1.4. Antibodies.....	127
1.5. Plasmids.....	128
1.6. Probes.....	128
1.7. Reagents.....	129
2. METHODS.....	129
2.1. Basic DNA techniques.....	129
2.1.1. Plasmid DNA preparation.....	129
2.1.2. DNA digestion with restriction enzymes.....	129
2.1.3. Dephosphorylation of DNA fragments.....	130

2.6.4.1. <i>Glucose</i>	144
2.6.4.2. <i>Insulin</i>	144
2.6.4.3. <i>Free fatty acids</i>	144
2.6.4.4. <i>Triglycerides</i>	144
2.6.4.5. <i>Leptin</i>	145
2.6.4.6. <i>Skeletal muscle triglyceride content</i>	145
2.7. Statistical analysis.....	146
VII. BIBLIOGRAPHY	147

Type 2 diabetes is the most common metabolic disease worldwide. Despite drug treatments are useful in the first stages of the disease, none of them have proven to prevent the glycaemic control loss in a long-term basis. Furthermore, all treatments present undesirable secondary effects. Thus, the development of new treatments for type 2 diabetes is nowadays an important cornerstone in scientific research. The development of Gene Therapy has provided a new tool to treat human diseases. However, successful gene therapy approaches for the treatment of type 2 diabetes have not been developed to date.

About 90% of type 2 diabetes is attributable to excessive body weight. The accumulation of triglycerides in peripheral tissues is linked to the appearance of insulin resistance and reduced glucose uptake. This leads to β -cell failure and ultimately to type 2 diabetes. Thus, promoting glucose uptake or fatty acid oxidation may prevent the development of type 2 diabetes. The skeletal muscle plays a key role in glucose homeostasis and possesses a big capacity to use fatty acids for energy production. It is also an ideal tissue for gene transfer since it is easily accessible and can be transduced by a diversity of gene therapy vectors. In this study, with the aim of finding a new gene therapy approach for type 2 diabetes, we transferred several genes with the ability to increase glucose uptake or bust the oxidative capacity of the skeletal muscle in a model of diet-induced diabetes by using AAV vectors. These vectors are safe and allow a long-term expression of the transgene in the skeletal muscle.

We previously demonstrated in transgenic mice that increasing glucose phosphorylation by the muscular overexpression of Glucokinase (*Gck*), can prevent obesity and insulin resistance induced by a high fat diet. Here, as a

first approach, we overexpressed *Gck* in the skeletal muscles of high fat diet-fed adult mice. This led to a 10% reduction in body weight gain during the diet along with normoinsulinemia and a prevention of high fat diet-induced insulin resistance.

PGC1 α is a master regulator of mitochondrial biogenesis and the oxidative function in the skeletal muscle. The muscular expression of this gene is reduced in type 2 diabetic patients, suggesting that it is involved in the pathogenesis of insulin resistance in this tissue. Additionally, the expression of PGC1 α increased glucose uptake in skeletal muscle cells. Thus, in the second part of this study, we overexpressed *Pgc1 α* in the skeletal muscles of high fat diet-fed adult mice alone or in combination with *Gck*. The overexpression of *Pgc1 α* led to a reduction of a 10% of the body weight gained during the diet. However it did not prevent the development of insulin resistance and worsened insulin sensitivity in the skeletal muscle. The co-overexpression of *Pgc1 α* and *Gck* did not prevent obesity or the development of insulin resistance, thus abolishing the beneficial effects observed when *Gck* was overexpressed alone.

In the skeletal muscle, PPAR δ is a ligand-inducible transcription factor that promotes fatty acid oxidation. Upon ligand binding, PPAR δ recruits coactivators which allow the transcription of its target genes. PGC1 α is one of these coactivators. Much of the actions of PPAR δ activation in the skeletal muscle resemble those observed by PGC1 α , suggesting that these actions are orchestrated by the interaction of both proteins. Thus, in the third part of this study, we overexpressed *Ppar δ* alone or in combination with *Pgc1 α* in the skeletal muscles of high fat diet-fed adult mice. The overexpression of *Ppar δ* during the diet did not prevent the development of obesity or insulin resistance. In contrast, the co-overexpression of *Ppar δ* and *Pgc1 α* led to a 10%

reduction in body weight gain along and with a prevention of the development of insulin resistance during the diet. Furthermore, muscles overexpressing both genes presented increased in insulin sensitivity and reduced accumulation of fatty acids.

Therefore, the muscular overexpression of *Gck* or the co-overexpression of *Ppar δ* and *Pgc1 α* , might represent potential new gene transfer approaches to treat type 2 diabetes.

1. GLUCOSE HOMEOSTASIS

Glucose is the main energy source for the cells in the body and therefore, its concentration in blood is tightly regulated. The homeostatic mechanism keeps blood glucose levels within a narrow range independently of the internal demand or the exogenous disposition of the sugar. The regulation of blood glucose concentration is the result of the coordinated action of two antagonistic hormones secreted by the pancreas, glucagon and insulin.

During fasting, basal glucose use is matched with the endogenous glucose production keeping glucose levels between 70 mg/dL and 100 mg/dL (American diabetes association 2013, ADA). In this situation, the majority of the total body glucose use, approximately a 50%, takes place in the brain. The rest is distributed between the liver, gastrointestinal tissues, the skeletal muscle and to a lesser extent the adipose tissue. On the other hand, approximately 85% of the endogenous glucose production is derived from the liver by processes such as gluconeogenesis and glycogenolysis and the remaining 15% is produced in the kidney (DeFronzo, 2004). The hepatic glucose production is regulated by glucagon, secreted by the pancreatic α -cells. In fasting conditions, blood glucagon levels rise in order to increase hepatic gluconeogenesis and match the glucose demand (Marliss et al., 1970). Following a postprandial situation, glucose levels rise rapidly thus challenging glucose homeostasis. Consequently, pancreatic β -cells immediately respond to hyperglycaemia by secreting insulin. Insulin acts on different tissues in order to restore glucose homeostasis. Glucagon secretion is inhibited by insulin action on pancreas, which in turn contributes to diminish hepatic glucose production. Glucose uptake is stimulated by the action of insulin on peripheral tissues mainly the skeletal muscle, but also in the liver and the adipose tissue. Additionally, insulin directly inhibits the hepatic glucose production. In the

adipose tissue, insulin inhibits lipolysis, the process by which this organ releases free fatty acids (FFA) from stored triglycerides. The decline in circulating FFA further increases muscle glucose uptake and contributes to the inhibition of hepatic glucose production (DeFronzo, 2004). The final consequence of insulin action is the return of glucose levels back to normal.

Thus, any alteration affecting the normal function of β -cells, liver, skeletal muscle or adipose tissue can lead to situations where glucose homeostasis is not preserved.

2. TYPE 2 DIABETES MELLITUS

2.1. Introduction

Diabetes Mellitus is a group of chronic metabolic diseases where glucose homeostasis is challenged by high blood glucose levels (hyperglycaemia). It arises when the pancreas does not produce enough insulin, or when the body loses its ability to effectively use it. If it remains untreated, chronic hyperglycaemia can result in long-term complications and damage to various organs and tissues. (American Diabetes Association, International Diabetes Federation, 2013).

The vast majority of diabetic patients fall into two broad etiopathogenetic categories: type 1 and type 2 diabetes.

Type 1 Diabetes Mellitus, results from an autoimmune attack against the insulin-producing cells in the Pancreas (β -cells) and, as a consequence, are severely damaged or destroyed. As a result of the increased β -cell death, insulin production is highly reduced or even eliminated. Consequently, the compensatory mechanisms to preserve glucose homeostasis are not initiated, leading to hyperglycaemia.

Type 2 Diabetes Mellitus is the most common form of the disease accounting for about 90% of the cases diagnosed with diabetes. The onset of this disease usually occurs after the age of 40, reason because it is also known as adult-onset diabetes. This type of Diabetes is related to the appearance of insulin resistance in peripheral tissues. As a result, insulin is less effective at stimulating glucose uptake in insulin-dependent tissues, such as the skeletal muscle and the white adipose tissue. In liver, the insulin-related halting of

gluconeogenesis and glycogenolysis is attenuated, resulting in an increased glucose production. Meanwhile, insulin resistance in the adipose tissue results in an enhanced release of FFA to the circulation. In turn, raised FFA further inhibit glucose uptake by the skeletal muscle (Kelley et al., 1993), and affect β -cell function and viability (McGarry et al., 1999). Moreover, pancreatic β -cells progressively increase the amount of secreted insulin in order to maintain glucose homeostasis. The development of diabetic hyperglycaemia occurs when β -cells fail to further secrete enough insulin to compensate for peripheral insulin resistance (DeFronzo, 2004). This β -cell failure is usually associated to alterations in both the functionality and reduced mass of β -cells (Rhodes, 2005). Although the primary cause of this disease is unknown, it is clear that insulin resistance plays an early role in its pathogenesis and that defects in insulin secretion by pancreatic β -cells are instrumental in the progression to hyperglycaemia (Lowell et al., 2005).

Type 2 diabetic patients suffer from an enhanced prevalence of several macro-vascular and micro-vascular complications. Patients present approximately a 4-fold increased risk of heart attack, and coronary heart diseases (AACE report, 2005). As a consequence, they have an increased mortality index compared to general population (Lutgers et al., 2009). Additionally, type 2 diabetes is the leading cause of kidney failure, new cases of blindness in adults and it can give rise to foot problems that can lead to amputations (Ripsin et al., 2009). It is estimated that about a 60% of diabetic patients suffer from one or more of these complications (AACE report, 2005).

Apart from the health threat, type 2 diabetes represents a huge economic cost for society. It is estimated that the total direct medical cost in treatments in the European region is over 105.5 billion US dollars a year, which represents approximately 1911 US dollars per patient/year (Zhang et al.,

2010b). Additionally, type 2 diabetes is a significant cause of lost workforce productivity (Goetzel et al., 2003).

2.2. Epidemiology of type 2 diabetes

Type 2 diabetes is the most common metabolic disease in the world and its prevalence is rapidly increasing. In 2010, over 285 million adults worldwide were estimated to be diabetic, 90% of whom had type 2 diabetes. Furthermore, the number of patients has more than doubled since 1980 and by 2030 the number of adults with diabetes is predicted to rise to 439 million people worldwide (Figure 1). In this predicted increase, there is a huge difference between developed and developing countries. The estimated number of adults with diabetes is likely to increase by 69% in developing regions, compared to 20% for the developed countries. In particular, Asia is yet considered as the “diabetes epicenter” in the world, as a result of rapid urbanization, changes in lifestyle and nutrition (Chan et al., 2009). China and India currently are the two top countries with higher number of diabetic patients in the world, and another three Asiatic countries (Pakistan, Indonesia and Bangladesh) are expected to be in the top 10 by 2030. However, North-America is the region with the highest prevalence of the disease (Shaw et al., 2010). Meanwhile in Europe, the number of adult diabetic patients is estimated to be 55 million people, being Russia and Germany the top countries with more patients suffering from the disease (Figure 1).

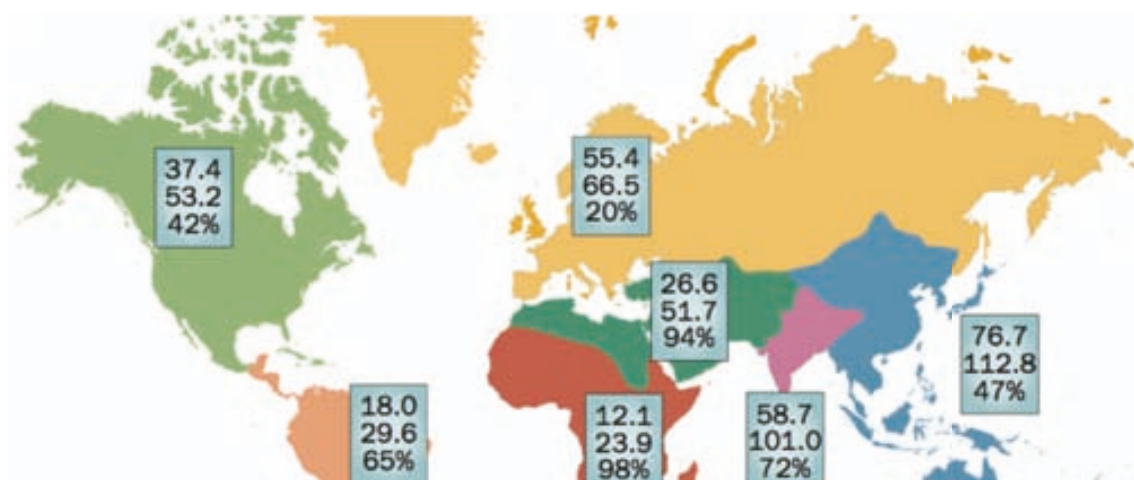


Figure 1. The number of people with diabetes mellitus (in millions) by region among adults aged 20–79 years for the years 2010 and 2030. (Chen et al., 2011).

In addition to the epidemic increase in the prevalence and number of diabetics, the age of onset of the disease is getting lower. Traditionally considered to be a metabolic disorder exclusively of adults, type 2 diabetes is increasingly appearing amongst younger people, even adolescents and children (Pinhas-Hamiel et al., 2005; Springer et al., 2013).

2.3. Risk factors for type 2 diabetes

Type 2 diabetes mellitus is a result of the interaction between a genetic predisposition and environmental factors that may affect the final incidence of the disease. However, there are several major aspects that predispose to the development of type 2 diabetes.

2.3.1. Obesity

The global epidemics of type 2 diabetes is associated to the rising rates of overweight and obesity. Obesity is characterised by increased fat accumulation in the adipose tissue and other organs, which lead to excessive weight gain to the extent that it may have an adverse effect on health. The Body Mass Index (BMI), defined as the weight in kilograms divided by the square of the height in metres (kg/m^2), is an index used to classify adults

based on their body weight (WHO, 2012). In 2005, a 23.2% of the global population was considered to be overweight (BMI of 25-30 Kg/m²) and 9.8% obese (BMI of \geq 30Kg/m²) and, by 2030, the total numbers of both conditions are expected to duplicate and almost triplicate, respectively (Kelly et al., 2008).

Nowadays, overweight and obesity are considered the single most important predictors of type 2 diabetes (Hu et al., 2001). In particular, about 90% of type 2 diabetes is attributable to excess weight (Hossain et al., 2007). However, how and where this excessive fat gets distributed in the body is proven of great importance. In humans, fat is mainly located beneath the skin (subcutaneous fat) or around the internal organs (visceral fat). Many investigations demonstrate that excessive fat accumulation in the visceral adipose tissue, but not in the subcutaneous adipose tissue, significantly correlate with insulin resistance and type 2 diabetes (Boyko et al., 2000; Lemieux et al., 1996; Pouliot et al., 1992). In fact, the removal of abdominal subcutaneous fat by liposuction has no net effect on insulin resistance (Klein et al., 2004a). This is in agreement with the fact that not all individuals categorized as obese develop type 2 diabetes (Lebovitz et al., 2005). Nevertheless, there is a clear relationship between excessive fat accumulation and increased risk of developing type 2 diabetes.

2.3.2. Environmental factors

The western and the modern way of life are important participants contributing to the rise of type 2 diabetes and obesity. In our modern society, decreased physical activity, regular overconsumption of high-caloric foods and sedentary lifestyle are common behaviours which are clearly related to the increased prevalence of type 2 diabetes (Hu et al., 2001). This relationship has been dramatically evidenced by studies in migrating populations where the adoption of the western lifestyle progressively increased their prevalence to develop

type 2 diabetes (Chan et al., 2009; Mohan, 2004; Motala et al., 2003). On the other hand, diabetic migrated populations returning to their previous way of life highly improved their metabolic profile (O'Dea, 1984).

Other environmental factors found to be independently associated with the risk of type 2 diabetes include smoking, sleeping disorders, depression, antidepressant medications and pollution (Chen et al., 2011).

The sum of maintaining a body-mass index of 25 or lower, low-calorie and rich fiber diets, regular exercise, smoking abstinence and moderate alcohol consumption is associated with a 90% reduced incidence of type 2 diabetes (Hu et al., 2001).

2.3.3. Genetic susceptibility

In addition to environmental components, there is compelling evidence that genetic factors also affect the pathogenesis of type 2 diabetes. For instance, a family history with type 2 diabetic relatives confers a 3-fold increased risk to develop the disease (Schafer et al., 2011). Additionally, some ethnic populations, such as Pima and Tohono O'odham Indians, present a higher prevalence of type 2 diabetes than other populations exposed to the same environmental risks of developing this disease (Knowler et al., 1978; Livingston et al., 1993).

Thanks to the development of genetic techniques such as the candidate gene approach or genome wide association studies (GWAS), various gene variants have been recently discovered to be associated with T2DM. To date, approximately 40 different risk genes for T2DM have been found (McCarthy, 2010). Although the precise molecular mechanisms for many of the gene variants are poorly understood, their influence on insulin sensitivity or insulin secretion have been uncovered on several cases. For instance, common

variants in PPARG (which encodes for the PPAR γ gene), ADIPOQ (which encodes for adiponectin, a well known insulin-sensitizing hormone) or IRS1 (encoding for the insulin receptor substrate 1, a key protein in the insulin signalling pathway) among others were reported to affect insulin sensitivity. On the other hand, variations in KCNJ11 (encoding for the Kir6.2 subunit of the ATP sensitive channel of β -Cells), SLC30A8 (encoding for ZnT-8, a zinc transporter protein present in insulin granules) or TCF7L2 (encoding for the transcription factor TCF7L2 which controls the expression of the insulin gene) are reported to affect insulin secretion. Actually, the vast majority of the T2DM risk genes appear to affect β -cell function (Schafer et al., 2011).

Although the evidence of the genetic influence in the pathogenesis of T2DM, individual risk genes are thought only to contribute to an inherent susceptibility to the disease. For instance, the common variants with the greatest effects on the risk of T2DM (TCF7L2 in Europeans and KCNQ1 in Asians) result in lifetime prevalence rates that are roughly double those seen in persons with none (McCarthy, 2010). The current rise in T2DM is considered to be mainly caused by environmental changes associated to lifestyle (Imamura et al., 2011).

2.3.4. *Another risk factors*

Low birth weight has been consistently found to be associated with an increased risk of T2DM in later life. Low birth weight due to nutritional deprivation *in utero* influences later susceptibility to obesity and T2DM (Chen et al., 2011). This has been related to the “thrifty phenotype” hypothesis, that postulates that a pregnant woman can modify the development of her unborn child such that it will be prepared for survival in an environment in which resources are likely to be short (Hales et al., 1992). For instance, adults

exposed to famine during fetal life had a worse glucose tolerance status than unexposed individuals. The risk of T2DM owing to inadequate fetal nutrition is likely to be exacerbated by to an affluent nutritional environment in adult life (Chen et al., 2011).

Gestational diabetes (GDM) is another clearly related risk factor for developing type 2 diabetes. GDM consists in high blood glucose levels during pregnancy in women without previously diagnosed diabetes. It is caused when, during pregnancy, the pancreas does not secrete enough insulin, leading to hyperglycaemia. It usually disappears after birth, however women that suffered GDM and their offspring have an increased risk of developing Type 2 diabetes (International Diabetes Federation 2012)

2.4. Etiopathogeny of type 2 diabetes

T2D is caused by insulin resistance in peripheral tissues and inappropriate compensatory insulin secretion response, due to the combination of decreased β -cell mass and function. It has been classically accepted that insulin resistance was the primary defect in the progression to Type 2 diabetes. However, now it is known that both peripheral insulin resistance and β -cell dysfunction occur early in the pathogenesis of type 2 diabetes, long before blood glucose values reach a level that is defined as pre-diabetes (fasting glucose levels between 100 mg/dL and 125 mg/dL, ADA). Although the primary cause of this disease is unknown, several mechanisms have been postulated to explain the progression to type 2 diabetes.

As already discussed, type 2 diabetes is linked to obesity and over-nutrition. Adipocytes, the cells that primarily compose adipose tissue, have a

large capacity to store triglycerides during feeding, as well as to hydrolyse and release triglycerides as FFAs and glycerol during fasting. Apart from their storage function, adipocytes secrete a large number of hormones and cytokines (known as adipokines) that affect energy metabolism in other tissues (Guilherme et al., 2008). As overfeeding develops, adipocytes enlarge as a result of increased triglyceride deposition. This enlargement rises the rates of lipolysis (Arner, 2005), consequently increasing the levels of circulating FFA, and also promotes the secretion of inflammatory cytokines. The action of such cytokines profoundly affects the adipocyte function by further increasing lipolysis and inhibiting TG synthesis (Guilherme et al., 2008). The release of FFA as a result of increased adipose lipolysis, may be the single most critical factor in modulating insulin sensitivity in peripheral tissues (Kahn et al., 2006). The excessive circulating FFAs cause accumulation of triglycerides into non-adipose tissues, such as liver and skeletal muscle, which contribute to the development of insulin resistance in these tissues. (Krssak et al., 1999; Perseghin et al., 1999). Specifically, FFA would promote insulin resistance by inhibiting glucose oxidation (Randle cycle)(Bevilacqua et al., 1990). Additionally, the cytosolic accumulation of triglycerides and derived lipid intermediates, such as ceramides and diacylglycerol (DAG), interfere with the insulin signalling pathway in these tissues, thus promoting insulin resistance. (Muoio et al., 2008). Along with the developing hyperglycaemia resulting from the insulin resistance in peripheral tissues, a chronic elevation in FFA impairs the β -cell secretory function and induces β -cell apoptosis, thus possibly contributing to the β -cell failure and reduced β -cell mass observed in the progression to T2DM (Poitout et al., 2008).

Apart from FFA, inflammatory cytokines derived from enlarged adipocytes might be other important factors contributing to the pathogenesis

of T2DM during obesity. In particular, TNF-alpha, IL-1 β and IL-6 might also have a direct role in the development of insulin resistance in skeletal muscle and liver, as well as β -cell dysfunction.

2.5. Current treatments for type 2 diabetes

Several approaches are being used to control type 2 diabetes.

2.5.1. Lifestyle interventions

Because of the effects of excessive body weight on insulin resistance and its correlation with T2DM, the first strategy to treat and prevent this disease focuses on lifestyle changes to reduce patient's BMI. In order to achieve this goal, lifestyle modification programs basically consist of diet and physical activity interventions. Low-calorie (500-1000 calorie deficit per day) and low-fat meals (25-30% calories from fat) are recommended to reduce body weight. Although many people can lose a 10% of weight in six months with such diets, regular physical activity is needed to maintain body weight and prevent weight regain. Thus, a minimum of 150 minutes of moderate activity per week is recommended. Furthermore, physical activity improves insulin sensitivity independent of weight loss. Short-term studies have demonstrated that moderate weight loss (5% of body weight) in patients with T2DM can improve insulin action, decrease fasting blood glucose and reduce the need for diabetes medications (Klein et al., 2004b). However, making long-term changes to eating and activity behaviours, and consequently keeping weight loss, is extremely difficult for most patients (Bantle et al., 2008).

2.5.2. Pharmacological treatment

When lifestyle interventions are not sufficient to keep glucose control a pharmacological treatment must be added. Due to the multiple

pathophysiologic changes involved in the progression to T2DM, multiple compounds have been developed with the aim of improving glycaemic control and slowing the onset of the disease. The vast majority of them are focused on improving insulin resistance or enhancing the β -cell function. However, the initial improvements in glycaemia are not sustained because of progressive β -cell dysfunction, making of insulin treatment a must. Furthermore, these treatments may also have undesired side effects, such as hypoglycaemia, weight gain and gastrointestinal complications.

Metformin

Metformin is the first-line drug of choice for the treatment of T2DM. It reduces the hepatic glucose production and improves insulin sensitivity in the skeletal muscle by activating AMP-Kinase. It does not cause hypoglycaemic episodes and is not associated with body weight gain. It appears to decrease heart attacks, strokes and another cardiovascular complications associated to T2DM (Global guideline for Type 2 Diabetes, IDF 2005). Gastrointestinal intolerance is the most common side-effect and metformin is not indicated for patients with renal insufficiency (Stumvoll et al., 2005).

Sulfonylureas

Sulfonylureas increase insulin release by closing the β -cell potassium channels. These drugs lead to moderate decreases in concentrations of plasma glucose in most patients with T2DM. However, they may induce hypoglycaemia as a result of excesses in insulin production and release. Another undesirable effect is that they promote weight gain (Stumvoll et al., 2005)

Thiazolidinediones

Thiazolidinediones (TZD) are PPAR γ agonists that act by redistributing triglycerides from visceral fat depots to other less lipolytic subcutaneous depots, thus lowering circulating FFA. TZDs improve insulin sensitivity in skeletal muscle and liver and ameliorate the inflammatory milieu of T2DM (Stumvoll et al., 2005). However, all TZDs promote weight gain and fluid retention leading to edema and heart failure to predisposed individuals (Tahrani et al., 2011). Additionally, of the two commercially available TZDs in the market, Rosiglitazone is no longer available in the European Union due to increased myocardial infarction (Nissen et al., 2010) and Pioglitazone has been recently associated with bladder cancer and consequently withdrawn from the market in France and Germany (Lewis et al., 2011).

Incretin Mimetics and DPP-4 inhibitors

Incretins are a group of gastrointestinal hormones that potentiate glucose-dependent insulin secretion and inhibit glucagon release. They also reduce the gastric emptying, consequently reducing food intake with a long-term effect to help with weight loss. The two main incretins are the glucagon-like peptide-1 (GLP-1) and gastric inhibitory peptide (GIP). However, incretins are rapidly inactivated by the enzyme dipeptidyl peptidase-4 (DPP-4) (Tahrani et al., 2011).

Some DPP-4-resistant GLP-1 analogues with GLP-1-receptor agonist properties have been developed to extend their half-life. Another incretin drug based approach has been to increase the circulating concentrations of active GLP-1 and GIP with the development of specific DPP-4 inhibitors. These compounds have been proven to be effective at improving glycaemic control without causing hypoglycaemia and at reducing body weight gain in the case of the GLP-1 analogues. However, these are relatively new drugs. Their long-term safety it is still unknown and some limiting side effects have been described,

particularly vomiting and nausea in the case of GLP-1 analogues, and an association with pancreatitis in the use of both (Ratner et al., 2010; Tahrani et al., 2011).

α -Glucosidase inhibitors

This class of drugs act as competitive inhibitors of enzymes needed to digest carbohydrates, specifically alpha-glucosidase enzymes in the brush border of the small intestines. It delays the digestion of complex carbohydrates to monosaccharides (glucose) thus reducing the postprandial glucose pics. Their main drawback is its tendency to cause gastrointestinal side effects (Tahrani et al., 2010).

Meglitidines

Meglitidines are a class of drugs that increase insulin release by closing the potassium channels in β -cells in a similar manner to sulfonylureas. However their onset of action and duration of effect is shorter than sulfonylureas. Their action is partially glucose-dependent and thus are less likely to hypoglycaemic episodes (Tahrani et al., 2010). However they still represent a potential side effect. Like sulfonylureas they promote weight gain (Tahrani et al., 2011).

Bile acid sequestrants

These drugs have been used as lipid-lowering agents but they also moderately reduce plasma glucose levels. However their glucose-lowering mechanism is currently unknown (Handelsman, 2011)

Usually metformin is the first drug to be used along with lifestyle interventions. However, monotherapy alone is not able to maintain long-term glucose control and a second drug needs to be introduced. At this point, there

is limited data available to guide endocrinologists on which drug is better to use as a second choice. Advantages and disadvantages of specific drugs for each patient must be considered, increasing the complexity of the treatment. As the progression of the disease advances, the addition of a third drug or even more compounds is necessary to keep glucose homeostasis, further complicating the treatment. When the combination of glucose-lowering drugs and lifestyle interventions are unable to maintain blood glucose control, exogenous insulin therapy is inevitably needed. However, insulin therapy is difficult since it is not easy to achieve and maintain an effective glucose control without significant hypoglycaemic episodes and weight gain (DeFronzo, 2009; Inzucchi et al., 2012). The difficulty and complexity of efficient long-term treatments makes of the development of new strategies based on a better understanding of the disease a must.

2.5.3. Bariatric Surgery

Bariatric surgery includes several gastrointestinal operations performed to promote weight loss that can powerfully ameliorate and even reverse T2DM. However, these operations are only recommended to T2DM patients with BMI >35 thus limiting its application to severely obese patients (Robinson, 2009).

3. THE SKELETAL MUSCLE

The skeletal muscle is the largest organ in the body comprising between 40-50% of body mass. As well as having a role in movement, posture, and force generation it also produces and maintains body heat and plays a central role in body metabolism.

The skeletal muscle is made up of large multinuclear cells known as myocytes or muscle fibres. Such fibres contain long bundles of contractile proteins in the cytoplasm, such as myosin and actin. The hydrolysis of ATP by the ATPase activity located in the heavy chain portion of the myosin molecule leads to the contraction of the fibre resulting in the generation of tension.

As Figure 2 shows, each individual fibre is separated by a connective tissue known as endomysium. These cells are grouped forming large bundles called fascicles, which are surrounded by a layer of connective tissue called perimysium. The perimysium is an inward projection of a bigger layer called epimysium that surrounds the group of fascicles that form the muscle. Skeletal muscles have an abundant supply of blood vessels and nerves that are distributed through the epimysium (Figure 2).

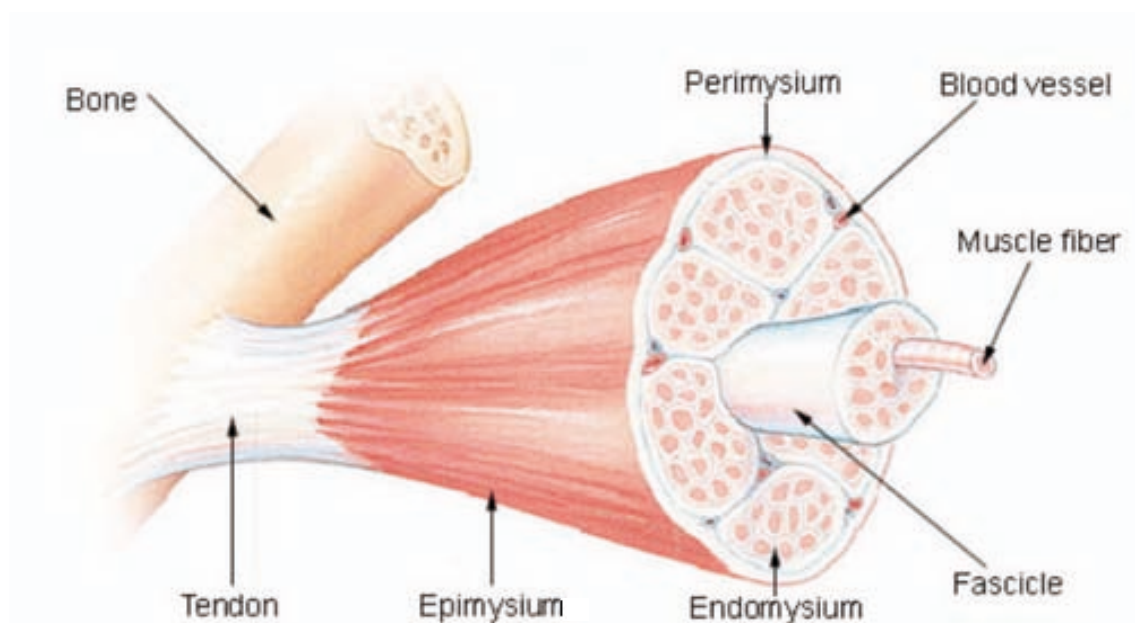


Figure 2. Structure of the skeletal muscle.

3.1. Fibre types

In humans, skeletal muscle fibres are classified as Type I, Type IIa and Type IIb depending on the myosin heavy chain (MHC) isoform that they express (Schiaffino, 2010). For instance, Type I fibres express a slow contracting isoform of myosin heavy chain, MHC I. Meanwhile, Type IIa and IIb fibres express a faster contracting isoform of myosin heavy chain, MHC IIa and MHC IIb respectively. Each different fibre type possesses specific metabolic and functional properties. Metabolically, Type I fibres obtain energy from the oxidation of substrates to CO₂, reason why they are also known as oxidative fibres. Accordingly, Type I fibres have an elevated number of mitochondria. In contrast, Type IIb fibres (also known as glycolytic fibres) produce energy by anaerobic processes and have a low mitochondrial density. Meanwhile, Type IIa fibres have intermediate metabolic properties between Type I and Type IIb fibres. Mouse skeletal muscles express a fourth type of myosin heavy chain protein, the MHC IIx. Type IIx fibres have properties intermediate between IIa and IIb. In Table 1 the characteristics of each fibre type are summarized. Each individual muscle is a mixture of these fibres but their individual proportions vary depending on the action of every specific muscle. Thus, muscles where fast contracting fibres predominate (type II) are adapted to activities that require short and powerful contractions. On the other hand, muscles rich in type I fibres are adapted to endurance activities and have a high resistance to fatigue (Pette et al., 1999). Lifestyle factors like training exercise, inactivity, and age induce fibre type transitions showing the great plasticity of the skeletal muscle in response to stimuli (Scott et al., 2001).

	Type I Fibres	Type IIa Fibres	Type IIx Fibres	Type IIb Fibres
Contraction time / fatigability	Slow	Medium	Fast	Very Fast
Activity	Aerobic	Long-Term anaerobic	Short-Term anaerobic	Short-Term anaerobic
Mitochondrial density	High	High	Medium	Low
Muscle colour	Red	Red	Red / White	White
Capillary density	High	Intermediate	Low	Low
Oxidative capacity	High	High	Intermediate	Low
Glycolytic capacity	Low	High	High	High
Creatine phosphate content	Intermediate	High	High	High
Glycogen content	Intermediate	Intermediate	High	High
IMTG content	High	Intermediate	Low	Low

Table 1. Basic Muscle Fibre Type and Metabolic Properties (Mann et al., 2010)

3.2. Skeletal muscle metabolism

Skeletal muscle can adapt its metabolism to use different energy sources, such as, glucose, free fatty acids, ketone bodies and amino acids depending on its energy demand. In resting conditions, FFAs are its main source of energy. They are metabolized to Acetyl-CoA in the mitochondria by the process of β -oxidation. The resulting Acetyl-CoA enters the Krebs Cycle (also known as the TCA cycle) where it is used to produce CO_2 and regenerate NADH. The NADH generated by the TCA cycle is fed into the oxidative phosphorylation pathway where it is used to produce energy in the form of ATP (Figure 3). When energy demands increase, such as during moderate exercise, skeletal muscle can use glucose and circulating ketone bodies in addition to FFA. Myocytes can use glucose derived from the circulation or produced from glucose stores in the cell as glycogen by the process of glycogenolysis. Glucose enters the glycolytic pathway where it is metabolized to acetyl-CoA which

immediately enters the TCA cycle. If exercise is very intense, oxygen supply is insufficient to oxidize enough FFA and glucose to produce ATP and satisfy the energy demand. In this situation, the skeletal muscle metabolises glucose to lactate, a process by which ATP is produced without the need of oxygen.

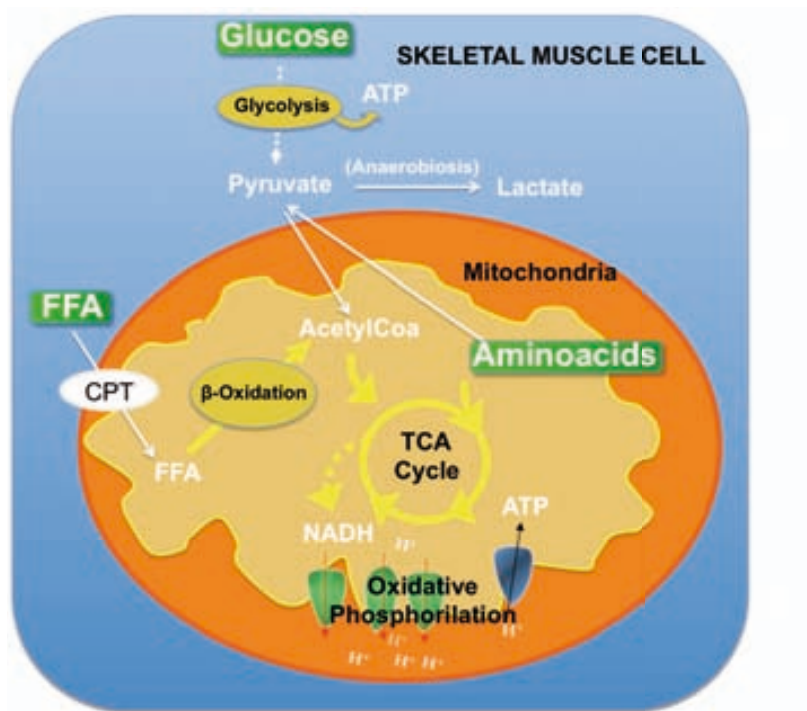


Figure 3. Main metabolic processes leading to ATP production in the skeletal muscle. Glucose is metabolized to pyruvate by the process of glycolysis thus producing energy in the form of ATP. In anaerobic conditions, pyruvate is metabolized to lactate. In aerobic conditions pyruvate is metabolized to AcetylCoA which enters the TCA cycle. FFAs enter the mitochondria through the carnitine-palmitoyl transferase system (CPT) where they are oxidized to AcetylCoA by the process of β -oxidation. Aminoacids can be metabolized to pyruvate, or enter directly as intermediates in the TCA cycle. The NADH produced in the TCA cycle is fed into the oxidative phosphorylation chain for ATP production.

3.2.1. Glucose metabolism in the skeletal muscle

The skeletal muscle plays a key role in maintaining glucose homeostasis. Following glucose ingestion, approximately 80% of glucose uptake occurs in the skeletal muscle. In this tissue, glucose uptake is facilitated by two different glucose transporters, GLUT1 and GLUT4 (DeFronzo, 2004) (Figure 4). GLUT1

is nearly ubiquitous and is thought to be the primarily responsible during the postabsorptive glucose uptake. However, its abundance in the skeletal muscle is substantially lower than that of GLUT4 (Marette et al., 1992). GLUT4 is the insulin-regulated glucose transporter. After exposure to insulin, GLUT4 moves from intracellular vesicles to the plasma membrane where catalyses glucose uptake into the cell (Olson et al., 1996). Once inside the cell, hexokinase (HK) enzymes catalyse the conversion of free glucose to glucose-6-phosphate (G-6-P). Of the known isoforms of HK, only HK-I and HK-II are expressed in the skeletal muscle. Insulin increases the expression of HK-II, but not HK-I, so HK-II is considered to be the isoform in skeletal muscle that is subject to insulin action (Vogt et al., 2000). Thus, HK-I, together with GLUT1, mediates the basal glucose uptake and HK-II, along with GLUT4, control the insulin-regulated glucose uptake in the skeletal muscle (Figure 4). Both hexokinases present a very high affinity for glucose and are allosterically inhibited by its product, G-6-P (DeFronzo, 2004).

Once phosphorylated by hexokinase II, glucose can be directed to glycogen or to the glycolytic pathway to be used as energy. However, with increasing insulin concentrations, glycogen synthesis predominates.

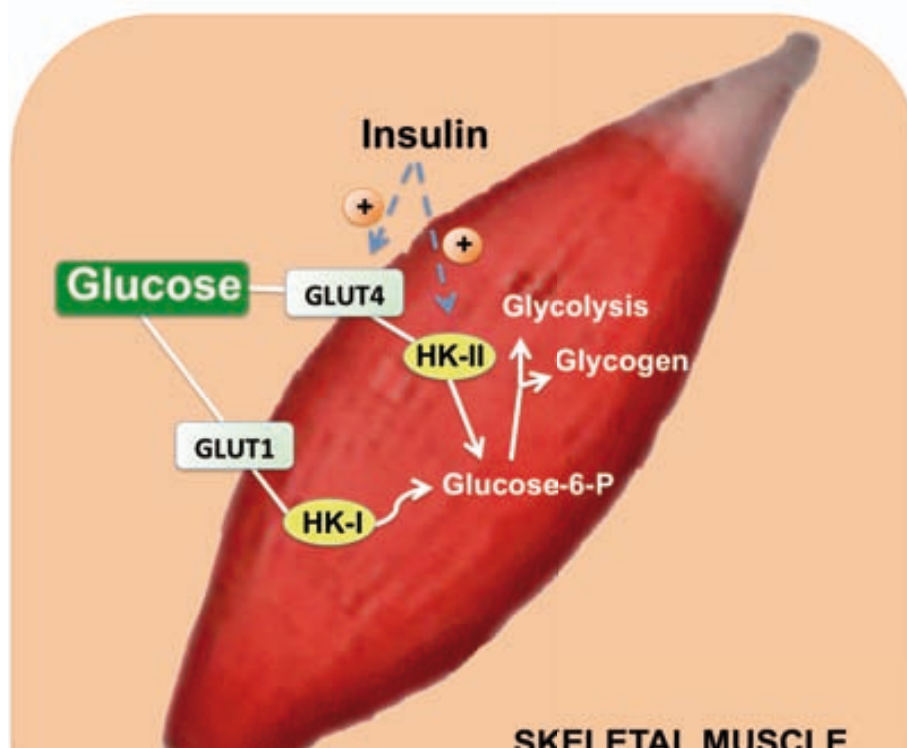


Figure 4. Role of skeletal muscle in glucose homeostasis. During postabsorptive states, glucose uptake is facilitated by the glucose transporter GLUT1. Once inside the cell, glucose is phosphorylated by HK-I. In fed conditions, elevated glucose levels lead to insulin release by the pancreas. Insulin induces the translocation of GLUT4 to the cell membrane and increases HK-II expression, which together increase glucose uptake and utilization by the skeletal muscle. Once in the cell, glucose is phosphorylated to glucose-6-phosphate by HKII. Glucose-6-phosphate is processed further for either storage, in the form of glycogen, or metabolised, mainly by glycolysis.

3.2.2. Lipid metabolism in the skeletal muscle

Free fatty acids can account for 90% of skeletal muscle total energy demand during fasting. However, the uptake of FFA by the skeletal muscle is not yet fully understood. The vast majority of FFA enter by a protein-mediated transport mechanism, although passive diffusion can also occur. Several FFA transporters have been identified including fatty acid translocase (FAT/CD36), plasma membrane-bound fatty acid binding protein (FABPpm) and tissue-specific fatty acid transport protein (FATP). Although the relative contribution of each one is not known, CD36 is thought to be the predominant transporter. Once fatty acids are transported into the cytosol, they are esterified to long chain acyl CoAs (LCACoA). A small proportion of LCACoA can be converted to lipid accumulation intermediates such as triglycerides, but also to diacylglycerols (DAG) and ceramides that can act as signalling molecules. However, most of LCACoA are transferred to the mitochondria for oxidation and energy production. LCACoAs enter the mitochondrial membrane by the Carnitine-dependent transport system. LCACoA are combined with carnitine by the carnitine palmitoyltransferase I (CPT1) to form acyl-carnitine, which is transported into the mitochondrial matrix by the carnitine translocase (CAT). Once there, acyl-carnitines are converted back to LCACoAs by the carnitine palmitoyltransferase 2 (CPT2). In this process, CPT1 is considered to be the

rate-limiting protein of β -oxidation of FFA. LCACoA then enter the β -oxidation pathway where acetylCoA, NADH and $FADH_2$ are produced as a result of the oxidation of the fatty acid. NADH and $FADH_2$ are directly fed into the oxidative phosphorylation pathway where they are used to produce energy in the form of ATP. Meanwhile, acetylCoA enters the TCA cycle in order to produce energy (Zhang et al., 2010a).

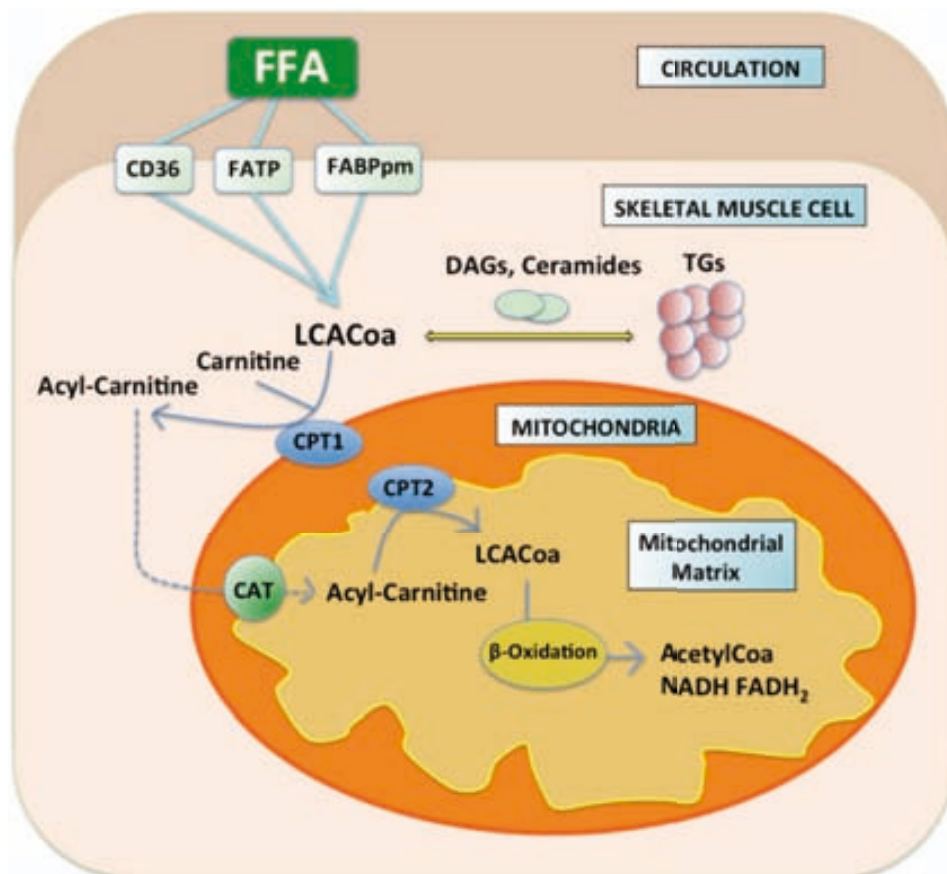


Figure 5. Lipid Metabolism in the skeletal muscle. FFAs enter the myocyte through the transporter proteins CD36, FATP or FABPpm where they are esterified to LCACoA. A small proportion of LCACoA can be stored in the form of triglycerides (TGs) and intermediate products such as ceramides and diacylglycerol. However, the majority of fatty acids are combined with carnitine, thanks to the action of CPT1, and translocated to the mitochondrial matrix by CAT. CPT2 disrupts the Acyl-carnitine complex and the fatty acid is esterified again to LCACoA. Once in the mitochondrial matrix LCACoAs are oxidized to AcetylCoA, NADH and $FADH_2$ by the process of β -oxidation.

3.2.3. Oxidative phosphorylation and mitochondrial uncoupling

The NADH and FADH₂ produced by the oxidation of the different energetic substrates are redirected to the inner mitochondrial membrane where the mitochondrial electron transport chain (ETC) produces ATP. ETC is made up of four protein complexes located in the inner mitochondrial membrane. These complexes accept electrons, given by NADH and FADH₂. The energy released by electrons flowing through the ETC is used to transport protons (H⁺) from the mitochondrial matrix towards the intermembranal space thus generating an electrochemical gradient between these two compartments. This gradient is tapped by allowing protons to flow back to the mitochondrial matrix through the enzyme ATP synthase. The energy produced by this movement is used by this enzyme to synthesize ATP from ADP and inorganic phosphate. The final destination of the electron flow is molecular oxygen, which is reduced to H₂O. Thus, substrate oxidation and oxygen reduction are coupled to the formation of ATP (Figure 6).

Although oxidative phosphorylation is a vital process, it also is a major site of Reactive oxygen species (ROS) production (Echtay, 2007). These oxygen species are highly damaging since they can react with lipids forming lipid peroxides, which induce mitochondrial and DNA damage. One of the mechanisms that the cell uses in order to reduce ROS and peroxide is to activate mitochondrial uncoupling. Mitochondrial uncoupling is the process by which protons are pumped out of the matrix back into the mitochondria in a process not coupled to ATP synthesis. Thus, part of the H⁺ gradient generated by the ETC is used by other proteins, known as uncoupling proteins (UCP), located in the inner mitochondrial membrane. This family of proteins is composed by five different members (UCP1-5). The skeletal muscle expresses

UCP2, UCP3 and UCP4 being UCP3 almost specific for the skeletal muscle. Although the role of mitochondrial uncoupling in skeletal muscle is nowadays still in discussion, its activation reduces the electrochemical proton gradient leading to reduced production of ROS by the ETC (Echtay, 2007). Additionally, UCPs would also export lipid peroxide species out of the mitochondria as a protective mechanism against oxidative damage during high rates of fatty acid oxidation (Schrauwen et al., 2004). Accordingly, UCP3 expression is elevated during states that are associated with increased fat metabolism like fasting (Millet et al., 1997) or acute exercise (Schrauwen et al., 2002). UCP3 may also increase fatty acid oxidation rates in the skeletal muscle by anion transport (Bezaire et al., 2005).

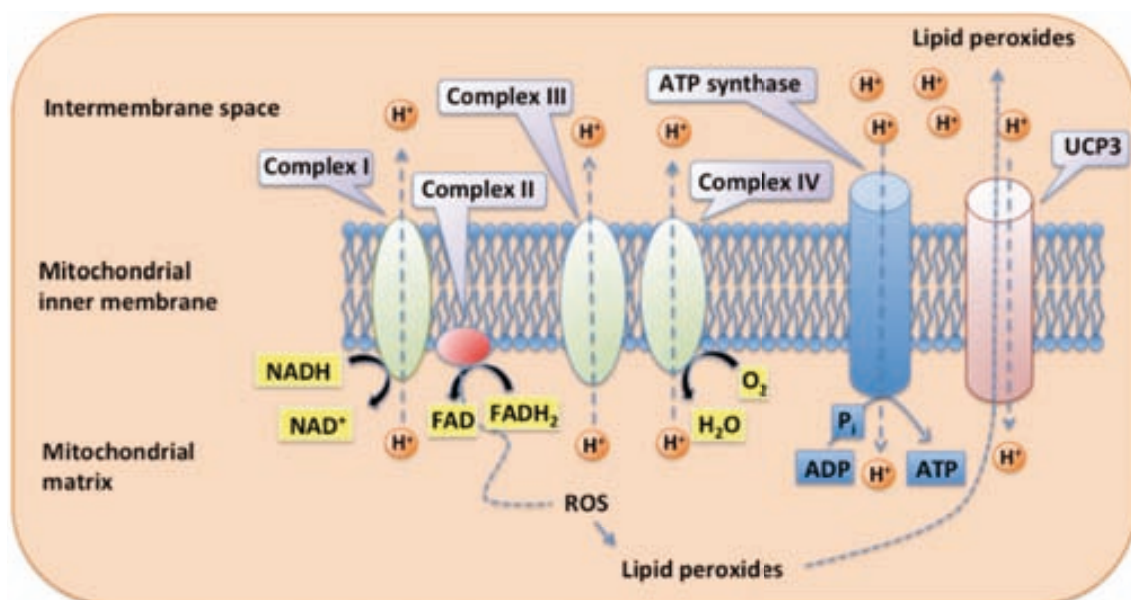


Figure 6. Scheme of the electron transport chain. All four complexes of the electron transport chain are found in the mitochondrial inner membrane. While electrons are transported across the chain, protons are pumped towards the intermembrane space. The energy of the proton gradient is used by the ATP synthase to generate ATP and/or by UCP3 to separate oxidative phosphorylation from ATP synthesis. ROS are produced by the electron transport chain

and react with phospholipids resulting in lipid peroxides. UCP3 exports lipid peroxide anions out of the mitochondrial matrix.

3.3. Skeletal muscle and type 2 diabetes

During post-prandial states, the skeletal muscle uses glucose as a primary source of energy in response to the increasing insulin concentrations in blood. However during fasting, when insulin levels are low, the metabolism of the skeletal muscle switches to fat oxidation. This switch is a measure to keep glucose homeostasis when blood glucose concentrations are low (during fasting) or suddenly rise and need to be rapidly decreased (post-prandial states). This adaptable capacity of the skeletal muscle is known as *metabolic flexibility*. However, during type 2 diabetes and in insulin resistance states this flexibility is greatly reduced. In these situations, the skeletal muscle is characterised by lower fasting lipid utilization and the inability to switch to carbohydrate uptake and oxidation in response to insulin (Kelley, 2005; Ukropcova et al., 2005). As a consequence lipids accumulate in the skeletal muscle and blood glucose levels rise (Figure 7).

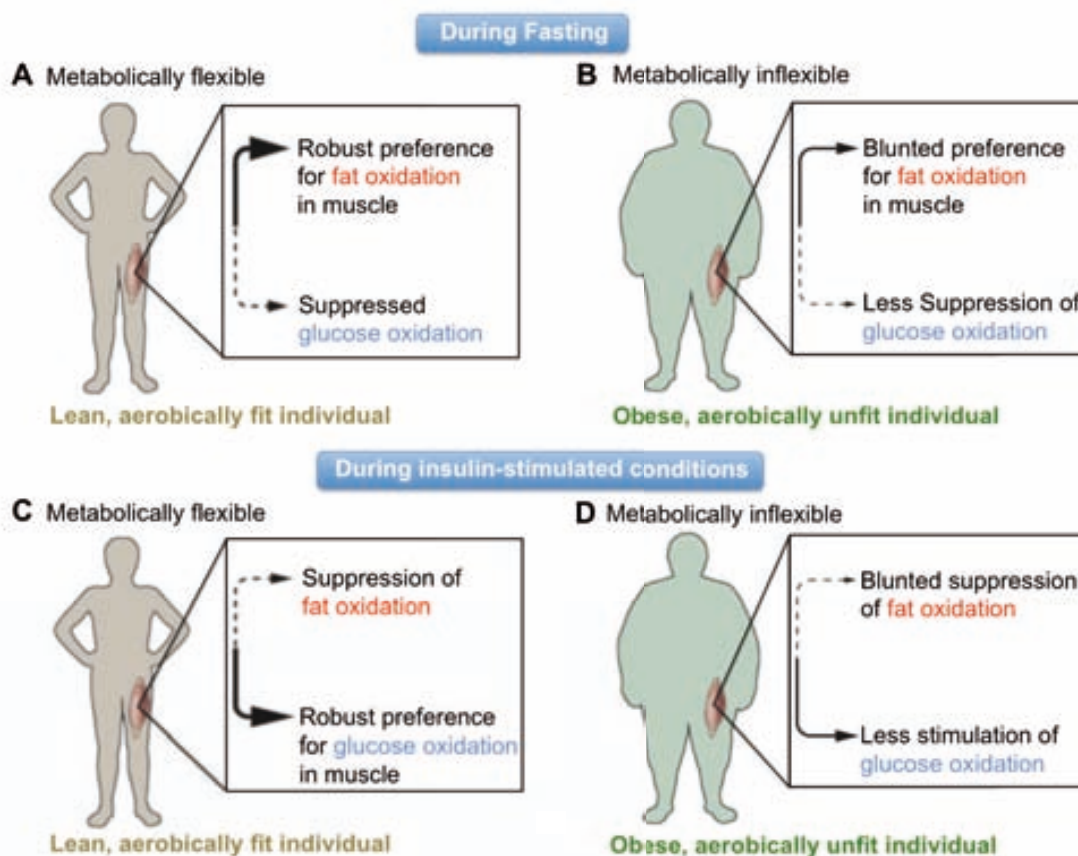


Figure 7. Muscle metabolic inflexibility during type 2 diabetes (Kelley, 2005).

3.3.1. Role of reduced glucose phosphorylation of the skeletal muscle in type 2 diabetes

During insulin resistance states the ability of insulin to induce glucose uptake by the skeletal muscle is greatly reduced. Both insulin-mediated glucose transport and phosphorylation have been shown to be impaired in type 2 diabetic subjects (DeFronzo, 2004). Accordingly, the activity of HK-II and the presence of GLUT4 in the plasma membrane are reduced in insulin resistance conditions (Pendergrass et al., 1998; Zierath et al., 1996). Thus, the skeletal muscle is unable to metabolize blood glucose normally. Even though glucose transport and phosphorylation are reduced, the fact that free glucose (non-phosphorylated) concentrations are increased in the skeletal muscle of type 2 diabetic patients evidences that the rate of intracellular glucose phosphorylation is impaired to a greater extent than glucose transport (Bonadonna et al., 1996). This suggests that reduced glucose phosphorylation in the skeletal muscle may be the rate-limiting step for glucose use in type 2 diabetic individuals (Abdul-Ghani et al., 2010).

3.3.2. Role of reduced oxidative capacity of the skeletal muscle in type 2 diabetes

Elevations in circulating FFA are common in insulin resistant conditions such as obesity and type 2 diabetes and excessive lipid accumulation of fatty acids and/or lipid metabolites in muscle has emerged as an important contributor to insulin resistance. Additionally, several studies have reported decreased fat oxidation in skeletal muscle of insulin resistant individuals

independent of the plasma FFA concentration (Blaak, 2004; Kelley et al., 1999). Since the majority of fat oxidation takes place in the mitochondria, impaired fat oxidation in the skeletal muscle of insulin resistant individuals suggests the presence of mitochondrial defects that contribute to the impaired fat oxidation. Accordingly, the activity of β -oxidative enzymes (Simoneau et al., 1999), the size and number of mitochondria (Morino et al., 2005; Ritov et al., 2005) as well as the activity of proteins in the respiration chain (Befroy et al., 2007; Szendroedi et al., 2007) have been found to be reduced in the skeletal muscle of type 2 diabetic individuals. Therefore, the increase in circulating FFA along with the decrease in fat oxidation capacity leads to the accumulation of fatty acids and triglycerides in the skeletal muscle.

3.3.3. Molecular mechanisms of lipid-induced insulin resistance in the skeletal muscle

When the uptake of fatty acids exceeds the rates of β -oxidation, intramuscular TG can accumulate. Associated with the accumulation of TG, the abundance of lipid metabolites such as LCACoAs, DAGs and ceramides increase in the skeletal muscle. The presence of these lipid species is associated with the activation of a number of different serine kinases that negatively modulate insulin action (Zhang et al., 2010a). For instance, DAG has been found to be increased in skeletal muscle from insulin-resistant rodents (Avignon et al., 1996) and humans (Itani et al., 2002). The accumulation of DAG is positively correlated with the increased activity of the protein kinase C Theta (PKC θ), known to impair insulin signalling via serine phosphorylation of IRS-1 (Itani et al., 2001; Itani et al., 2000; Yu et al., 2002). Nowadays, DAG activation of PKCs is considered a major determinant of lipid-induced insulin resistance (Timmers et al., 2008). Ceramides have been postulated to inhibit muscular insulin action

via the inhibition of Akt phosphorylation in obese insulin resistant humans (Adams et al., 2004; Hajdуч et al., 2001). Thus, the accumulation of triglycerides in the skeletal muscle and its derivate metabolites is associated with the development of insulin resistance.

3.4. Novel Strategies to counteract type 2 diabetes by the genetic modification of the skeletal muscle

Strategies to increase glucose phosphorylation have been tested in order to increase glucose use by the skeletal muscle and hence to ameliorate insulin resistance. Transgenic mice overexpressing HK-II in the skeletal muscle showed an increase in insulin mediated muscular glucose uptake (Chang et al., 1996). However, this effect was lost when diabetes was induced in these animals by feeding with a high fat diet (Fueger et al., 2004). The expression of the liver hexokinase-IV enzyme (HK-IV, also known as Glucokinase) in the skeletal muscle of transgenic mice led to increased glucose use by the skeletal muscle (Otaegui et al., 2000). Furthermore, the overexpression of HK-IV showed to ameliorate type 2 diabetes in diabetic Zucker fatty rats (a model of type 2 diabetes and obesity) and in mice fed with a high fat diet (Jimenez-Chillaron et al., 2002; Otaegui et al., 2003). These results suggest that the expression of Gck in the skeletal muscle could become a good therapeutic approach or type 2 diabetes.

Some strategies to prevent lipid accumulation and hence, improve insulin sensitivity, are based on the concept of enhancing fatty acid β -oxidation in the skeletal muscle. For instance, the overexpression of CPT-1 in the skeletal muscle of HFD fed mice resulted in enhanced rates of fatty acid oxidation and improved high-fat diet-induced insulin resistance. These improvements were associated with a reduction in the muscular TG content along with reductions in

DAG and ceramides (Bruce et al., 2009). Knock-out animals for acetyl-CoA Carboxylase 2 (ACC2), an enzyme that catalyses the production of the allosteric CPT-1 inhibitor Malonyl-CoA, showed enhanced fat oxidation, improved insulin sensitivity and reductions in DAG and PKC activity in the skeletal muscle (Choi et al., 2007b). The specific muscular overexpression of UCP3 led to protection against high fat diet-induced obesity with improved insulin sensitivity in mouse (Choi et al., 2007a). Thus, the modulation of the oxidative capacity in the skeletal muscle represents a possible therapeutic target for type 2 diabetes mellitus. In agreement, the increase in the activities of the peroxisome proliferator-activated receptor-gamma co-activator 1 alpha (PGC1 α), a master regulator of the oxidative function and mitochondrial biogenesis in the skeletal muscle, and the peroxisome proliferator activated receptor-delta (PPAR δ), a master transcriptional regulator of the fatty acid catabolism program in the skeletal muscle, have been proposed as promising strategies to counteract type 2 diabetes and obesity (McCarty, 2005; Salvado et al., 2012).

4. GLUCOKINASE

The hexokinase-IV, or glucokinase (GCK), is one of the four mammalian hexokinases that catalyse the conversion of glucose to G-6-P by ATP. Like the other hexokinases, GCK shows the ability to phosphorylate different hexoses

including manose, fructose, D-deoxyglucose and glucose, being this last one its physiologic substrate (Printz et al., 1993). However, glucokinase shows some distinguished features form other hexokinases:

- 1) It has a lower affinity to glucose. The half saturation level (concentration of substrate at which the enzyme is 50% saturated and active, also known as $S_{0.5}$) of GCK is around 7.5 mM for glucose (Matschinsky et al., 2006). The rest of hexokinases show half saturation in a range of glucose concentrations that varies from 0.003 to 0.3 mM (Wilson, 2003).
- 2) Glucokinase shows a positive cooperative dependence with respect to glucose concentrations which is most apparent at glucose concentrations above the normal fasting level, 5 mM (Storer et al., 1976).
- 3) GCK is not inhibited by its product G-6-P.

These kinetic properties allow GCK to be extremely sensitive to variations in blood glucose levels in cells with a high capacity of glucose transport activity in the plasma membrane. Consequently, the activity of GCK is largely increased after meals, when glucose levels rise and need to get back to normal, and it is kept low during fasting periods.

4.1. Metabolic role of glucokinase

GCK is expressed in hepatocytes and β -cells and its kinetic characteristics are well adapted to the presumed roles of glucose phosphorylation in these different locations. In the liver, GCK facilitates both glycolysis and glycogen production in periods of transient hyperglycaemia, such as after meals. In β -cells, glucose-induced insulin secretion requires the stimulation of glucose metabolism. The ATP generated from glycolysis and glucose oxidation increases the cellular ATP/AMP ratio thus triggering a signalling cascade that results in insulin secretion. All of these processes depend on glucose phosphorylation by GCK as an initial step and, consequently, they make of this hexokinase a key regulator of glucose homeostasis.

GCK is also expressed in neurones from the hypothalamus and the brainstem, in the pituitary and entero-endocrine K and L cells. However, the role of GCK in these cells and the contribution to glucose homeostasis is still under discussion (Matschinsky et al., 2006).

4.2. Regulation of glucokinase activity

In the Liver, the activity of GCK is regulated by a protein-protein interaction between GCK and a protein named GCK regulatory protein (GCKR). As the glucose supplies diminish during periods of fasting, GCKR participates in the observed decrease in GCK activity by binding and inhibiting free cytoplasmic GCK. The binding of GCKR with GCK also affects the cellular localization of GCK, moving it into the nucleus where it is held in an inactive form (Shiota et al., 1999).

The association between the two proteins is ligand dependent. Ligands for GCKR are fructose-6-phosphate (F-6-P) and fructose-1-phosphate (F-1-P). During fasting, the processes of gluconeogenesis and glycogenolysis in liver increase the concentration of F-6-P. Binding of F-6-P to GCKR favours the

GCKR-GCK interaction, thus facilitating the glucose release by the liver. In the other hand, the concentration of F-1-P is increased by the ingestion of carbohydrates. F-1-P weakens the GCK-GCKR complex, allowing for the rapid export of GCK from the nuclei (Iynedjian, 2009).

GCKR expression has also been detected in small amounts in pancreatic islets, periventricular neurons, and lungs, but its physiological function in these tissues remains uncertain (Alvarez et al., 2002).

4.3 Transgenic expression of glucokinase in the skeletal muscle

Several models of *Gck* expression in the skeletal muscle have been described in the literature. *Gck* gene transfer in the skeletal muscle of rats using adenoviral vectors resulted in increased glucose uptake and utilization by the skeletal muscle (Jimenez-Chillaron et al., 1999). When the same approach was tested in muscles of diabetic Zucker fatty rats these animals showed improved insulin-sensitive glucose uptake. However, the diabetic phenotype was not completely corrected since these animals still developed systemic hyperinsulinemia and obesity (Jimenez-Chillaron et al., 2002). In our laboratory, we generated a transgenic mouse model expressing *Gck* specifically in the skeletal muscle. The presence of *Gck* increased glucose disposal by the skeletal muscle and reduced type 1 diabetic hyperglycaemia (Otaegui et al., 2000). When these animals were challenged with a high fat diet they did not develop obesity and remained insulin sensitive, showing only a mild increase in circulating insulin levels. Furthermore these animals showed increased expression of *Ucp-3* in the skeletal muscle, providing an explanation for their reduced body weight gain (Otaegui et al., 2003). Thus, these results suggest that the expression of *Gck* in the skeletal muscle could become a good therapeutic approach for obesity and type 2 diabetes.

5. ROLE OF THE PEROXISOME PROLIFERATOR-ACTIVATED RECEPTOR-GAMMA COACTIVATOR 1-ALPHA IN THE SKELETAL MUSCLE

The peroxisome proliferator-activated receptor-gamma coactivator 1 alpha (PGC1 α) is a transcriptional coactivator that was first described in the brown adipose tissue (Puigserver et al., 1998). As a coactivator, PGC1 α controls gene transcription by binding and regulating the activity of a large amount of transcription factors in different tissues. Thus, PGC1 α is involved in the transcriptional regulation of various biological programs. Among tissues, PGC1 α is highly expressed in tissues with a high oxidative capacity and elevated energy demands such as the brown adipose tissue (BAT), Heart and the skeletal muscle. However, PGC1 α is also enriched in liver, brain and kidney (Finck et al., 2006). In most of these tissues, the activity of PGC1 α controls a whole complete array of biologic processes directed to increase the oxidative capacity when needed. For instance, fasting activates the expression of PGC1 α in heart where it promotes the transcription of genes related to fatty acid oxidation and respiratory function (Huss et al., 2004). In brown adipose tissue, PGC1 α expression is induced by cold exposure, where it activates the transcription of UCP1 and other key mitochondrial enzymes of the respiratory chain necessary for adaptive thermogenesis (Puigserver et al., 1998). PGC1 α gene expression is activated in liver by fasting, where it regulates gluconeogenesis and fatty acid oxidation by activating the expression of some of its key genes (Koo et al., 2004; Yoon et al., 2001). Additionally, PGC1 α has

been shown to be a master regulator of mitochondrial biogenesis in mammals (Scarpulla, 2008).

In the skeletal muscle, PGC1 α expression is strongly induced by exercise (Baar et al., 2002; Goto et al., 2000). These observations, combined with the ability of PGC1 α to induce mitochondrial biogenesis have led to the notion that PGC1 α mediates many of the genomic adaptations of the skeletal muscle to exercise. Specifically, endurance exercise leads to fibre type transformation (Bassel-Duby et al., 2006), angiogenesis (Chinsomboon et al., 2009), increases in enzymes related to fatty acid oxidation (Mole et al., 1971), increases in enzymes of the respiratory chain (Garcia-Roves et al., 2006), mitochondrial biogenesis and other adaptive changes along with improved insulin sensitivity (Thyfault et al., 2007). All of these adaptations are similar to those induced in animal and cellular genetic models of altered PGC1 α expression, providing evidence for the importance of this protein in the muscular oxidative metabolic adaptations to exercise (Lira et al., 2010).

5.1. Regulation of PGC1 α transcription in the skeletal muscle

PGC1 α gene transcription is activated by exercise in the skeletal muscle. However the molecular mechanisms leading to this up-regulation are currently under discussion. Contractile activity induces the hydrolysis of ATP thus increasing the concentration of cyclic AMP (cAMP) and a decrease in the ATP/AMP ratio. This situation leads to the activation of the AMP-activated protein Kinase (AMPK), a protein that increases glucose uptake and lipid oxidation in order to restore ATP (Long et al., 2006). The activation of AMPK by chemical agonists increases the expression of PGC1 α in the skeletal muscle (Suwa et al., 2006; Suwa et al., 2003). Furthermore, transgenic animals expressing a dominant negative form of AMPK are unable to up-regulate PGC1 α .

in response to metabolic stress (Zong et al., 2002) providing evidence that PGC1 α expression is influenced by AMPK activity.

Increased contractile activity translates into a sustained increase in intracellular calcium (Ca) concentration, which activates the calcium-dependent phosphatase calcineurin (CaN) and the Ca-calmodulin dependent kinase (CaMK). In experiments using muscular cells, the activation of CaN increases the expression of PGC1 α by activating the myocyte enhancer factor-2c (MEF2c), a transcription factor that binds to and activates the PGC1 α promoter (Handschin et al., 2003). Meanwhile, CaMKIV activates the cAMP response element-binding protein (CREB), a transcription factor that binds to the PGC1 α promoter thus starting transcription (Handschin et al., 2003). These in vitro models are consistent with the increased expression of PGC1 α observed in transgenic animals overexpressing a constitutive active form of either CaN (Ryder et al., 2003) or CaMKIV (Wu et al., 2002) in the skeletal muscle.

5.2. PGC1 α and Skeletal Muscle Fibre type conversion

It is now well established that PGC1 α is an important regulator for type I fibre specification. In accordance, the expression of PGC1 α is enriched in type I oxidative fibres. Transgenic expression of PGC1 α in fast muscle fibres leads to the expression of proteins involved in mitochondrial oxidation and other proteins characteristic of slow muscle fibres, such as troponin I and myoglobin (Lin et al., 2002). Furthermore, these muscles presented an increased number of mitochondria (Choi et al., 2008). Accordingly, muscles isolated from these transgenic animals showed an increased resistance to electrically stimulated fatigue, a characteristic of a more oxidative type I based muscle (Lin et al., 2002). Thus, PGC1 α might mediate in the fast to slow fibre type switch adaptations of the skeletal muscle to endurance exercise.

5.3. PGC1 α , respiration and mitochondrial biogenesis

PGC1 α is considered to be a master regulator of the mitochondrial biogenesis and function. The expression of this coactivator increases the mRNA levels and the activity of the nuclear respiratory factors 1 and 2 (NRF1-2). These are transcription factors linked to the transcriptional control of a wide number of genes related to mitochondrial respiration and biogenesis (Kelly et al., 2004). Furthermore, NRF-1 is coactivated by PGC1 α thus starting the transcription of the mitochondrial transcription factor A (Tfam), a key protein in the duplication of the mitochondrial genome (Wu et al., 1999). Other proteins controlled by the coactivation of the NRFs by PGC1 α include various important proteins in the oxidative phosphorylation pathway, like the cytochrome c, various subunits of the respiratory complexes and subunits of the ATP synthase (Wu et al., 1999). Various animal models of altered PGC1 α expression provide evidence for the importance of this coactivator in mitochondrial biogenesis and function. Transgenic animals overexpressing PGC1 α in heart and skeletal muscle have consistently shown an increased number of mitochondria and increased expression of genes related to mitochondrial biogenesis and oxidative phosphorylation. (Choi et al., 2008; Lehman et al., 2000; Lin et al., 2002). On the other hand, total Knock-out (KO) mice for PGC1 α showed reduced mitochondrial density along with decreased respiratory function in the skeletal muscle (Leone et al., 2005) and muscle-specific PGC1 α KO showed reduced expression of genes related to oxidative phosphorylation along with altered mitochondrial function (Handschin et al., 2007).

5.4. PGC1 α and lipid metabolism

Transgenic animals overexpressing PGC1 α in the skeletal muscle show increased rates of fatty acid oxidation along with increased expression of genes related to lipid metabolism. Among them, the overexpression of PGC1 α induced the expression of β -oxidation genes like CPT-1, CPT-2 and the medium-chain acyl-coenzyme A dehydrogenase (MCAD) and also genes related to fatty acid uptake like CD36 (Choi et al., 2008). The regulation of lipid metabolism by PGC1 α in the skeletal muscle is thought to occur in part through the coactivation of the peroxisome proliferator-activated receptors (PPARs). These are members of a nuclear receptor superfamily that function as fatty acid-activated transcription factors. The PPAR δ isoform is constitutively expressed and it might be the most important form at regulating the lipid catabolism in the skeletal muscle (Evans et al., 2004). Importantly, the effects of PPAR δ on lipid catabolism would be dependent on PGC1 α coactivation (Kleiner et al., 2009). Thus, PGC1 α has the capacity to increase lipid catabolism.

5.5. PGC1 α and muscular glucose uptake

One of the adaptations of the skeletal muscle during exercise is the rapid increase in the expression of GLUT4 (Ren et al., 1994). The fact that PGC1 α is also rapidly induced by exercise, led to the notion that PGC1 α would directly regulate the expression of GLUT4 in the skeletal muscle. Accordingly, the overexpression of PGC1 α in muscle cells leads to the expression of GLUT4 along with increased rates of glucose transport (Michael et al., 2001). This was also the case when PGC1 α was modestly overexpressed in skeletal muscles of adult mice (Benton et al., 2010; Benton et al., 2008). The control of PGC1 α in the GLUT4 gene transcription seems to be mediated by MEF2 coactivation (Michael et al., 2001). Thus, these studies indicate that PGC1 α may have the

capacity to increase glucose uptake in the skeletal muscle in vivo by activating GLUT4 gene transcription.

5.6. PGC1 α and type 2 diabetes

Given the relation between the deregulation in fatty acid metabolism, mitochondrial dysfunction and insulin resistance in the skeletal muscle of type 2 diabetic patients and the importance of PGC1 α at inducing mitochondrial biogenesis, oxidative function and lipid catabolism in the skeletal muscle, it has been suggested that PGC1 α may have a role in the pathology of type 2 diabetes. In agreement, PGC1 α expression along with the expression of multiple of its target genes, was found to be decreased in muscles of type 2 diabetic patients as well as in subjects at high risk for T2DM (Mootha et al., 2003; Patti et al., 2003). Similarly, PGC1 α expression in the skeletal muscle has been found to be decreased in several animal models of insulin resistance and type 2 diabetes (Bonnard et al., 2008; Jove et al., 2004). The Gly482Ser missense variation in the PGC1 α gene has been associated with an increased risk of developing type 2 diabetes and with reduced insulin sensitivity in humans (Fanelli et al., 2005; Hara et al., 2002). Furthermore, the expression of PGC1 α in the skeletal muscle diminishes as insulin levels increase due to age-related insulin resistance (Ling et al., 2004). Thus, it has been suggested that a decrease in PGC1 α in the skeletal muscle could lead to a reduced oxidative capacity. As a consequence, triglyceride levels would accumulate in the skeletal muscle along with increased levels of circulating fatty acids leading to insulin resistance and finally to type 2 diabetes (Patti et al., 2003).

6. ROLE OF THE PEROXISOME PROLIFERATOR-ACTIVATED RECEPTOR-DELTA IN THE SKELETAL MUSCLE

PPARs are a family of nuclear receptor proteins that act as ligand-inducible transcription factors. This family of nuclear receptors is activated by free fatty acids and their derivatives, and thus serve as lipid sensors with the ability to turn on the transcription of genes related to lipid metabolism, storage, and transport. They are found forming heterodimers with the retinoid X receptors and bound to consensus DNA sites, named peroxisome proliferator

response elements (PPRE), located in the promoters of their target genes. When bound to the ligand (FFA), PPARs suffer a conformational change that results in the release of repressors in exchange for coactivators. Thus, they recruit the transcriptional machinery resulting in enhanced target gene expression. Importantly, PGC1 α coactivates every member of these family (Berger et al., 2002).

To date, three members of the family have been identified, PPAR α , PPAR γ and PPAR δ (also known as PPAR β). PPAR α was the first PPAR to be described. It is expressed predominantly in liver, where it has a key role at promoting fatty acid oxidation to generate ketone bodies in response to fasting (Kersten et al., 1999). However it is also expressed at significant levels in heart, kidney, small intestine and, to a lesser extent, the skeletal muscle where it also controls fatty acid catabolism (Rakhshandehroo et al., 2010). PPAR α -selective agonists are used to treat hypertriglyceridemia (Staels et al., 2008).

PPAR γ is expressed predominantly in adipose tissue, but also in macrophages, muscle and liver. It has a key role in the adipose tissue where it is a master regulator in the formation of new adipocytes. The expression of PPAR γ in the adipocyte activates the expression of genes related to fatty acid uptake and storage. This receptor is the molecular target of the antidiabetic drugs TZDs and therefore it has a very important role in insulin sensitivity (Feige et al., 2006).

Meanwhile, PPAR δ is expressed throughout all the body with very high levels in small intestine, liver and Colon (Girroir et al., 2008). *In vitro* and *in vivo*

studies using specific agonists and tissue-specific overexpression or knockout mouse models have demonstrated the involvement of this receptor in different biological activities. For instance, PPAR δ has been related to lipoprotein metabolism (Oliver et al., 2001), inflammation (Lee et al., 2003), incretin secretion (Daoudi et al., 2011), neuronal differentiation (Cimini et al., 2003), wound healing and keratinocyte differentiation (Michalik et al., 2001). Moreover, PPAR δ has been shown to be a key regulator in the transcriptional program of fatty acid oxidation and mitochondrial uncoupling in heart (Cheng et al., 2004a; Cheng et al., 2004b), adipose tissue (Wang et al., 2003b) and skeletal muscle (Wang et al., 2004). Due to its role in lipid metabolism, PPAR δ has been suggested as a new target against obesity and type 2 diabetes.

In the skeletal muscle, PPAR δ is the most abundant PPAR isoform. It is expressed at levels 10-fold and 50-fold greater than PPAR α and PPAR γ , respectively. Consequently, despite PPAR δ and PPAR α share some redundant functions in this tissue, PPAR δ is considered to be the prevalent PPAR isoform (Muoio et al., 2002). In this tissue, PPAR δ has been related to fibre type switching, mitochondrial function, lipid metabolism and glucose uptake (Ehrenborg et al., 2009). Much of these actions resemble those observed by PGC1 α in the skeletal muscle thus suggesting that they might be mediated by PGC1 α coactivation of PPAR δ . Accordingly, PGC1 α and PPAR δ strongly interact *in vivo* and *in vitro* (Wang et al., 2003b)

6.1. PPAR δ transcription in the skeletal muscle

PPAR δ expression in the skeletal muscle is increased by a different number of physiologic stimuli. Short-term exercise (Mahoney et al., 2005) and endurance training (Luquet et al., 2003) have shown to produce a rapid

increase in PPAR δ expression in this tissue. Accordingly, mice overexpressing a constitutively active form of CaN in the skeletal muscle showed an increased expression of PPAR δ (Long et al., 2007). Fasting has also shown to lead to a rapid up-regulation of PPAR δ mRNA in the skeletal muscle (Holst et al., 2003). Despite exercise and fasting elevate the levels of circulating FFA, there is no evidence that FFA directly increase the expression of this receptor per se (Ehrenborg et al., 2009). However, exercise and fasting also up-regulate PGC1 α expression in the skeletal muscle, thus suggesting that this coactivator may have an active role at regulating the transcription of PPAR δ . Accordingly, PPAR δ (like PGC1 α) is also enriched in type I fibres (Wang et al., 2004).

6.2. PPAR δ and fibre type conversion

Several animal models of altered PPAR δ expression in the skeletal muscle have provided evidence for the importance of this receptor as a modulator in the development of oxidative type I fibres. Transgenic mice with targeted skeletal muscle overexpression of either the wild type (Luquet et al., 2003) or an activated form (Wang et al., 2004) of PPAR δ had an increased proportion of type I muscle fibres. Accordingly, these animals presented an increased resistance to fatigue when placed on a treadmill, being able to run twice the distance of wild-type mice (Wang et al., 2004). Meanwhile, mice with a selected ablation of PPAR δ in the skeletal muscle showed less type I skeletal muscle fibres. These animals also ran a 30% less the distance of a wild-type mice, in accordance to a type II fibre based skeletal muscle (Schuler et al., 2006). Thus, these studies suggest that PPAR δ is a key protein controlling the development of type I oxidative fibres.

6.3. PPAR δ , lipid metabolism and oxidation

In the skeletal muscle, the activation of PPAR δ increases the expression of genes related to fatty acid metabolism. Accordingly, skeletal muscle cells stimulated with specific PPAR δ agonists *in vitro* show a strong expression of genes related to fatty acid catabolism like CPT1, long-chain acyl-coenzyme A dehydrogenase (LCAD) and of genes related to fatty acid uptake like CD36, resulting in increased rates of fatty acid oxidation (Holst et al., 2003; Muoio et al., 2002; Wang et al., 2003b). Similarly, the overexpression of an activated form of PPAR δ in the skeletal muscle of transgenic mice lead to similar muscular increases of CPT1. These animals were protected against HFD-induced obesity and the accumulation of triglycerides in the skeletal muscle was reduced suggesting enhanced muscular fatty acid oxidation. These increases in fatty acid oxidation were accompanied with an enhanced expression of genes related to oxidative phosphorylation and mitochondrial uncoupling (Wang et al., 2004). A phenotype opposite to that of PPAR δ transgenic mice was revealed in the skeletal muscle specific PPAR δ knock-out mice. Deletion of PPAR δ decreased the expression of many genes for fatty acid β -oxidation and mitochondrial respiration leading to an increased body weight gain (Schuler et al., 2006). Thus, PPAR δ has the ability to activate a complete transcriptional program directed to increase fatty acid oxidation.

6.4. PPAR δ and type 2 diabetes

Given the ability of PPAR δ agonists to increase fatty acid catabolism and oxidation in the skeletal muscle, there has been an increasing interest in testing these compounds as drugs to ameliorate insulin resistance and type 2 diabetes. The specific PPAR δ agonist, GW501516, has been shown to be effective at ameliorating the phenotype of various type 2 diabetic animal models. HFD-fed mice treated with this compound showed reduced body weight gain as a result

of enhanced fatty acid utilization. Accordingly, these animals presented reduced lipid accumulation in liver and skeletal muscle along with reduced insulin levels and improvements in insulin sensitivity (Tanaka et al., 2003). Similarly, the administration of GW501516 in the genetically predisposed obese *ob/ob* mice improved insulin resistance (Tanaka et al., 2003). PPAR δ agonism has also shown to decrease insulin levels in spontaneously obese, insulin resistant middle-aged rhesus monkeys (Oliver et al., 2001) and in obese humans (Riserus et al., 2008). Many of the improvements in metabolic profiles noted in response to PPAR δ agonists are mirrored in mice with transgenic overexpression of PPAR δ in skeletal muscle (Wang et al., 2004) suggesting that much of these effects are a consequence of PPAR δ activation in the skeletal muscle. All together, these studies indicate that the modulation of PPAR δ in the skeletal muscle is an attractive strategy against type 2 diabetes.

7. GENE THERAPY

Although current treatments for type 2 diabetes have greatly improved the patient's quality of life, all existing therapies still present drawbacks and secondary side effects. Additionally, the mechanisms leading to the pathogenesis of the disease are still largely unknown. Thus, a better understanding of the disease and its mechanisms is mandatory in order to find new therapeutic targets to counteract type 2 diabetes. Due to its importance in metabolism and type 2 diabetes, the modulation of the oxidative function in the skeletal muscle provides new therapeutic possibilities to counteract the disease. In this regard, the transfer of candidate genes to the skeletal muscle *in vivo* may offer great potential in order to find new possible treatments for type 2 diabetes.

7.1. Introduction to gene therapy

The basic concept of gene therapy can be defined as the introduction, using a vector, of nucleic acids into target cells with the intention of altering gene expression to prevent, halt, or reverse a pathological process (Kay, 2011). Gene addition, gene alteration and gene knockdown are the three basic strategies by which gene therapy can alter gene expression. Gene addition consists on the introduction of foreign genetic material to provide therapeutic benefit by increasing the expression of an endogenous gene or to supply a protein that is missing (Kay, 2011). Gene alteration is based on the use of DNA recombination technologies and zinc fingers to alter genomic sequences to correct or create a mutation (Kay, 2011; Urnov et al., 2010). Finally, interference RNA has provided gene therapy with a tool to efficiently knockdown the expression of endogenous genes in order to provide

therapeutic benefit (Davidson et al., 2011). Initially gene therapy was established to treat patients with hereditary diseases caused by single gene defects, such as muscular dystrophy or hemophilia. However, at present, many gene therapy efforts are also focused on curing polygenic or non-inherited diseases with high prevalence, such as cancer, cardiovascular diseases and hepatitis C (Kay, 2011).

Two types of approaches in gene therapy can be distinguished: *in vivo* gene therapy is based on the introduction of a therapeutic gene into a vector which then is administered directly to the patient. This vector will transfer the gene of interest in the target tissue to produce the therapeutic protein. Meanwhile, *ex vivo* gene therapy, is based on the transfer of the vector carrying the therapeutic gene into cultured cells from the patient. Subsequently, these genetically engineered cells are reintroduced to the patient where they now express the therapeutic protein.

An ideal vector should be able to efficiently transduce target cells without activating undesirable immune response either against itself or the therapeutic gene. Over recent years, a large number of vectors have been developed, each one with its own characteristics. However, a universal vector to treat any disease does not exist. The choice of one or another depends on factors such as the target tissue to manipulate or whether the disease may require short-term or chronic treatment. Two large groups of vectors can be distinguished according to their origin: **viral vectors** and **non-viral vectors** (Verma et al., 2005).

7.2. Non-viral Vectors

As its name implies, non-viral vectors are any kind of vector that is not derived from a virus. In most applications, the therapeutic gene is part of a larger structure of double-stranded DNA called a plasmid. In its simplest form, non-viral gene therapy consists in the injection of plasmids directly into tissues, where they will be captured by target cells, although with very low efficiency. For this reason, different physical and chemical methods that allow an increased delivery efficiency of the nucleic acid have been developed. Physical methods increase the cell membrane permeability to plasmids by using electrical pulses, which is known as electrotransference, or by applying sound waves, which is known as sonoporation. With regard to chemical methods, plasmids can be covered with cationic liposomes or polymers to form organized structures called lipoplexes and polyplexes, respectively. In both cases, these structures protect and stabilize the nucleic acid and increase its uptake by the cell. The use of non-viral vectors has certain advantages over viral vectors. For example, there is no limit in the size of the therapeutic gene to transfer and also, no immune responses are triggered against the vector, so it can be readministered. However, the *in vivo* transfer efficiency achieved is usually lower than that of viral vectors (Kay, 2011; Verma et al., 2005).

7.3. Viral Vectors

Viral vectors derive from viruses. Viruses are infectious agents that have evolved to be highly efficient at transferring their genetic material into host cells in order to produce new viral particles. Gene therapy has taken advantage of this feature of the virus to introduce therapeutic genes to target cells. To this end, much or all of the viral genes are replaced by the therapeutic gene, turning the virus into a viral vector. These viral vectors retain the original infective capacity of the virus, mediating the introduction of the genetic material into the cell nucleus (process known as transduction) but are not able

to produce new virions. Additionally, viral vectors are incapable of causing disease as the viral pathogenic genes have been eliminated (Kay et al., 2001).

Viral Vectors currently available in gene therapy are based on the biology of different virus with different inherent features. Consequently, the choice of one or another will depend on the type of disorder. Table 2 summarizes the different properties of the most commonly used vectors in gene therapy.

Vector	Advantages	Disvantages
Retrovirus	<ul style="list-style-type: none"> • Stable expression • Production in High titers • Low immunogenicity 	<ul style="list-style-type: none"> • Random integration in the host genome • Limited encapsidation capacity (8 Kb) • Infects only diving cells
Lentivirus	<ul style="list-style-type: none"> • Infects dividing and quiescent cells • Stable expression for long periods of time • Low immunogenicity 	<ul style="list-style-type: none"> • Random integration into the host genome • Limited encapsidation capacity (8 Kb) • Production in Low titers • More studies needed to asses lack of Pathogenicity
Adenovirus	<ul style="list-style-type: none"> • Infects dividing and quiescent cells • Long encapsidation capacity (36 Kb) • Production in high titers (First generation) • Remains episomal • High transduction efficiency 	<ul style="list-style-type: none"> • High immunogenicity (first and second generation) • Difficult to produce • Toxicity when high sistemic doses are used • Transitory expression
Adenoassociated Virus (AAV)	<ul style="list-style-type: none"> • Large number of serotypes with tropism variety • Infects dividing and quiescent cells • Non pathogenic • Production in high titers 	<ul style="list-style-type: none"> • Low encapsidation capacity (4.7 kb)

Table 2. Summary of the characteristics of the viral vectors used in gene therapy (Ayuso et al., 2010b).

7.4. Adeno-associated vectors (AAV)

Adeno-associated vectors derive from the human adeno-associated virus. These viruses are non-pathogenic human parvovirus that normally require

a helper virus, such as an adenovirus or herpesvirus, to mediate a productive infection. There are not known associated diseases with AAV infections, making it an ideal candidate for gene therapy. In this regard, most strategies for treating human genetic diseases by means of *in vivo* gene therapy are exploiting AAV and the most promising results to date have been achieved using these vectors (Mingozzi et al., 2011).

7.4.1. Biology of wild-type adeno-associated viruses

The adeno-associated virus is a small, icosahedral and non-enveloped virus. To date, 14 serotypes have been identified based on the receptor they use for cell entry and in the epitopes recognized by the immune system (Buning et al., 2008). All serotypes share a similar structure and genome organization. The AAV capsid has approximately 22 nm and encapsidates a linear single-stranded DNA genome of about 4.7 kb. Flanking both ends of the genome, in the termini, there exist two 145 nucleotide-long inverted terminal repeat sequences (ITR) containing all the *cis*-acting functions required for genome replication and packaging. The AAV genome encodes two large open reading frames (ORF), one encoding replication proteins (Rep) and the other encoding for capsid proteins (Cap). A total of four Rep proteins (Rep 78, Rep 68, Rep 52 and Rep 48) and three Cap proteins (VP1, VP2 and VP3) are produced through alternative splicing and the use of different promoters within the AAV genome (Figure 8) (Coura Rdos et al., 2007; Kay et al., 2001).

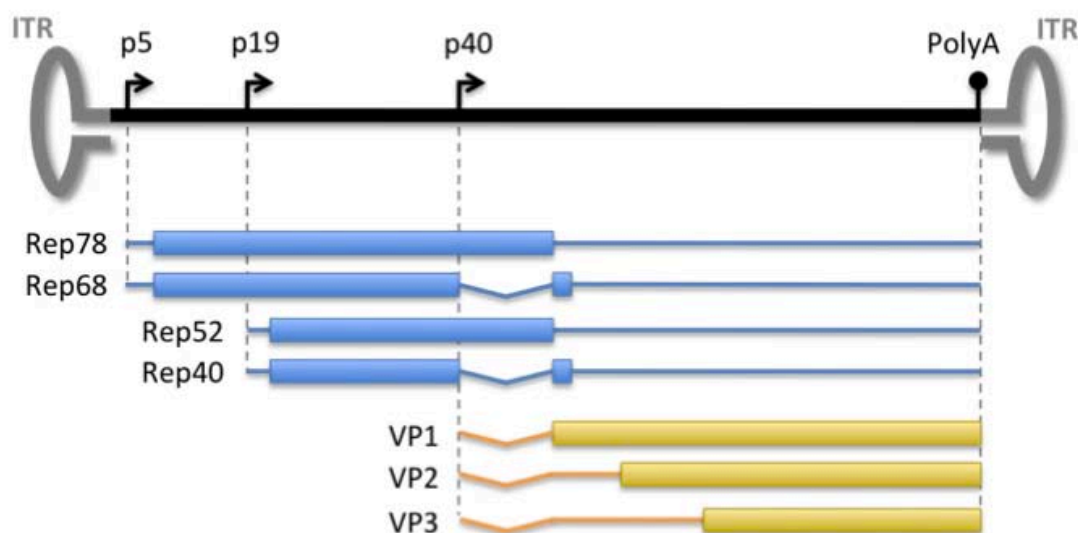


Figure 8. Schematic representation of the AAV serotype 2 genome. AAV genome is flanked by two inverted terminal repeat (ITR) and the three arrows indicate each of the three promoters at positions 5, 19 and 40. Regulatory proteins (Rep78, Rep68, Rep52 and Rep40) are encoded by the *rep* gene. Structural proteins are encoded by the *cap* gene. There are three capsid proteins VP1, VP2, VP3 transcriptionally regulated by p40 promoter. All AAV transcripts share the same polyadenylation signal (polyA). (Ayuso et al., 2010a)

7.4.2. Recombinant adeno-associated viral vectors

AAV based vectors can be produced in the laboratory by replacing the *rep* and *cap* ORFs by the therapeutic gene flanked by the original viral ITRs to retain the packaging ability. As a consequence, the resulting vectors lack viral genes preventing transduced cells from being recognized and killed by the immune system.

The most common method to produce AAVs in the laboratory is the triple transfection protocol (Figure 9). The expression cassette is cloned into a plasmid containing the AAV ITRs (vector genome), whereas *Rep* and *Cap* proteins are provided by a second plasmid (AAV Helper). Adenoviral Helper functions are provided by a third plasmid (Ad Helper) encoding the adenoviral helper genes virus-associated (VA) RNA, E2A and E4. The three plasmids are transfected into 293HEK cells expressing the E1 adenoviral gene, necessary for AAV replication. After the transcription and translation of the Rep and VP proteins, the transgene in the vector genome plasmid is replicated along with the flanking ITRs and encapsidated in the pre-assembled capsids (Ayuso et al., 2010a). Cells are then lysed and AAV vectors are purified by density gradient centrifugation using cesium chloride (CsCl) or iodixanol, and/or by column chromatography. After purification, the vector yield contains empty capsids

that dilute the total amount of effective vector particles resulting in reduced transgene expression and vector transduction efficiency. Recently, our laboratory developed a method based on polyethylene glycol (PEG) and CsCl-based purification that dramatically reduces empty capsids and protein impurities which ultimately results in higher transduction *in vivo* (Ayuso et al., 2010b).

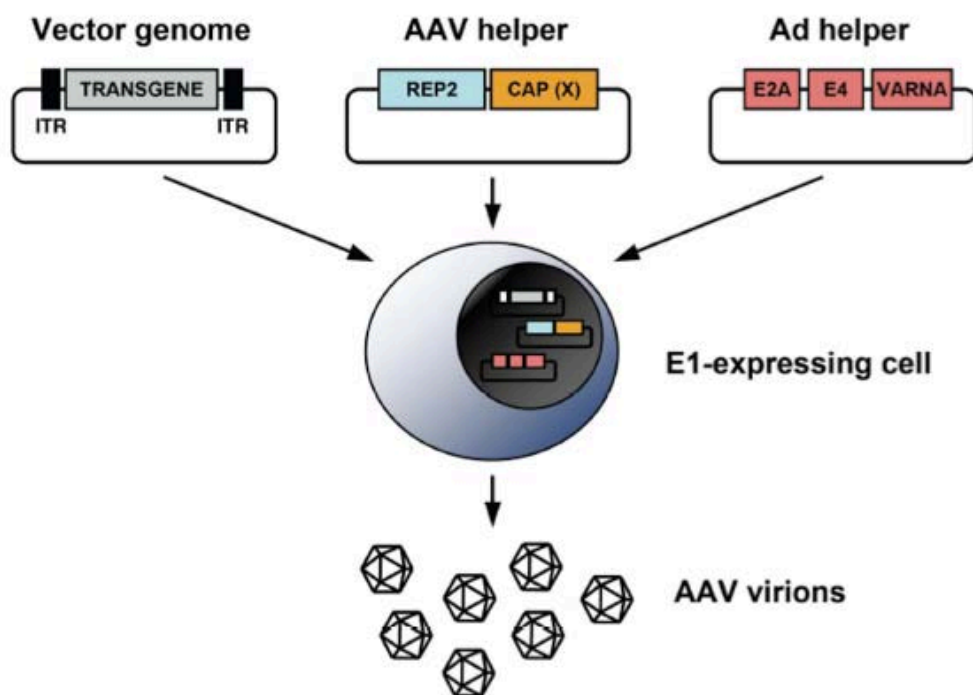


Figure 9. Triple transfection method for recombinant AAV production. For the production of rAAV, both viral ORFs are replaced by the transgene. For packaging, *rep* and *cap* are provided in *trans* on a helper plasmid. Helper virus functions are provided by transfection of a third plasmid coding for adenoviral genes needed for AAV production. Vector particles are harvested from the cells and are purified by density gradient and/or chromatography

AAV vectors have emerged as a very attractive tool for gene transfer, since they can mediate highly efficient cell entry and produce long-term expression of the desired therapeutic gene with both low toxicity and low immunogenicity. These vectors can transfect both dividing and non-dividing cells and the AAV genome remains episomal in the cell nucleus. The natural tropism of any viral vector, including recombinant AAVs, is a fundamental limitation to efficient gene transfer. In this regard different AAV serotypes (AAV1, AAV2, AAV5...) also have different tropism (Buning et al., 2008). Among them, the AAV1 serotype is considered to be the best serotype to transduce the skeletal muscle.

Thus, the use of AAV1 vectors to transfer target genes to the skeletal muscle might represent a good strategy to find new potential approaches to treat type 2 diabetes and obesity.

Treatments for type 2 diabetes are only short-term effective and most of them still present drawbacks and undesirable secondary effects. Thus, new effective strategies must be developed to treat this disease. Type 2 diabetes is highly related to obesity. The accumulation of triglycerides in peripheral tissues is linked to the appearance of insulin resistance and, consequently, hyperglycemia. The skeletal muscle has a huge capacity of using both glucose and fatty acids as an energy source. Thus, the transfer of genes to increase the oxidative capacity or the glucose uptake of the skeletal muscle may represent a new potential strategy to treat type 2 diabetes.

The *overall aim* of this study was *to find a new gene therapy approach for type 2 diabetes using AAV1-mediated transfer of candidate genes into the skeletal muscle of high fat diet fed mice.*

This general aim was subdivided into three specific aims:

1. To study the metabolic effects of the muscular overexpression of Glucokinase.
2. To study the metabolic effects of the muscular overexpression of *Pgc1 α* alone or in combination with Glucokinase.
3. To study the metabolic effects of the muscular overexpression of *Ppar δ* alone or in combination with *Pgc1 α* .

1.1. Transduction of the skeletal muscle with AAV vectors

The skeletal muscle is a good target tissue for genetic manipulation since it is easily accessible. Consequently, there has been extensive research at identifying efficient vectors to transduce it. Adeno-associated serotype 1 viral vectors (AAV1) are very efficient at transducing the mouse skeletal muscle after an intramuscular injection. Moreover, these are safe vectors and allow long-term expression of the gene of interest in mice (Arruda et al., 2004; Mas et al., 2006; Riviere et al., 2006). We can obtain high expression levels of exogenous genes in the skeletal muscle, such as the green fluorescence protein (GFP) (Figure 1).

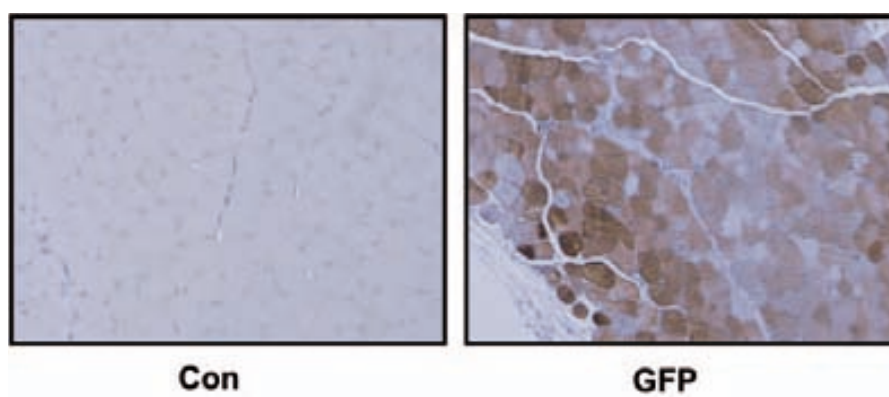


Figure 1. Skeletal muscle transduction after intramuscular administration of AAV1-GFP vectors. GFP immunostaining of *tibialis anterior* muscle sections of animals injected with Saline (Con) or with 1×10^{10} viral genomes (vg) of AAV1-GFP (GFP) into the muscle two months after administration.

In the present we took advantage of our expertise on the use of AAV1 vectors to transfer genes into the skeletal muscle to test potential targets towards developing new gene therapy approaches to counteract insulin resistance and obesity.

1.2. Experimental design

The ability to modulate the development of insulin resistance and obesity of the muscular overexpression of *Gck*, *Pgc1 α* , *Ppar δ* genes and combinations between them was evaluated in this study. To this aim, an AAV1 vector carrying each gene was designed and produced in our laboratory. Two-month old C57Bl6 mice received intramuscular injections of either the corresponding AAV1 vector or a saline solution (Control). Each animal was injected into the *Gastrocnemius*, *Quadriceps*, and *Tibialis anterior* muscles of both legs. After administration, animals were given one-week to recover from the intervention and then they were fed a high-fat diet (HFD) in order to induce insulin resistance and obesity. At the same time, a group of control animals was placed under a regular (chow) diet to be used as a reference for normal parameters. During the first 9 weeks, the evolution of their body weight and their food intake were measured weekly. At week 10, in order to study the *in vivo* glucose homeostasis, glucose measurements and an intra-peritoneal insulin tolerance test (ITT) were performed in conscious, fed animals. To let mice recover from the ITT test, no further analysis was performed for two weeks, at which time animals were euthanized for tissue sampling and further evaluation of metabolic parameters (Figure 2).

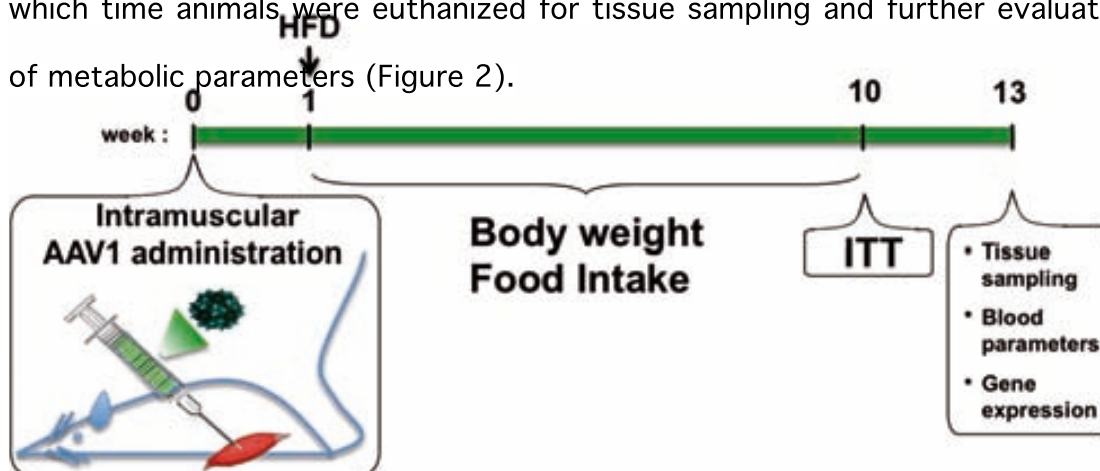


Figure 2. Experimental design. ITT: Insulin tolerance test, HFD: High-fat diet

As mentioned above, in this study the muscular overexpression of three key genes in the control of glucose homeostasis and combinations between them were tested. In a first set of experiments, an AAV1 vector was used to express *Gck* in the skeletal muscle. In a second set, an AAV1 vector was used to overexpress *Pgc1 α* alone, or in combination with *Gck* in the same skeletal muscle. In the last set of experiments, AAV1 vectors were used to overexpress *Ppar δ* alone or in combination with an overexpression of *Pgc1 α* in the same skeletal muscle (Table 1).

Set of Experiments	Gene overexpressed
<i>First</i>	<i>Gck</i>
<i>Second</i>	a) <i>Pgc1α</i> b) <i>Gck + Pgc1α</i>
<i>Third</i>	a) <i>Pparδ</i> b) <i>Pparδ + Pgc1α</i>

Table 1. Genes and combinations of genes overexpressed in each set of experiments.

Previous studies in our laboratory demonstrated that the expression of the Glucokinase (*Gck*) in the skeletal muscle of transgenic mice conferred preventive benefits against high fat diet-related diabetogenic complications (Otaegui et al., 2003). These animals did not become obese and remained insulin sensitive when challenged with a HFD. Moreover, *Gck*-expressing mice showed increased energy expenditure, which was probably responsible for their reduced body weight gain during the diet (Otaegui et al., 2003). Thus, based on the preventive aspects of *Gck* overexpression observed in transgenic animals, we wondered whether *Gck* would be a good candidate gene to deliver to the skeletal muscle as a first step towards developing a gene therapy approach to treat T2DM and obesity. To this end, in the first part of this study we examined the metabolic effects of overexpressing *Gck* in skeletal muscle of mice fed a high fat diet.

2.1. Design of an AAV1 vector carrying the *Gck* gene

To transfer *Gck* into the skeletal muscle of adult mice, an AAV1 vector carrying this gene (AAV*Gck*) was designed. To this aim, the cDNA sequence of the Rat *Gck* was cloned into the pGG2 plasmid (pGG2-*Gck*) upstream of the polyadenylation signal (Poly A) and under the transcriptional control of the cytomegalovirus (CMV) promoter (Figure 3). This promoter is ubiquitously expressed in murine tissues and has been extensively used to control the expression of exogenous genes in skeletal muscle (Callejas et al., 2013; Mas et al., 2006). The pGG2-*Gck* was then used to produce the AAV1 vectors, as stated in Material and Methods. Two different doses of the AAV1 vector were

used in two separate experiments, 6×10^9 vector genomes per animal (vg/animal) and 1.8×10^{10} vg/animal.

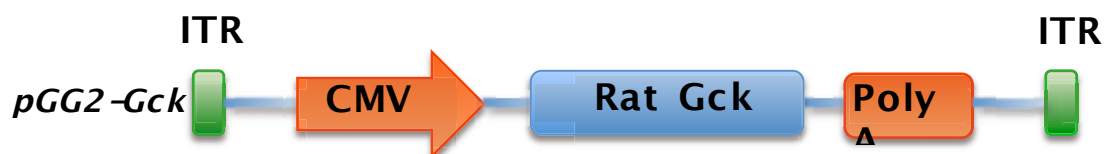


Figure 3. Schematic representation of the construct used to produce the AAVGck vector. CMV: cytomegalovirus promoter; poly A: Simian Virus 40 Polyadenylation signal; ITR: Inverted terminal repeat; Rat Gck: Rat Glucokinase.

2.2. Metabolic effects of the *Gck* expression in the skeletal muscle of high-fat fed mice

With the aim of characterising the metabolic effects of expressing *Gck* during a high fat diet, a total dose of 6×10^9 vg/animal of AAVGck was injected in the skeletal muscles of C57BL6 mice. After the administration, animals were placed under a high fat diet as indicated in the experimental design (Figure 2).

2.2.1. Glucokinase expression in the skeletal muscle

The muscular *Gck* expression in treated animals was analysed at week 13 after the administration. To this aim, total RNA was extracted from the skeletal muscle and analysed by Northern blot with a specific probe against *Gck*. Glucokinase expression was clearly detected in AAVGck injected muscles. As expected, control animals did not show any expression of glucokinase since this gene is not endogenously expressed in the skeletal muscle (Figure 4). These results indicate that the intramuscular injection of AAVGck allowed for a sustained glucokinase expression during the entire experiment.

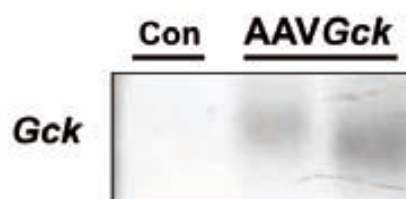


Figure 4. Glucokinase expression in the skeletal muscle of AAVGck injected animals. Total RNA from AAVGck (6×10^9 vg) or saline (Con) treated animals was extracted from Tibialis Cranialis at week 13. The RNA obtained was analysed by Northern blot. A representative blot hybridised with a *Gck* specific probe is shown.

2.2.2. Body weight gain and adiposity

Mice fed with a HFD progressively gain weight faster than animals fed a regular chow diet (Winzell et al., 2004). Ten weeks after the initiation of the experiment, body weight gain of control animals fed the chow diet increased about 20% (Figure 5a). Meanwhile, both control and AAVGck-treated animals fed a HFD gained about a 50% of body mass, indicating that they developed obesity (Figure 5a). Food intake was also measured weekly during the study. All groups of mice, independently of the diet or treatment that they were receiving, ate the same amount of food, approximately 2.5 g/day (Figure 5b). However, as the amount of calories per gram is higher in a HFD, the total caloric intake was higher in high-fat fed animals. Thus, the expression of *Gck* in the skeletal muscle did not change neither the body weight gain percentage induced by a high-fat diet nor the food intake.

During a high fat feeding, the increase in body weight is mainly due to an enhanced accumulation of fat in white adipose tissue (WAT) depots. At week 13, animals were euthanized and the epididymal white adipose tissue (eWAT) was weighted. The eWAT mass in control and AAVGck-injected animals fed a high-fat diet was doubled compared to chow-fed mice, in agreement to their increased body weight (Figure 5c).

Finally, circulating leptin levels were also determined. Leptin is an adipokine which circulates at levels that increase with the amount of body fat. Consequently, leptin levels are higher during obesity. In agreement with the

observed increase in their eWAT mass, control animals in HFD showed a 13-fold increase in circulating leptin levels compared to chow fed mice (Figure 5d). AAV*Gck*-injected animals in HFD, showed similar circulating increased values as those obtained in their high-fat fed control counterparts (Figure 5d).

Overall, these results suggest that the muscular expression of *Gck* using a total dose of AAV*Gck* of 6×10^9 vg per animal did not significantly change the body weight gain induced by a HFD.

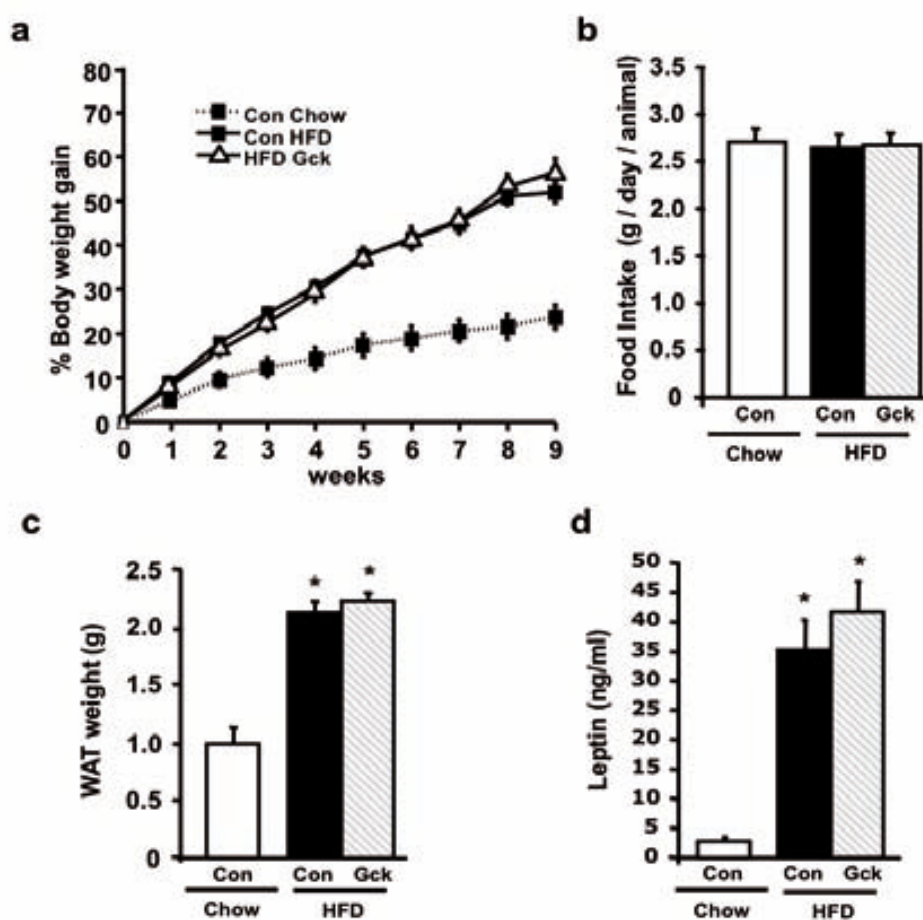


Figure 5. Body weight gain, food intake, eWAT weight and Leptin measurements. (a) Body weight gain was measured weekly in control (Con) or AAV*Gck* injected animals (Gck) under a high fat diet (HFD) or fed with a chow diet (chow) for nine weeks. (b) Food intake. Food was measured weekly after week one. Results are expressed as grams of food consumed per day and animal. (c) Epididymal white adipose tissue weight was measured at week 13. (d) Circulating leptin levels were measured at week 13 as stated in Materials and Methods. Data are means \pm SEM of minimum 8 animals per group. * $p < 0.05$ vs. Con Chow.

2.2.3. Hepatic triglyceride content

Another consequence of a prolonged high fat diet is the accumulation of triglycerides in the liver, known as hepatic steatosis. Liver sections stained with Hematoxylin/Eosin showed that both groups of animals fed with a HFD presented a large increase in hepatic lipid accumulation compared to chow fed mice. This was clearly revealed by the appearance of big lipid droplets in hepatocytes (Figure 6a). The amount of triglycerides in the liver was also quantified. In agreement with the morphologic observations, both control and AAV*Gck*-treated HFD-fed mice presented a 4-fold increase in lipid content compared to chow-fed control animals (Figure 6b). Thus, the muscular expression of *Gck* did not change the HFD-related fat accumulation in the liver.

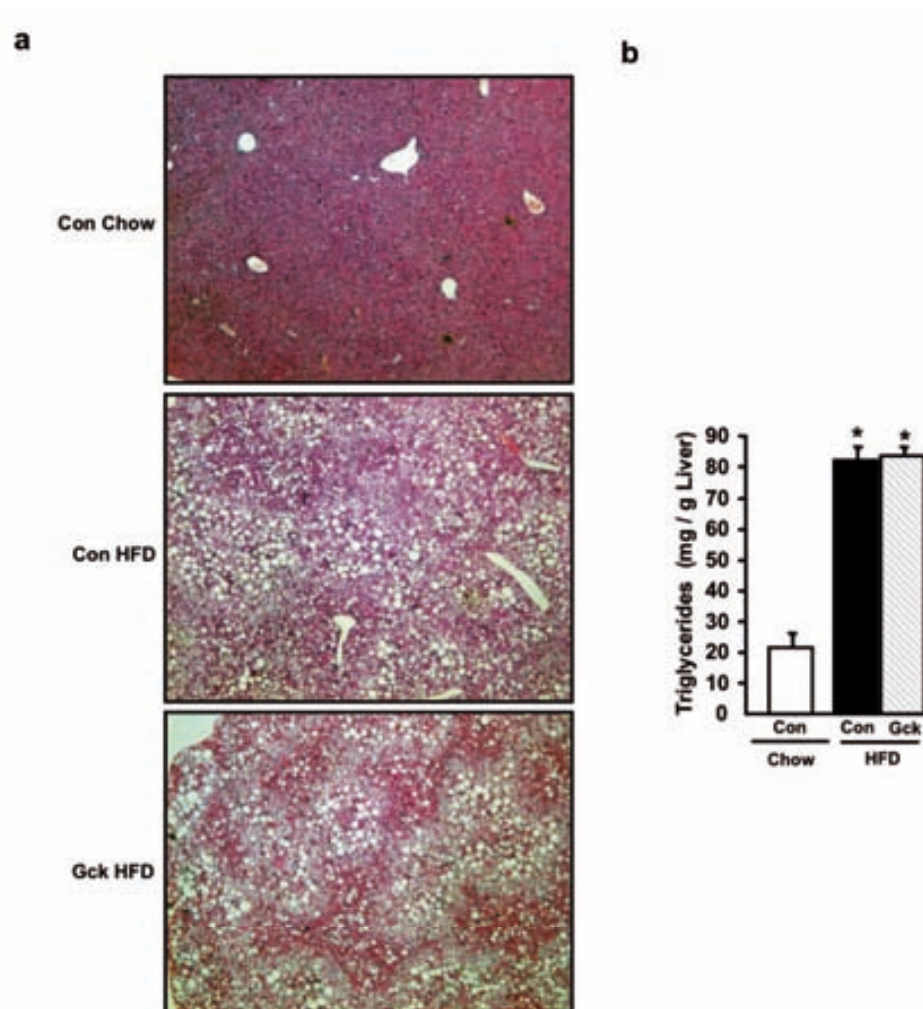


Figure 6. Hepatic triglyceride content. (a) Representative liver sections stained with Hematoxylin/Eosin from control animals fed a chow diet (Con Chow), control animals fed a High fat diet (Con HFD) and AAV*Gck*-treated animals fed a high fat diet (Gck HFD) are shown. Lipid accumulation inside hepatocytes is observed as an increase in the number and size of lipid droplets (40x). (b) Hepatic Triglyceride quantification. Analysis was performed as stated in materials and methods. Data are means \pm SEM of minimum 5 animals per Group. * $p < 0.05$ vs. Con Chow.

2.2.4. Study of glucose homeostasis

Increased fat accumulation in peripheral tissues is highly associated with the development of insulin resistance, usually characterized by elevated levels of glycaemia and insulinemia. Thus, fed blood glucose and serum insulin levels were determined. All groups of mice presented a similar glycemia (Figure 7a). Nevertheless, insulin circulating levels in control HFD-fed animals were 2-fold higher than those observed in chow-fed animals (Figure 7b), indicating that more insulin was needed to maintain normoglycaemia. In contrast, AAV*Gck*-injected mice were nearly normoinsulinemic, suggesting that they were insulin sensitive despite being obese (Figure 7b).

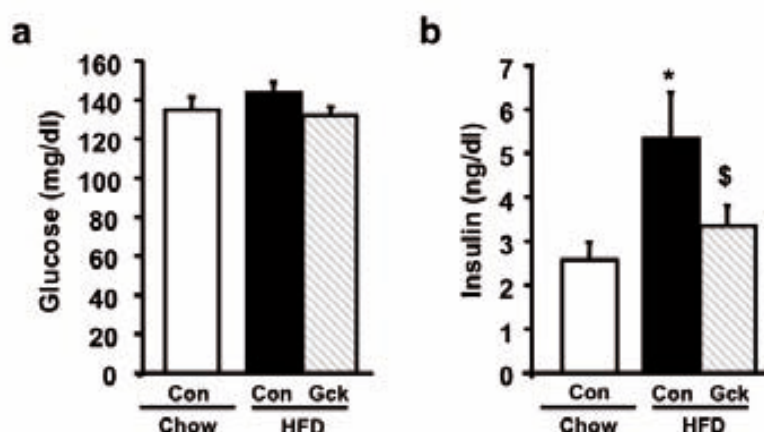


Figure 7. Glycemia and Insulinemia in HFD-fed *Gck*-expressing mice. (a) Blood Glucose and (b) Serum Insulin levels were measured in control (Con) and AAV*Gck*-treated (Gck) animals fed either with a chow diet (chow) or a High-fat diet (HFD). Measurements were performed at week 13 of the experiment as stated in Material and Methods. Data are means \pm SEM of a minimum of 8 animals per group. * $p < 0.05$ vs. Con Chow; \$ $p < 0.05$ vs. Con HFD.

To determine the insulin sensitivity of the AAV*Gck*-treated mice, an intra-peritoneal insulin tolerance test (ITT) was performed in fed conscious animals. Thirty minutes after the insulin administration, glucose levels in chow fed animals were reduced by 40%. Blood glucose levels were also reduced in high-fat fed control animals but only by 15%, confirming that these animals had developed insulin resistance (Figure 8). In contrast, AAV*Gck*-treated animals in HFD behaved similarly to chow fed control animals. They showed a 40% blood glucose reduction after 30 minutes and thereafter maintained lower glucose levels than those seen in their high-fat fed control counterparts (Figure 8). Overall, these results indicate that the muscular expression of *Gck* using a total dose of AAV*Gck* 6×10^9 vg per animal, protected mice against high-fat diet-induced insulin resistance.

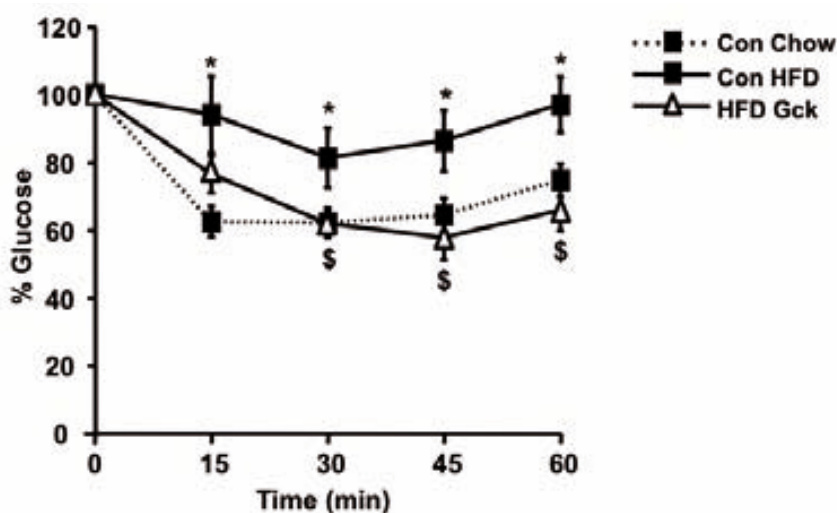


Figure 8. Insulin tolerance test. Insulin (0.75 U/kg) was injected intraperitoneally into fed animals. Blood samples were taken from the tail vein at indicated time points. Results are expressed as percentage of blood glucose values at time 0. Data are means \pm SEM of minimum 6 animals per Group. * $p < 0.05$ vs. Con Chow; \$ $p < 0.05$ vs. Con HFD.

2.2.5. Insulin signalling in the skeletal muscle

The Insulin signalling pathway is initiated upon binding of insulin to its cellular receptor. The activation of this pathway leads to the phosphorylation and activation of the protein kinase B (PKB, also known as AKT). This activation is important at regulating various cellular processes, like the translocation of the insulin-responsive glucose transporter 4 (GLUT4) to the cell membrane (Taniguchi et al., 2006). However, during insulin resistance conditions and obesity this activation is impaired (Tonks et al., 2013).

As an indicator of insulin sensitivity, the basal (without exogenous insulin stimulation) ratio between phosphorylated and total AKT levels was measured in the skeletal muscles of fed mice. To this aim, muscle protein extracts were analysed by Western blot with specific antibodies against phosphorylated AKT (P-AKT) and total AKT (T-AKT). As Figure 9a shows, P-AKT and T-AKT levels appeared to be similar between all groups of mice. To calculate the P-AKT/T-AKT ratio, a densitometric analysis of the Western blot was performed. Accordingly, all groups of animals presented a similar P-AKT/T-AKT ratio (Figure 9b), indicating that the expression of *Gck* did not modify the basal phosphorylation levels of AKT. However, AAV*Gck*-treated animals had a normal AKT activation being normoinsulinemic, while high-fat fed animals needed hiperinsulinemia to maintain the same levels of AKT activation. Thus, this result suggests that the skeletal muscles injected with AAV*Gck* were more sensitive to the insulin action.

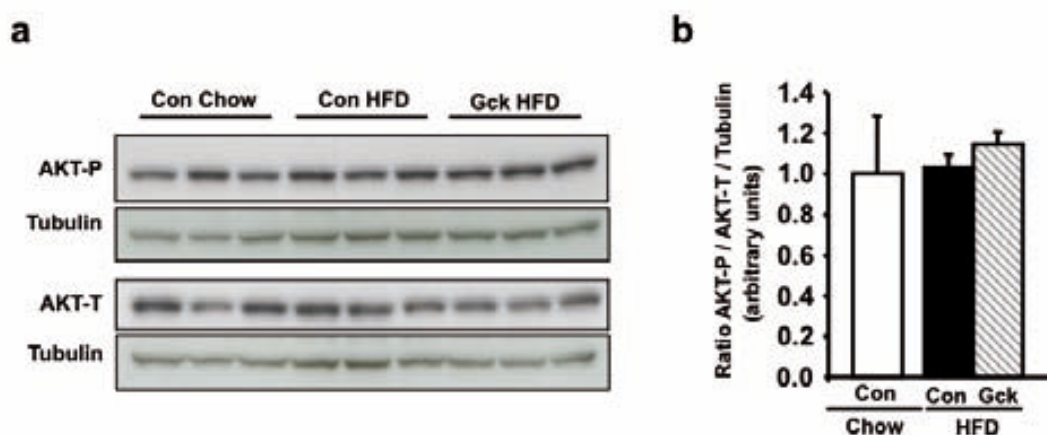


Figure 9. Insulin signalling in the skeletal muscle. (a) Representative Western blot analysis of phosphorylated (P)Ser473-AKT (AKT-P) and total AKT (AKT-T) from control animals fed a chow diet (Con Chow), control animals fed high-fat fed (Con HFD), and AAV*Gck* treated animals fed a HFD (Gck HFD). *Quadriceps* muscle protein lysates were used. (b) Band quantification by densitometric analysis of phosphorylated (P)Ser473-AKT and total AKT. Results are expressed as means \pm SEM of the ratio between P^{Ser473}-AKT and total AKT prior respective Tubulin correction (n=3).

2.2.6. Determination of circulating metabolites

During obesity and insulin resistance conditions, insulin is less effective at inhibiting lipolysis in WAT due to the insulin resistance in this tissue. As a result, the levels of circulating free fatty acids (FFA) and Glycerol are higher. Accordingly, control and AAV*Gck*-injected animals in HFD presented a trend to have increased levels of circulating FFA (Figure 10a). Similarly, glycerol levels were increased by a 25% in HFD-fed control animals and presented a trend to be increased in AAV*Gck*-injected mice (Figure 10b). However, no significant differences were found between high-fat fed control and AAV*Gck*-injected animals, suggesting that lipolysis, and hence WAT insulin resistance, were similar in both groups.

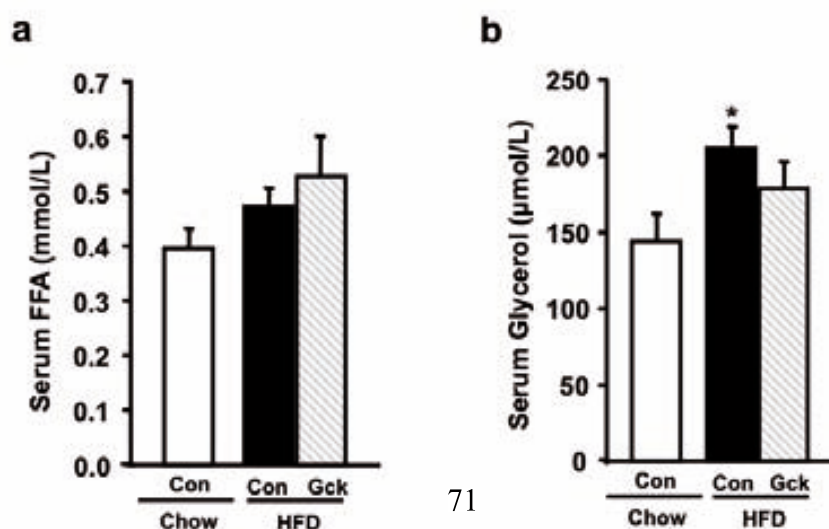


Figure 10. Serum levels of FFA and Glycerol. (a) Free fatty acid and (b) Glycerol circulating levels were measured in control (Con) and AAV*Gck*-treated (*Gck*) animals fed either with a chow diet (chow) or a High-fat diet (HFD). Measurements were performed at week 13 of the experiment as stated in Material and Methods. Data are means \pm SEM of minimum 8 animals per Group. * $p < 0.05$ vs. Con Chow.

2.3. Metabolic effects of the expression of high levels of *Gck* in the skeletal muscle

Results obtained by using a dose of AAV*Gck* 6×10^9 vg/animal demonstrated that expressing *Gck* in the skeletal muscle of adult mice resulted in the prevention of high-fat diet-induced insulin resistance. However, this dose was not able to ameliorate the increases in body weight gain. Since the expression of *Gck* in skeletal muscle proved to prevent obesity in our transgenic model (Otaegui et al., 2003), we wondered whether achieving a higher *Gck* expression could also lead to reductions in body weight gain while keeping animals insulin sensitive during a HFD. To this end, we next studied the effects increasing the dose of AAV*Gck* to 1.8×10^{10} vg per animal, which represents a 3-fold increase compared to the previous used dose. Hence, mice were administered and placed in a HFD regime as indicated in the experimental design (Figure 2).

2.3.1. Glucokinase expression in the skeletal muscle

The levels of the *Gck* expression in skeletal muscle using the higher AAV*Gck* dose, were determined and compared to those obtained with the

previous dose. To this aim, total RNA from injected *tibialis cranialis* was obtained and analysed by Northern blot at week 13. The expression of *Gck* obtained using a dose of AAV*Gck* 1.8×10^{10} vg per animal was markedly higher than that detected in muscles injected with AAV*Gck* 6×10^9 vg/animal (Figure 11). Thus, by increasing the dose of AAV*Gck* we also increased the expression of *Gck* in the skeletal muscle.

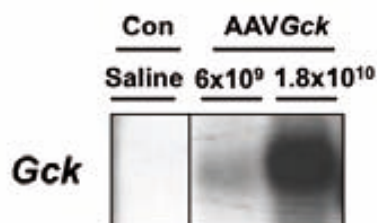


Figure 11. Glucokinase expression in the skeletal muscle of AAV*Gck* injected animals. Total RNA from *Tibialis Cranialis* was extracted from saline (Con) or AAV*Gck* injected animals using a dose of AAV*Gck* 6×10^9 vg/animal or 1.8×10^{10} vg/animal at week 13 post-administration. The RNA obtained was then analysed by Northern blot. A representative blot hybridised with a *Gck* specific probe is shown.

2.3.2. Body weight gain and adiposity

After nine weeks, the body weight gain of control animals fed the HFD increased by a 70% indicating that they became obese compared to chow-fed control mice (Figure 12a). In contrast, mice treated with AAV*Gck* (1.8×10^{10} vg) presented a body weight gain that was a 10% lower compared to their control HFD-fed counterparts. This difference started at week one after feeding a HFD, and remained until the end of the experiment. No significant differences

in food intake were found between control and AAV*Gck*-injected animals suggesting that the observed reduction in body weight gain was not due to a different eating behaviour (Figure 12b). In agreement to their reduced body weight gain, WAT mass in AAV*Gck* 1.8×10^{10} vg treated mice presented a trend to be decreased compared to high-fat fed control mice (Figure 12c). However, no-significant differences in circulating leptin levels were found between control and AAV*Gck*-injected mice in HFD (Figure 12d).

Thus, these results suggest that the increase in the muscular *Gck* expression using the higher dose of AAV*Gck*, was able to partially reduce the body weight gain during a HFD.

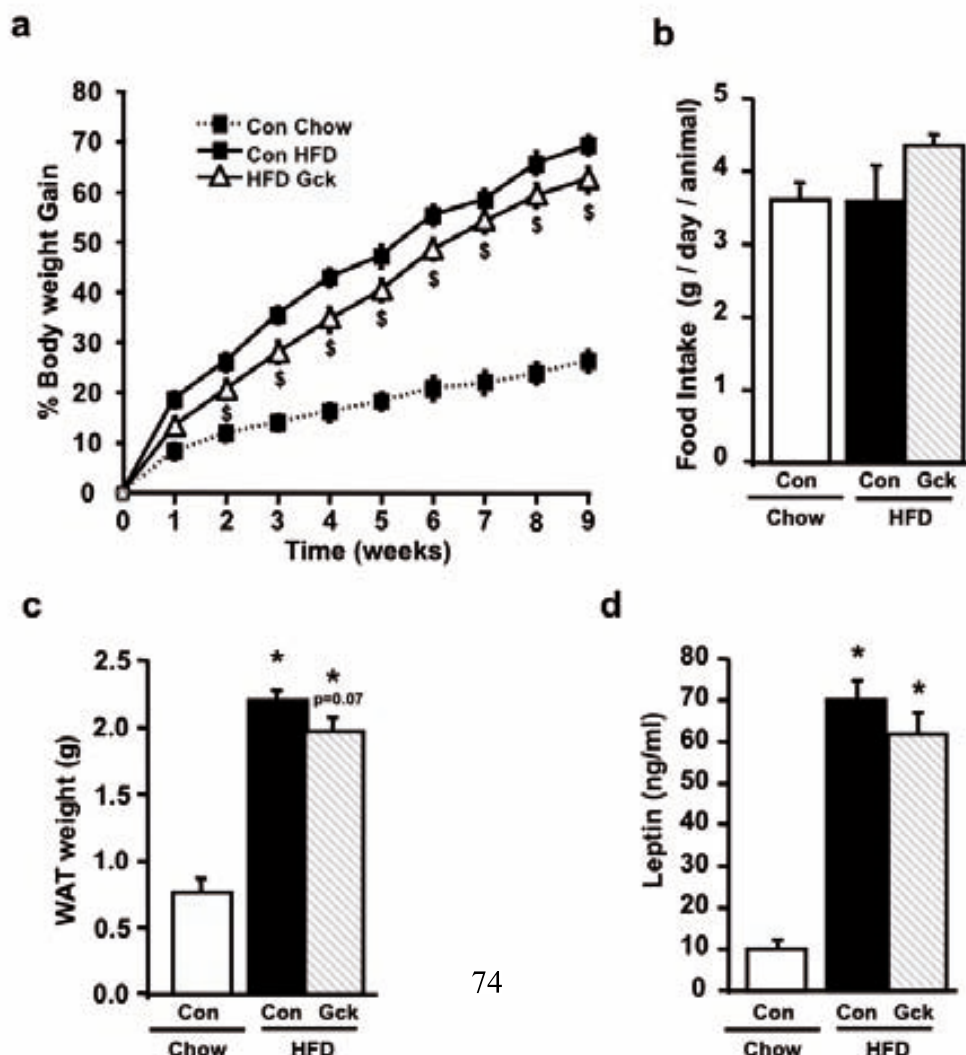


Figure 12. Body weight gain, food intake, eWAT weight and Leptin measurements. (a) Body weight gain was measured weekly in control (Con) or AAVGck (1.8×10^{10} vg/animal) Injected animals (Gck) under a High fat diet (HFD) or fed with a chow diet (chow) during nine weeks after the start of the high fat feeding (week 1). (b) Food intake. Food was measured weekly after week one. Results are expressed as grams of food consumed per day and animal. (c) Epididymal white adipose tissue weight was measured at week 13. (d) Circulating Leptin levels were measured at week 13 as stated in Materials and Methods. Data are means \pm SEM of minimum 8 animals per Group. * $p < 0.05$ vs. Con Chow; $p = 0.07$ vs. Con HFD.

2.3.3. Hepatic triglyceride content

Liver sections stained with Haematoxylin/Eosin from both control and AAVGck-treated animals fed with a HFD showed an increase in lipid accumulation compared to chow fed mice (Figure 13a). However, whereas control animals fed a HFD developed massive steatosis, AAVGck-treated animals presented areas with notorious less lipid accumulation (Figure 13a). In agreement with these morphometric observations, livers from AAVGck animals presented approximately a 20% reduction in hepatic lipid accumulation compared to HFD-fed control mice (Figure 13b). Thus, in agreement with their reduced body weight gain, animals treated with AAVGck using a dose of 1.8×10^{10} vg reduced the HFD-related hepatic lipid accumulation

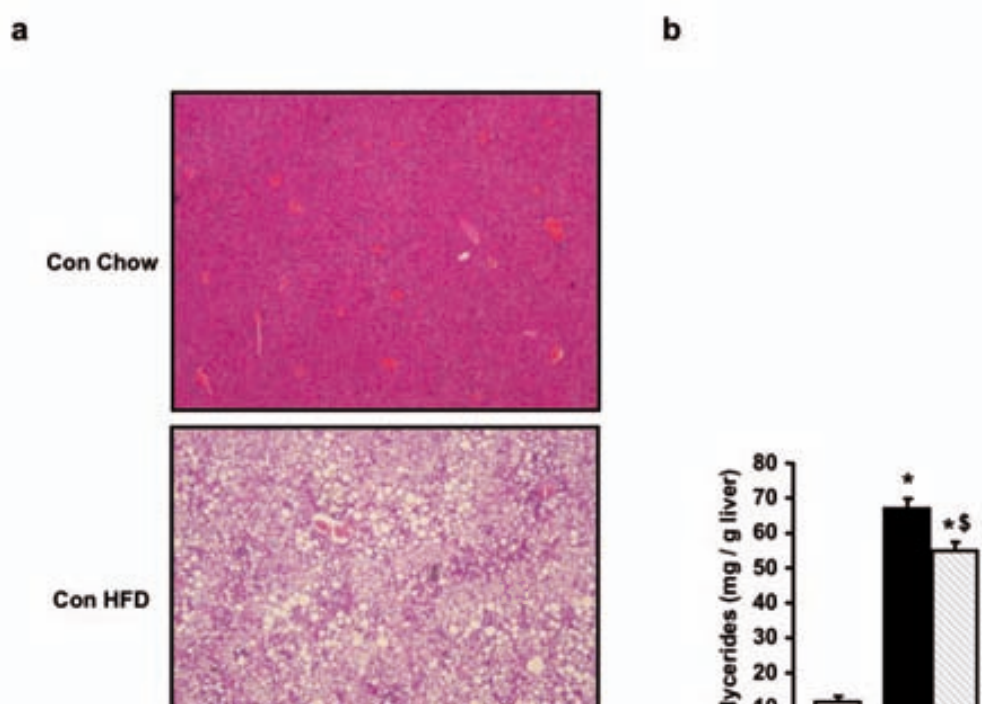


Figure 13. Liver histology and hepatic triglyceride content. (a) Representative liver sections stained with Hematoxylin/Eosin from control animals fed a chow diet (Con Chow), control animals fed a High fat diet (Con HFD) and AAV*Gck*-treated animals fed a high fat diet (Gck HFD) are shown (40x). (b) Hepatic Triglyceride quantification. Analysis was performed as stated in Materials and Methods. Data are means \pm SEM of minimum 5 animals per Group. * $p < 0.05$ vs. Con Chow; $^{\$}p < 0.05$ vs. Con HFD.

2.3.4. Triglyceride content and fatty acid oxidation in the skeletal muscle

During prolonged high fat diets and obesity, triglycerides also tend to accumulate in the skeletal muscle. Thus, the accumulation of triglycerides in skeletal muscles was also measured. Control animals fed a HFD presented a 2.7-fold increase in muscular triglycerides compared to control mice fed a chow diet (Figure 14). Muscles treated with AAV*Gck* presented a similar lipid accumulation than that obtained in muscles from high-fat fed control animals (Figure 14). Thus, the expression of *Gck* in the skeletal muscle did not significantly change the muscular lipid accumulation during prolonged high fat diets.

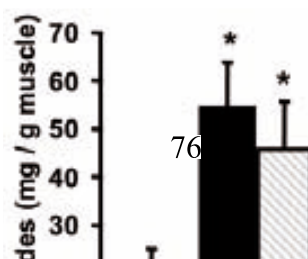


Figure 14. Skeletal muscle triglyceride content. Animals were euthanized at week 13 and *Gastrocnemius* muscle samples were obtained. The Analysis was performed as stated in Materials and Methods. Data are means \pm SEM of minimum 5 animals per Group. * $p < 0.05$ vs. Con Chow.

Cpt1 is the rate-limiting enzyme of mitochondrial β -oxidation by controlling mitochondrial entry of long-chain fatty acids in the skeletal muscle (He et al., 2012). As a measure of the status of the fatty acid oxidation, *Cpt1* mRNA expression was determined in skeletal muscles under HFD conditions. As Figure 15 shows, the expression levels of *Cpt1* in *Gck*-treated muscles approximately doubled those obtained in samples from Control animals in HFD. This result suggests that, despite the expression of *Gck* did not significantly change the accumulation of triglycerides in the skeletal muscle, the fatty acid oxidation was probably enhanced compared to control animals fed a HFD.

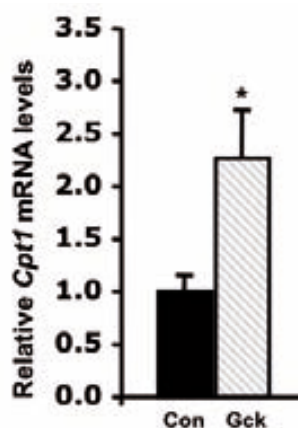


Figure 15. *Cpt1* expression in skeletal muscle expressing *Gck*. *Cpt1* expression was analysed by quantitative Real Time PCR in *Tibialis cranialis* samples from High-fat fed Control (Con) and AAV*Gck* (Gck) treated animals euthanized at week 13 after vector administration. The abundance of *Cpt1* was normalized by the expression of the housekeeping gene *36B4* as

indicated in Materials and Methods. Data are means \pm SEM of minimum 4 animals per Group. * $p < 0.05$ vs. Con HFD.

2.3.5. Study of glucose homeostasis

Glucose homeostasis was determined in animals treated with the higher dose of AAVGck. No significant differences in fed glucose levels were found between the different groups of animals (Figure 16a). To study their insulin sensitiveness an insulin tolerance test was performed at week 10. Once the exogenous insulin was injected, the initial glycaemia in chow fed control animals was reduced approximately by a 50%. Meanwhile, high-fat fed animals only showed a 30% reduction indicating that they had become insulin resistant. In contrast, AAVGck-treated mice showed a similar evolution in blood glucose levels to that observed in chow fed animals, indicating that they remained insulin sensitive despite being fed with a HFD (Figure 16b). Thus, as previously observed after treatment with low doses of AAVGck, these results indicate that higher doses of AAVGck were also able to maintain insulin sensitivity in HFD fed mice.

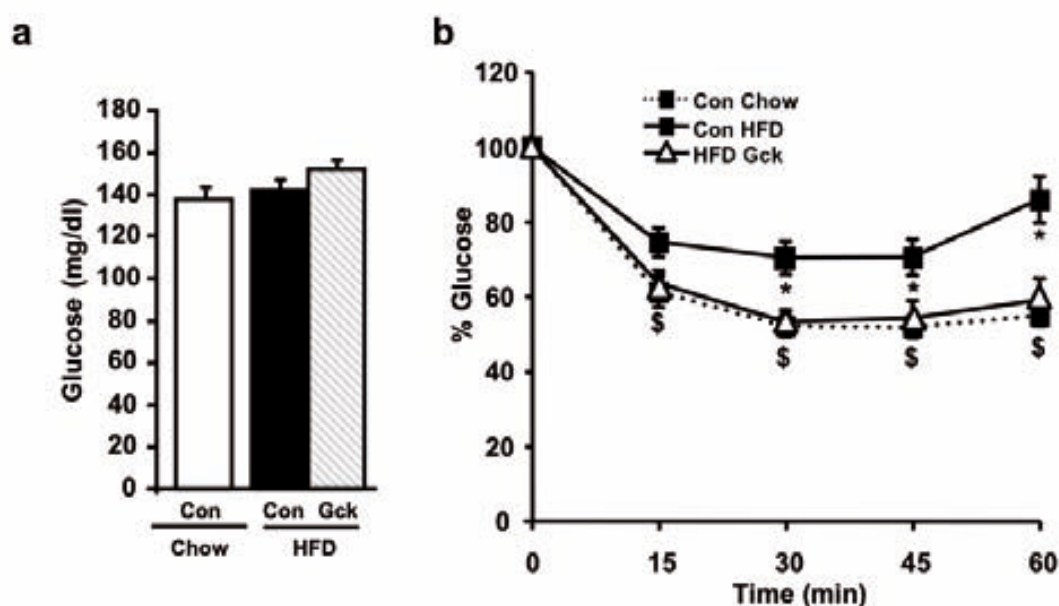


Figure 16. Glucose levels and insulin tolerance test. (a) Glucose levels measured in serum of control chow fed animals (Con) and AAV*Gck*-treated (Gck) animals fed either with a chow diet (chow) or a High-fat diet (HFD). Measurements were performed at week 10. (b) Insulin Tolerance Test. Insulin (0.75 U/kg) was injected intraperitoneally into fed animals. Blood samples were taken from the tail vein at indicated times. Results are expressed as percentage of blood glucose values at time 0. Data are means \pm SEM of minimum 6 animals per Group. * $p < 0.05$ vs. Con Chow; $^{\$}p < 0.05$ vs. Con HFD.

2.3.6. Insulin signalling in the skeletal muscle

To study the insulin signalling in muscles treated with the higher dose of AAV*Gck*, phosphorylated and total AKT levels were measured by Western blot analysis (Figure 17a). Once the blotted bands were densitometred, the P-AKT/T-AKT ratio was calculated, muscles treated with AAV*Gck* tended to have a higher ratio compared to their HFD-fed control counterparts (Figure 17b). Thus, this data suggests that the muscles injected with a higher dose of AAV*Gck* were probably more insulin sensitive than those from HFD-fed animals.

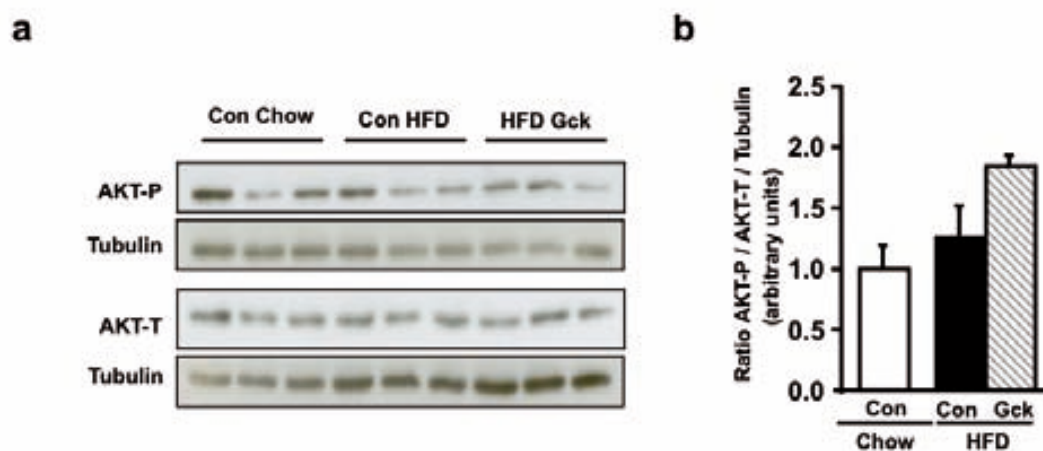


Figure 17. Insulin signalling in the skeletal muscle. (a) Representative Western blot analysis of phosphorylated (P)Ser473-AKT (AKT-P) and total AKT (AKT-T) from control Chow (Con), high-fat fed (HFD), and AAV*Gck* treated (Gck HFD) animals. *Quadriceps* muscle protein lysates were used. (b) Band quantification by densitometric analysis of phosphorylated

(P)Ser473-AKT and total AKT. Results are expressed as means \pm SEM of the ratio between P^{Ser473}-AKT and total AKT prior respective Tubulin correction (n=3).

2.3.7. Determination of circulating metabolites

Circulating free fatty acids presented a non-significant trend to be increased in HFD-fed animals compared to animals fed with the chow diet (Figure 18a). Similarly, glycerol levels were highly increased in animals fed with the high fat diet (Figure 18b). Meanwhile, both parameters appeared to be significantly decreased in AAV*Gck* treated mice compared to their HFD-fed control counterparts suggesting that lipolysis was less active in these animals (Figure 18a,b).

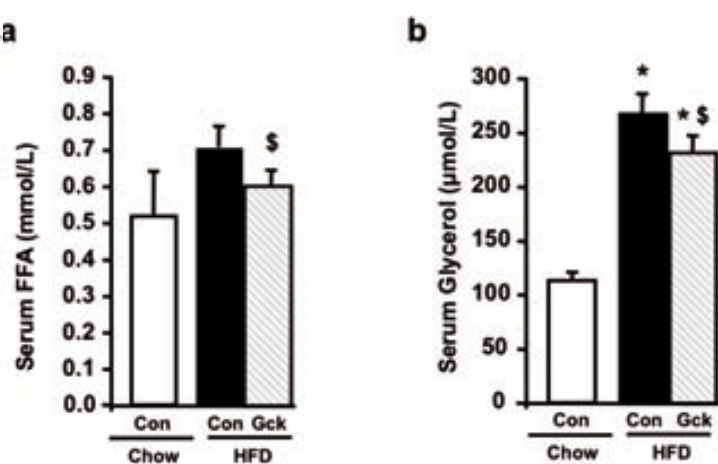


Figure 18. Serum levels of metabolites. (a) Free fatty acid and (b) Glycerol blood circulating levels measured in control (Con) and AAV*Gck*-treated (Gck) animals fed either with a chow diet (chow) or a High-fat diet (HFD). Measurements were performed at week 13 of the experiment as stated in Material and Methods. Data are means \pm SEM of minimum 8 animals per Group. * p <0.05 vs. Con Chow; $^{\$}$ p <0.05 vs. Con HFD.

The results obtained expressing *Gck* in the skeletal muscle suggest that expression of this enzyme is enough to prevent the development of high-fat diet-derived insulin resistance. Moreover, increasing the expression of *Gck* resulted in a partial reduction of weight gain (about 10%).

Despite the mild reduction observed in body weight gain when the higher AAV*Gck* dose was used, *Gck*-treated animals still developed severe obesity. Along with a decreased capacity to phosphorylate glucose, the skeletal muscles of type 2 diabetic patients show alterations in the capacity to metabolize fat along with a reduced oxidative capacity. Thus, we wondered whether increasing the oxidative function of the skeletal muscle, could further improve the degree of prevention of the high-fat diet derived consequences observed when *Gck* was expressed alone.

Given the key role of PGC1 α at regulating the oxidative function of the skeletal muscle, in the second part of this study we checked the metabolic effects of overexpressing *Pgc1 α* in the skeletal muscles of mice during a high fat diet. Moreover, PGC1 α expression has been related to the over-expression of GLUT4 and consequently, to increase the rates of glucose uptake by muscular cells. Since hexokinase-II is unable to phosphorylate large amounts of glucose, this makes of *Pgc1 α* an interesting gene to be over-expressed in combination with *Gck*. Thus, we also evaluated whether the co-overexpression of *Gck* along with *Pgc1 α* , could ameliorate the preventive effects mediated by *Gck* during a HFD.

3.1. Design of an AAV1 with the *Pgc1 α* gene

In order to over-express *Pgc1 α* in the skeletal muscle of adult mice, an AAV1 vector carrying this gene (AAVPGC) was designed. To this aim, the cDNA sequence of the mouse *Pgc1 α* was cloned into the pGG2 plasmid (pGG2-PGC) upstream of the polyadenylation signal (Poly A) and under the transcriptional control of the CMV promoter (Figure 19). The pGG2-PGC was then used to produce the AAV1 vectors, as stated in Material and Methods.



Figure 19. Schematic representation of the construct used to produce the AAV-PGC vector. CMV: cytomegalovirus promoter; poly A: Simian Virus 40 Polyadenylation signal; ITR: Inverted terminal repeat.

3.2. Metabolic effects of the *Pgc1 α* expression in the skeletal muscle of high-fat fed mice

With the aim of characterising the metabolic effects of over-expressing *Pgc1 α* during a high fat diet, a total dose of AAVPGC 1.8×10^{10} vg/animal was injected in the skeletal muscles of mice. After the injection, animals were placed under a high fat diet and the experimental design detailed in Figure 2 was followed.

3.2.1. *Pgc1 α* expression in the skeletal muscle

Thirteen weeks after the intramuscular AAVPGC administration, *Pgc1 α* expression was measured in the skeletal muscles of injected animals. The basal levels of *Pgc1 α* expression were not modified by the HFD since both, chow-fed and high fat-fed control animals, expressed the same levels of the coactivator (Figure 20). Meanwhile, *Pgc1 α* expression in the skeletal muscle of the AAV-treated animals was approximately six times higher than that of control animals (Figure 20). Thus, the intramuscular administration of AAVPGC (1.8×10^{10} vg), allowed to overexpress high levels of *Pgc1 α* .

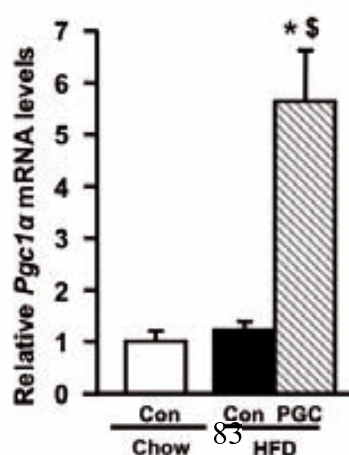


Figure 20. PGC1 α expression in the skeletal muscle. *Pgc1 α* expression was analysed by quantitative Real Time PCR in *Tibialis cranialis* samples from control (Con) and AAVPGC (PGC) treated animals fed with a chow diet (Chow) or a High fat diet (HFD) euthanized at week 13. The abundance of *Pgc1 α* was normalized by the expression of the housekeeping gene *36b4* as indicated in Materials and Methods. Data are means \pm SEM of minimum 4 animals per Group. * $p < 0.05$ vs. Con Chow; $^{\S}p < 0.05$ vs. Con HFD.

3.2.2. Body weight gain and adiposity

As expected, animals in high-fat diet started to gain weight soon. After nine weeks, animals fed a chow diet had gained a 20% in body weight, whereas high-fat fed control mice had increased body weight gain by a 70%, thus becoming obese (Figure 21a). In contrast, although AAVPGC-treated animals in HFD also developed obesity, they presented a 10% reduction in body weight gain. The reduction in body weight gain was not due to changes in daily food intake, since no significant differences were found between groups (Figure 21b). This indicated that muscular overexpression of *Pgc1 α* was able to reduce the HFD-induced body weight gain. The epididymal fat pad weight in animals under a HFD was approximately three times higher compared to chow fed mice (Figure 21c). Meanwhile, and in agreement with the reduced body weight during the HFD, the eWAT weight in AAVPGC treated animals was also reduced by a 10% compared to high-fat fed mice. In addition, control animals in HFD showed a 3-fold increase in leptin levels (Figure 21d) while AAVPGC-treated animals presented a non-significant decrease in leptin levels compared to high-fat fed animals (Figure 21d). Taken together, these results suggest that the muscular over-expression of *Pgc1 α* was able to reduce the HFD-induced body weight gain, probably in part by a reduction in eWAT weight.

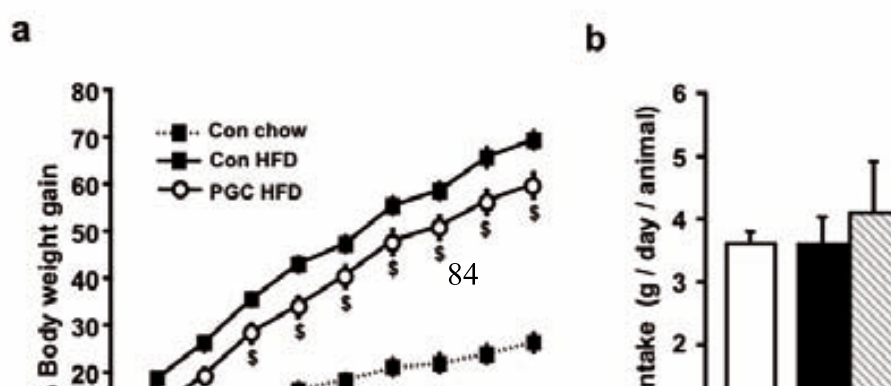


Figure 21. Body weight gain, food intake, eWAT weight and Leptin levels. (a) Body weight gain was measured weekly in control (Con) or AAVPGC injected animals (PGC) under a High fat diet (HFD) or fed with a chow diet (chow) during nine weeks after the start of the high fat feeding (week 1). (b) Food intake. Food was measured weekly after week one. Results are expressed as grams of food consumed per day and animal. (c) Epididymal white adipose tissue weight was measured at week 13. (d) Circulating Leptin **Levels** were measured at week 13 as stated in Materials and Methods. Data are means \pm SEM of minimum 8 animals per Group. * $p < 0.05$ vs. Con Chow; § $p < 0.05$ vs. Con HFD.

3.2.3. Hepatic triglyceride content

Hematoxylin and eosin stainings of liver sections of animals in HFD showed an increased storage of triglycerides, clearly revealed by the appearance of numerous lipid droplets (Figure 22a). However, hepatocytes in AAVPGC-treated animals appeared to have slightly less lipid accumulation than HFD-fed controls. This was specially noticeable in areas surrounding the hepatic portal vein (Figure 22a). When triglyceride content was quantified, livers from control animals in HFD presented approximately seven times more triglyceride accumulation than livers from animals in chow fed (Figure 22b). Nevertheless, livers from AAVPGC-treated animals presented a trend to accumulate less

triglycerides than livers from control high fat-fed animals. Altogether, these results suggest that livers from AAVPGC treated animals accumulated slightly less triglycerides during the HFD than control animals.

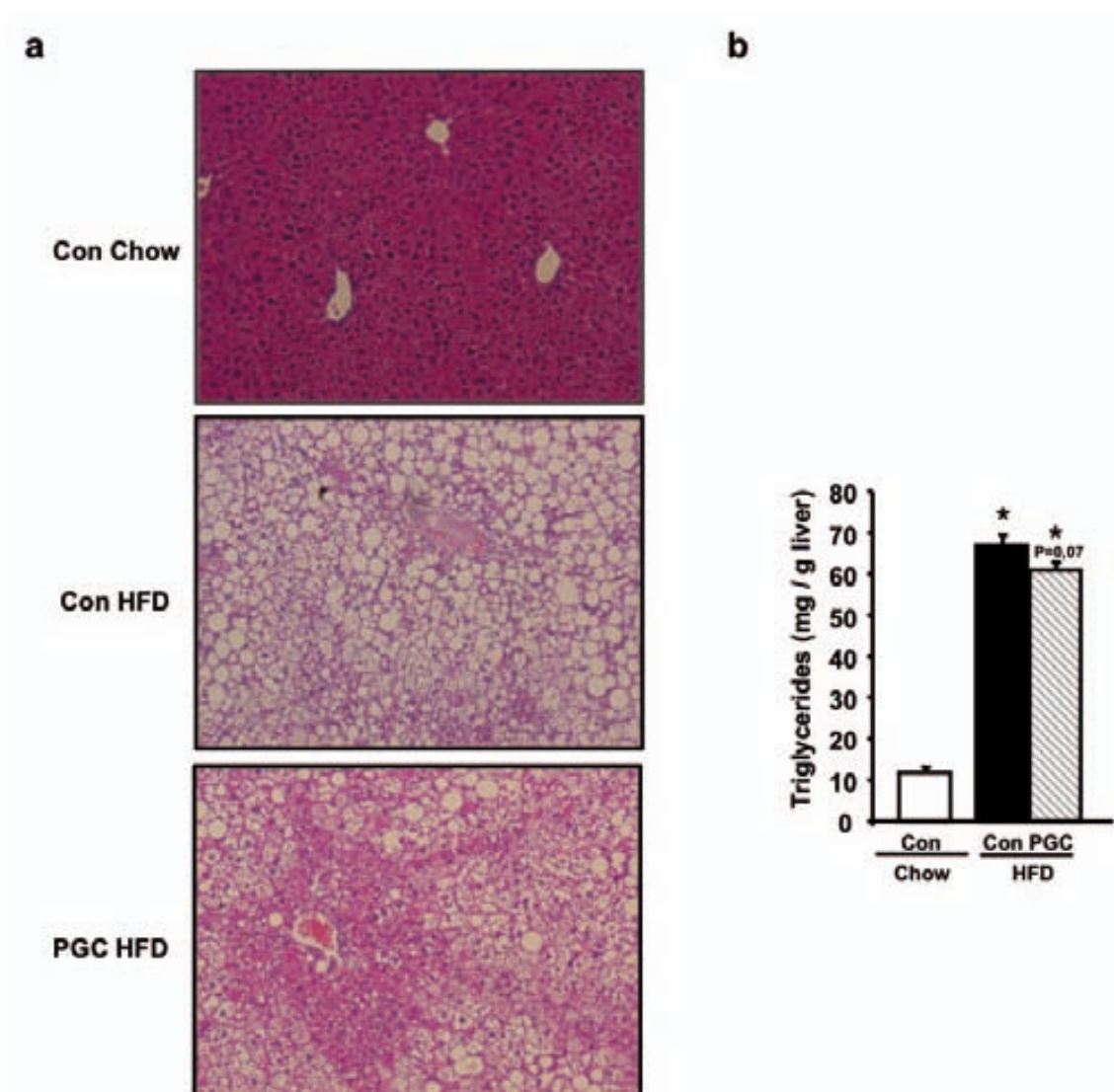


Figure 22. Liver histology and hepatic triglyceride accumulation. (a) Representative liver sections from control animals fed a chow diet (Con Chow), control animals fed a High fat diet (Con HFD) and AAVPGC treated animals in a high fat diet (PGC HFD) stained with Haematoxylin/Eosin are shown. Lipid accumulation inside hepatocytes was observed as an increase in the number and size of lipid droplets (100x). (b) Hepatic Triglyceride quantification. Analysis was performed as stated in Materials and Methods. Data are means \pm SEM of minimum 5 animals per Group. * $p < 0.05$ vs. Con Chow; $p = 0.07$ vs. Con HFD.

3.2.4. Triglyceride content and fatty acid oxidation in the skeletal muscle

Triglyceride accumulation in skeletal muscles was next studied. The triglyceride content in control muscles from high-fat fed animals was highly increased compared to muscles from animals fed a chow diet (Figure 23). Nevertheless, the overexpression of *Pgc1 α* in the skeletal muscle did not significantly change the lipid accumulation in this tissue (Figure 23).

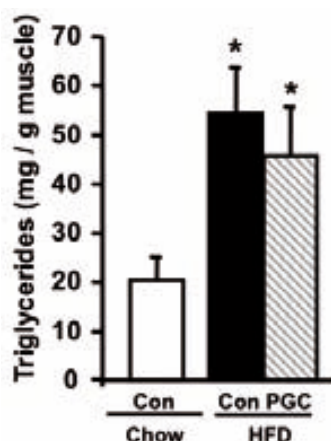


Figure 23. Skeletal muscle triglyceride content. Animals were euthanized at week 13 and *Gastrocnemius* muscle samples were obtained. The Analysis was performed as stated in Materials and Methods. Data are means \pm SEM of minimum 5 animals per Group. * p <0.05 vs. Con Chow.

To determine whether the muscular fatty acid oxidation was affected by the expression of *Pgc1 α* , the expression of *Cpt1* was studied by Real Time PCR analysis. The abundance of *Cpt1* in AAVPGC-treated muscles was approximately 50% higher compared to control muscles in mice fed a high fat diet (Figure 24). Thus, this result suggests that skeletal muscles overexpressing *Pgc1 α* may have a higher capacity to burn fat despite presenting a similar accumulation of triglycerides compared to control muscles.

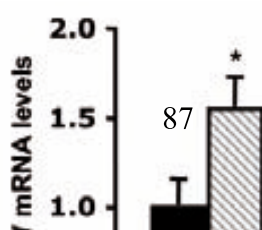


Figure 24. Expression of *Cpt1* in the skeletal muscle. *Cpt1* expression was analysed by quantitative Real Time PCR in *Tibialis cranialis* samples from High-fat fed Control (con) and AAVPGC (PGC) treated animals at week 13 after AAV administration. The abundance of *Cpt1* was normalized by the expression of the housekeeping gene *36B4* as indicated in Materials and Methods. Data are means \pm SEM of minimum 4 animals per Group. * $p < 0.05$ vs. Con HFD.

3.2.5. Study of glucose homeostasis

At week 10, glucose levels were measured in fed animals. No differences between groups were found in this parameter and all animals were normoglycemic (Figure 25a). To study the insulin responsiveness of AAVPGC-injected animals, an intra-peritoneal insulin tolerance test was performed. Chow-fed animals responded to the insulin challenge by decreasing their blood glucose levels by a 50% after 30 minutes (Figure 25b). In contrast, initial glucose values in control mice fed a HFD were only reduced by a 30%, indicating that these animals had become insulin resistant. AAVPGC treated animals showed a 35% reduction in glycemia, indicating that the muscular over-expression of *Pgc1 α* did not ameliorate the high-fat diet-induced insulin resistance (Figure 25b).

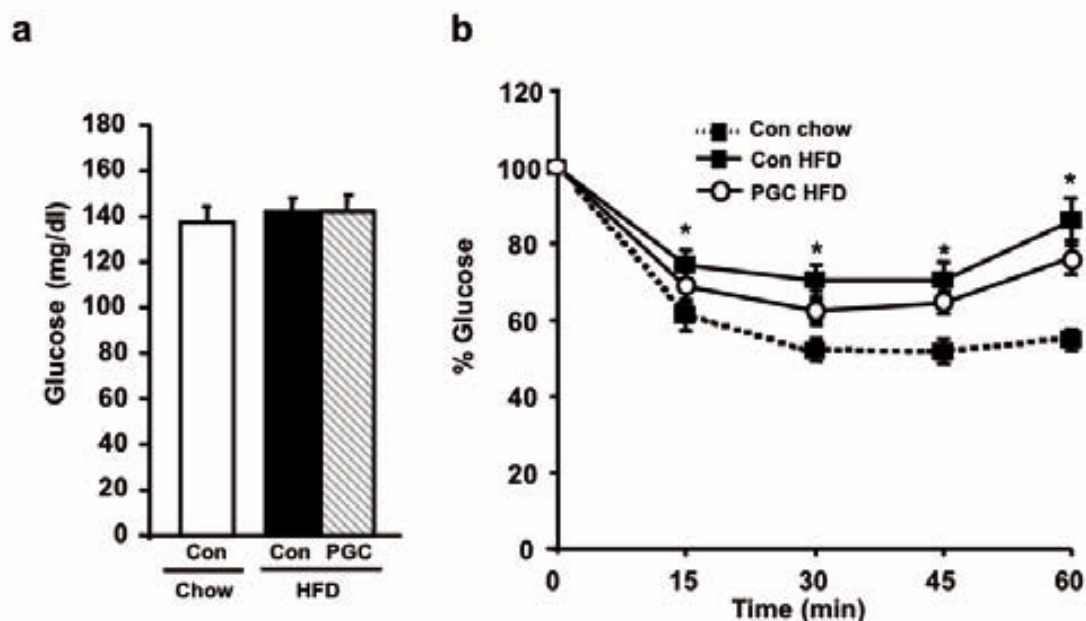


Figure 25. Glycemia and Insulin Tolerance Test. (a) Glucose levels measured in serum of control chow fed animals (Con) and AAVPGC-treated (PGC) animals fed either with a chow diet (chow) or a High-fat diet (HFD). Measurements were performed at week 10. **(b)** Insulin Tolerance Test. Insulin (0.75 U/kg) was injected intraperitoneally into fed animals. Blood samples were taken from the tail vein at indicated times. Results are expressed as percentage of blood glucose values at time 0. Data are means \pm SEM of minimum 6 animals per Group. * $p < 0.05$ vs. Con Chow.

3.2.6. Insulin signalling in the skeletal muscle

To study the insulin signalling in muscles over-expressing *Pgc1 α* under a high-fat diet environment, insulin-stimulated AKT phosphorylation was checked by Western blot analysis. *Pgc1 α* expressing muscles presented a decrease in AKT-phosphorylation compared to control muscles when they were stimulated with insulin (Figure 26a). This observation was corroborated when the bands were quantified by densitometry and the fold increase in AKT phosphorylation between basal and insulin-stimulated conditions was measured. AAVPGC-treated muscles presented approximately a 60% decrease in fold-increase AKT phosphorylation after insulin stimulation compared to HFD control muscles (Figure 26b). Thus, these results suggest that the over-expression of *Pgc1 α* in the skeletal muscle of adult mice reduced the activation of the insulin signalling

pathway and consequently, these muscles were more insulin resistant than their high-fat fed counterparts.

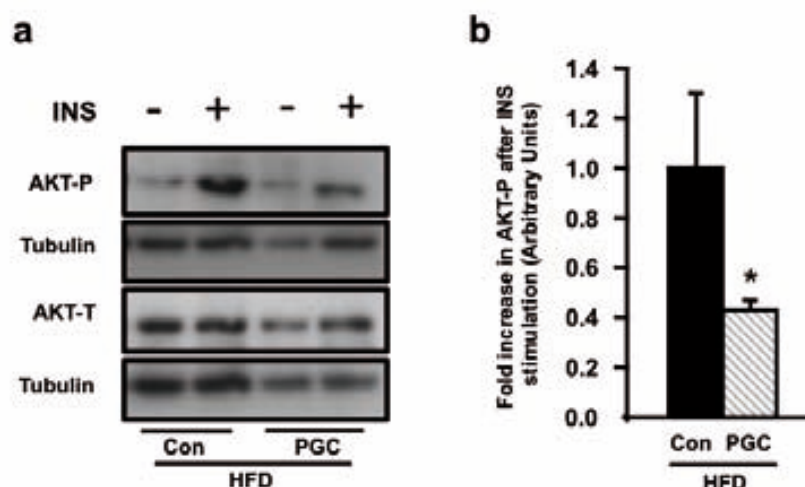


Figure 26. Western blot analysis of the insulin signalling pathway in skeletal muscle. (a) Representative Western blot analysis of phosphorylated (P)Ser473-AKT (AKT-P) and total AKT (AKT-T) from control high-fat fed (HFD), and AAVPGC treated (HFD PGC) animals stimulated with (+) or without (-) insulin (5 U/Kg). *Gastrocnemius* muscle protein lysates were used. (b) Band quantification by densitometric analysis. Results are expressed as means \pm SEM of the fold-increase in AKT-P after Insulin stimulation and relative to Con HFD. Fold-increase was obtained by calculating the ratio between P^{Ser473}-AKT and total AKT in basal and stimulated conditions. Tubulin was used as a loading control. (n=3). * $p < 0.05$ vs. Con Chow, [#] $p < 0.05$ vs. Con HFD. These experiments were performed at week 13 after AAV administration.

3.2.7. Determination of circulating metabolites

No differences in circulating free fatty acids were found between groups, despite control animals fed the HFD presented a trend to have higher levels than chow-fed control animals (Figure 27a). Glycerol levels in HFD-fed control animals presented approximately a 2.5-fold increase compared to chow-fed control mice (Figure 27b). The muscular over-expression of *Pgc1 α* during the HFD did not change glycerol levels compared to HFD-fed control animals despite a trend to decrease could be observed. These results suggest that lipolysis was not significantly modified by the muscular overexpression of *Pgc1 α* .

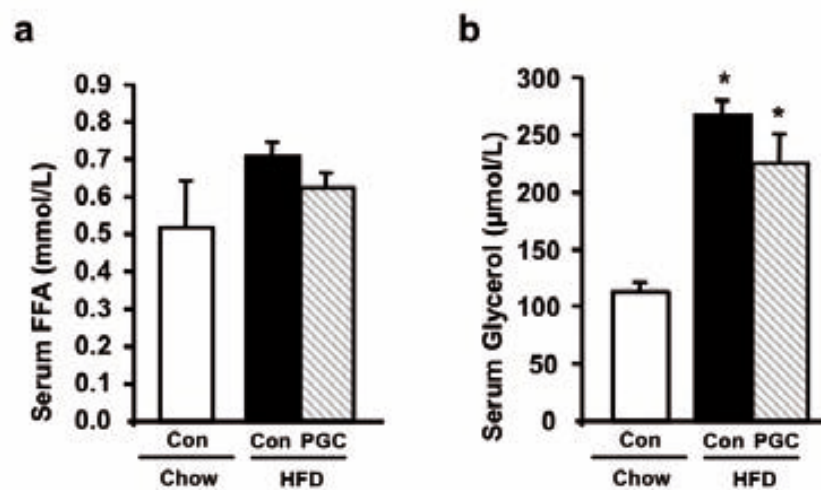


Figure 27. Serum levels of metabolites. (a) Free fatty acid and (b) Glycerol levels in serum were measured in control (Con) and AAVPGC-treated (PGC) animals fed either with a chow diet (chow) or a High-fat diet (HFD). Measurements were performed at week 13 of the experiment as stated in Material and Methods. Data are means \pm SEM of minimum 8 animals per Group. * $p < 0.05$ vs. Con Chow. § $p < 0.05$ vs. Con HFD.

3.3. Metabolic effects of *Gck* and *Pgc1α* overexpression in the skeletal muscle of high-fat fed mice

The muscular overexpression of *Pgc1α* led to a mild improvement in the HFD-induced body weight gain. However, this situation was not associated with an improvement in insulin sensitivity. Hence, the muscular overexpression of *Pgc1α* alone was not able to ameliorate the complications related to a prolonged high fat diet. Next we wondered whether the muscular expression of Glucokinase, along with an overexpression of *Pgc1α*, could have beneficial effects during a HFD. Specifically, we aimed to enhance the reduction in body weight gain observed when *Pgc1α* and *Gck* were overexpressed individually while keeping animals insulin sensitive. To this end, a dose of 1.8×10^{10} vg of AAV*Gck* and of 1.8×10^{10} vg AAVPGC was coinjected in skeletal muscles. After vector administration, animals were fed a high-fat diet as indicated in Figure 2.

3.3.1. *Pgc1α* and *Gck* expression in the skeletal muscle

Thirteen weeks after the AAV administration, the expression of *Pgc1α* and *Gck* was measured in skeletal muscles by real time PCR and compared to the expression obtained when each AAV was injected separately. Skeletal muscles injected with AAVPGC and AAV*Gck* (AAVPGC/*Gck*) expressed the same amount of glucokinase as that seen in muscles from animals injected with AAV*Gck* alone (Figure 28a). Similarly, muscles receiving both AAVs showed the same level of *Pgc1α* expression to that achieved when AAVPGC was injected alone (Figure 28b). Thus, the co-administration of AAVPGC and AAV*Gck* allowed us to over-express *Pgc1α* and *Gck* in the same skeletal muscle. Furthermore, co-administration of both AAV vectors did not affect the

individual performance of each vector, since the expression levels of *Gck* and *Pgc1 α* in skeletal muscles receiving both AAV vectors was the same as the skeletal muscles receiving just one of the genes.

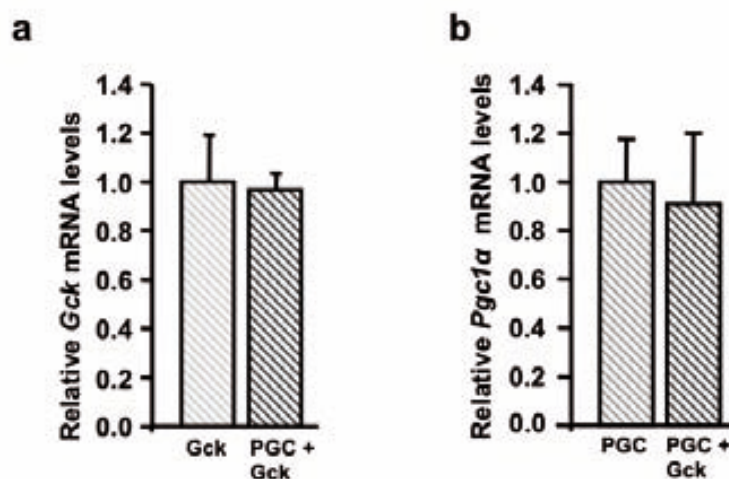


Figure 28. Expression of *Pgc1 α* and *Gck* genes in the skeletal muscles treated with AAVPGC and AAV*Gck*. (a) Glucokinase and (b) *Pgc1 α* expression was analysed by Quantitative Real Time PCR in skeletal muscles of AAV*Gck*-treated (Gck), AAVPGC-treated (PGC) or AAV*Gck* and AAVPGC-treated (PGC+Gck) animals fed a high-fat diet at week 13. The abundance of *Gck* and *Pgc1 α* expression was normalized by the expression of the housekeeping gene *36B4* as indicated in Material and Methods. Data are means \pm SEM of minimum 4 animals per group.

3.3.2. Body weight gain and adiposity

Control animals on HFD very rapidly developed obesity, gaining approximately three times more body weight than mice in chow-diet (Figure 29a). Meanwhile, the body weight gain in animals co-expressing *Pgc1 α* and *Gck* in the skeletal muscle did not change compared to their high-fat fed control counterparts. As Figure 29b shows, all groups of animals ate to the same extent either placed on a high fat or chow a diet. In agreement with the body weight gain, the eWAT weight and the circulating leptin levels were similarly increased in both the AAVPGC/*Gck* treated animals and the control animals in HFD (Figure 29c, d).

Thus, these results suggest that the muscular co-expression of *Pgc1 α* and *Gck* did not change the gain in body weight induced by a high-fat diet.

Furthermore, the co-expression of both genes abolished the body weight gain reductions seen when these genes were over-expressed individually.

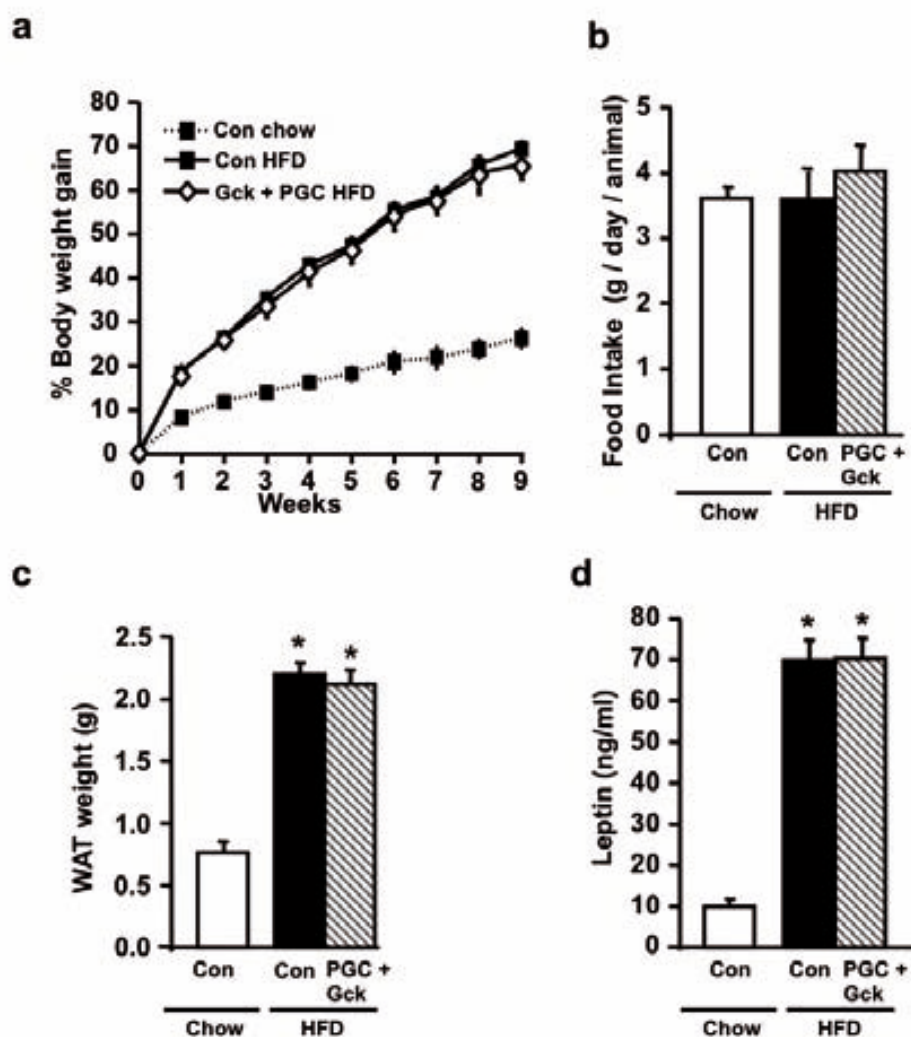


Figure 30. Body weight gain, food intake, eWAT weight and Leptin measurements. (a) Body weight gain was measured weekly in control (Con) or AAVPGC and AAVGck treated animals (PGC+Gck) under a High fat diet (HFD) or fed with a chow diet (chow), during nine weeks after the start of the high fat feeding (week 1). (b) Food intake. Food was measured weekly after week one. Results are expressed as grams of food consumed per day and animal. (c) Epididymal white adipose tissue weight was measured at week 13. (d) Circulating Leptin Levels were measured at week 13 as stated in Materials and Methods. Data are means \pm SEM of minimum 8 animals per Group. * $p < 0.05$ vs. Con Chow.

3.3.3. Hepatic triglyceride content

The liver from control and AAVPGC/*Gck*-treated mice fed a high fat diet presented a large amount of triglycerides compared to chow-fed control mice, revealed by the appearance of numerous lipid droplets (Figure 31a). The hepatic lipid content was similarly increased in both control and AAVPGC/*Gck*-injected animals fed a HFD (Figure 31b). Thus, muscular co-overexpression of *Pgc1 α* and *Gck* did not change the hepatic lipid accumulation induced by a HFD. Furthermore, these results indicate that the reduction in liver triglyceride accumulation observed when *Gck* and *Pgc1 α* were expressed individually, was now lost by the co-overexpression of these two genes.

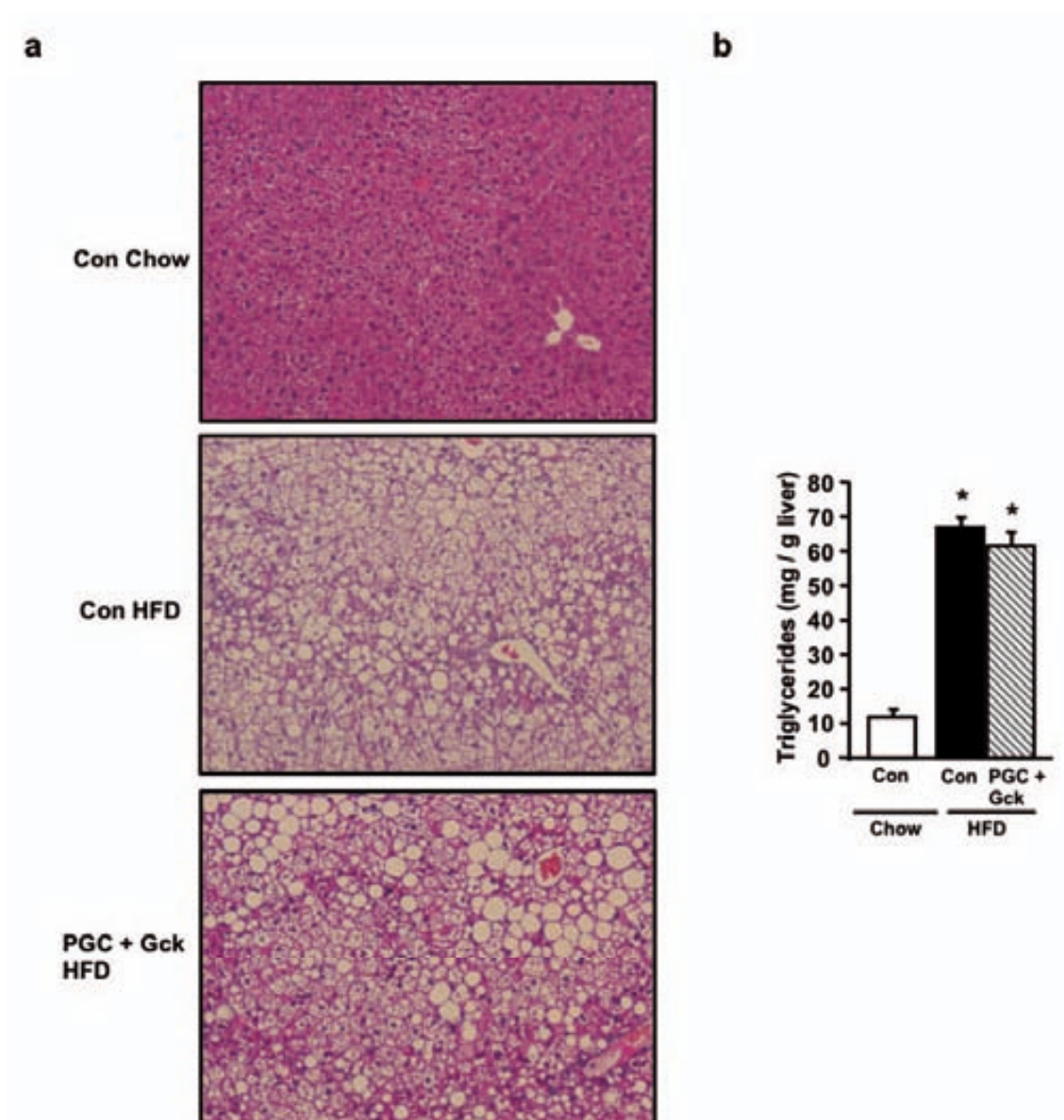


Figure 31. Liver histology and hepatic triglyceride accumulation. (a) Representative liver sections from control animals fed a chow diet (Con Chow), control animals fed a High fat diet (Con HFD) and AAVPGC/*Gck* treated animals in a high fat diet (PGC + *Gck* HFD) stained with Haematoxylin/Eosin are shown. Lipid accumulation inside hepatocytes is observed as an increase in the number and size of lipid droplets (100x). (b) Hepatic triglyceride quantification. Analysis was performed as stated in Materials and Methods. Data are means \pm SEM of minimum 5 animals per Group. * $p < 0.05$ vs. Con Chow.

3.3.4. Triglyceride content and fatty acid oxidation in the skeletal muscle

The lipid content was also measured in the skeletal muscle. Control animals in HFD showed an accumulation of triglycerides that was approximately three-fold higher than that observed in chow-fed control mice (Figure 32). Nevertheless, AAVPGC/*Gck* injected muscles showed a non-significant decrease in the accumulation of triglycerides compared to muscles from control animals in HFD (Figure 32).

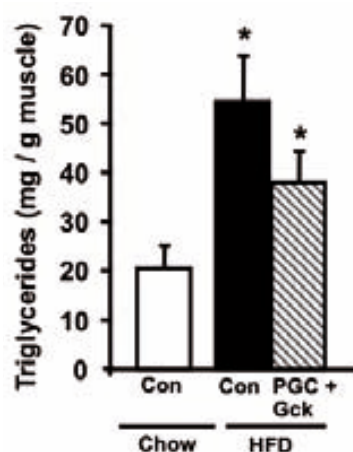


Figure 32. Skeletal muscle triglyceride content. Animals were euthanized at week 13 and *Gastrocnemius* muscle samples were obtained. The analysis was performed as stated in Materials and Methods. Data are means \pm SEM of minimum 5 animals per Group. * $p < 0.05$ vs. Con Chow.

In agreement with the trend observed in triglyceride accumulation, the expression of *Cpt1* in AAVPGC/*Gck*-treated muscles was approximately three-

fold higher compared to muscles from control mice fed the HFD (Figure 33). All together, these results suggest that fatty acid oxidation could be increased in muscles overexpressing *Pgc1 α* and *Gck* compared to muscles from HFD-fed mice.

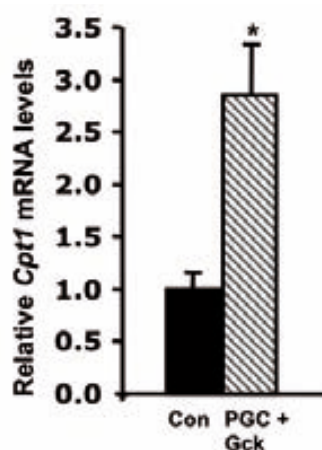


Figure 33. Expression of *Cpt1* in the skeletal muscle. *Cpt1* expression was analysed by quantitative Real Time PCR in *Tibialis cranialis* samples from high-fat fed Control (Con) and AAVPGC/*Gck* (PGC+*Gck*) treated animals euthanized at week 13. The abundance of *Cpt1* was normalized by the expression of the housekeeping gene *36b4* as indicated in Materials and Methods. Data are means \pm SEM of minimum 4 animals per group. * $p < 0.05$ vs. Con HFD.

3.3.5. Study of the glucose homeostasis

After nine weeks on HFD, blood glucose levels were measured in fed awake animals. No significant differences were found between groups (Figure 34a).

In order to study the insulin responsiveness, an insulin tolerance test was performed in AAVPGC/*Gck* treated animals. As expected, control animals in HFD showed a 20% lower reduction in their initial glucose levels than chow-fed

control mice in all time points measured, indicating that they were insulin resistant (Figure 34b). In contrast, AAVPGC/*Gck*-injected animals behaved like control animals in high fat diet. Thus, the muscular co-expression of *Pgc1 α* and *Gck* not only did not ameliorate the HFD-related insulin resistance, but abolished the insulin sensitising effects obtained when *Gck* was expressed individually (Figures 8, 26).

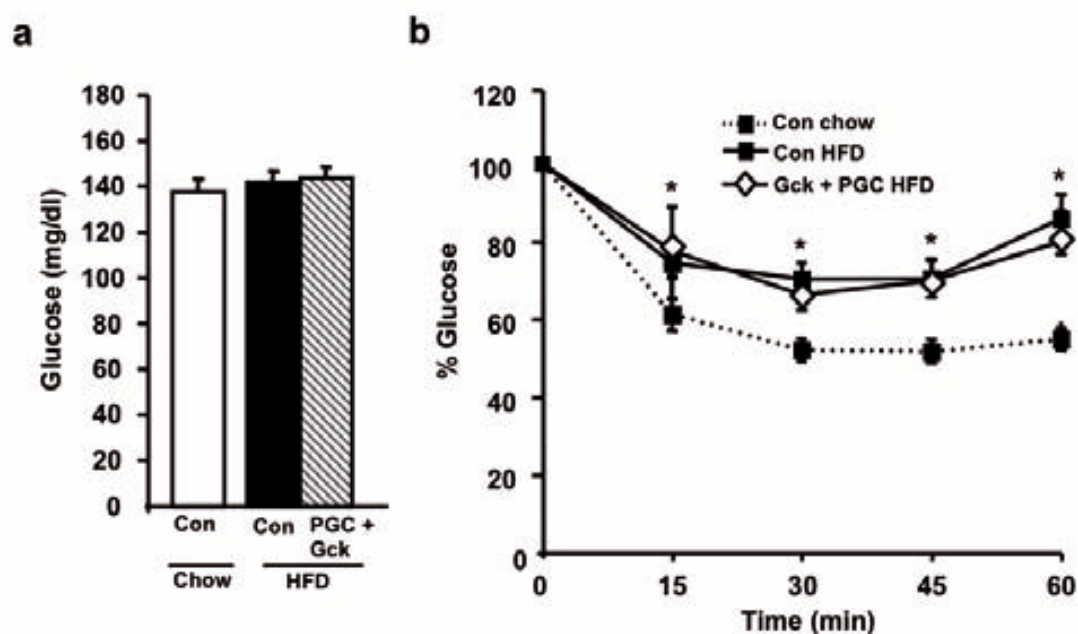


Figure 34. Glycemia and insulin tolerance test. (a) Blood Glucose levels measured in control chow fed animals (Con) and AAVPGC/*Gck*-treated (PGC+Gck) animals fed either with a chow diet (chow) or a High-fat diet (HFD). Measurements were performed at week 10. (b) Insulin Tolerance Test. Insulin (0.75 U/kg) was injected intraperitoneally into fed animals. Blood samples were taken from the tail vein at indicated times. Results are expressed as percentage of blood glucose values at time 0. Data are means \pm SEM of minimum 6 animals per group. * $p < 0.05$ vs. Con Chow.

3.3.6. Determination of circulating metabolites

At week 13 circulating free fatty acids levels presented a trend to be increased in high fat-fed animals compared to chow-fed mice (Figure 35a). Similarly, control animals in high fat diet showed a 2.5-fold increase in glycerol levels compared to chow-fed animals (Figure 35b). The co-expression of *Pgc1 α* and *Gck* did not significantly change the free fatty acid and glycerol levels compared to HFD-fed control mice.

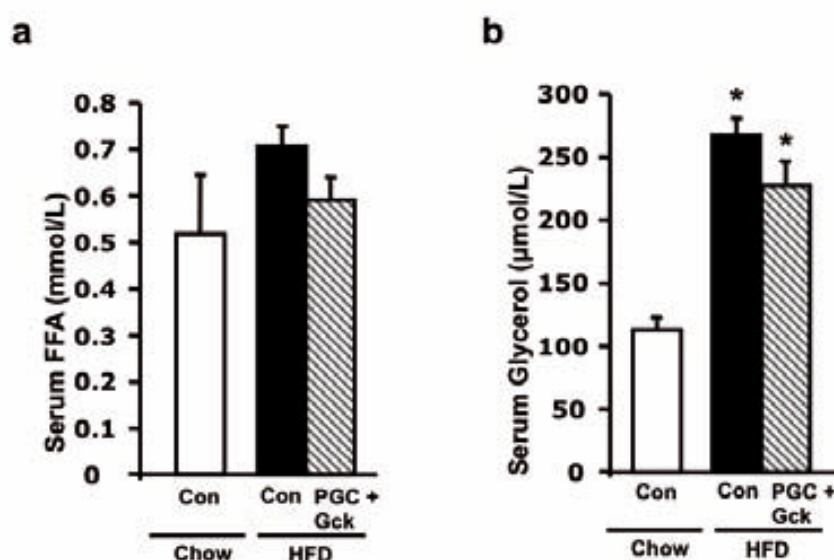


Figure 35. Serum levels of metabolites. (a) Free fatty acid and (b) Glycerol circulating levels were measured in control (Con) and AAVPGC-treated (PGC) animals fed either with a chow diet (chow) or a High-fat diet (HFD). Measurements were performed at week 13 of the experiment as stated in Material and Methods. Data are means \pm SEM of minimum 8 animals per Group. * $p < 0.05$ vs. Con Chow.

Thus, the muscular co-overexpression of *Pgc1 α* and *Gck* during a high fat diet did not prevent the diabetogenic consequences related to a high fat

feeding. Furthermore, most of the individual effects observed when *Pgc1 α* and *Gck* were overexpressed separately were lost when both genes were co-overexpressed in the same skeletal muscles.

The overexpression of *Pgc1 α* alone led to a mild decrease in body weight gain evolution during the high fat diet. This reduction was accompanied with a lower eWAT weight indicating that these animals could be burning more fat than their control counterparts. In agreement with that, the muscular expression of *Cpt1* was increased by the overexpression of *Pgc1 α* . However, this increase did not result in a significant reduction in muscle lipid accumulation suggesting that the expected *Pgc1 α* enhancement of lipid oxidation was not enough to potentially reduce the accumulation of lipids in this tissue. Furthermore, no improvements in insulin sensitivity were observed related to the overexpression of *Pgc1 α* .

As a coactivator, PGC1 α binds to a large number of transcription factors. However, the increase in lipid oxidation mediated by PGC1 α in the skeletal muscle is thought to occur mainly through the coactivation of PPAR δ

(Wang et al., 2003b). In fact, the sole overexpression of PPAR δ in the skeletal muscle of transgenic mice proved to be sufficient to protect these animals against the metabolic abnormalities related to a HFD (Wang et al., 2004). These animals remained insulin sensitive and lean when challenged with this diet. Hence, we wondered whether *Ppar δ* could be a good candidate gene to be overexpressed in the skeletal muscle with the aim of preventing the deleterious consequences of a prolonged HFD. Furthermore, in a different study we also evaluated whether overexpressing *Pgc1 α* and *Ppar δ* in the same skeletal muscle could also be a protective combination against a HFD feeding.

4.1. Design of an AAV1 with the *Ppar δ* gene

In order to over-express *Ppar δ* in the skeletal muscle of mice, an AAV1 vector carrying this gene (AAVPPAR) was designed. To this aim, the cDNA sequence of the mouse *Ppar δ* was cloned into the pGG2 plasmid (pGG2-PPAR) upstream of the polyadenylation signal (Poly A) and under the transcriptional control of the cytomegalovirus (CMV) promoter (Figure 36). The pGG2-PPAR was then used to produce the AAV1 vectors as stated in Material and Methods.



Figure 36. Schematic representation of the construct used to produce the AAVPPAR vector. CMV: cytomegalovirus promoter, poly A: Simian Virus 40 Polyadenylation signal; ITR: Inverted terminal repeat; PPAR δ : Peroxisome-proliferator-activated receptor delta

4.2. Metabolic effects of *Ppar δ* overexpression in the skeletal muscle of high-fat fed mice

With the aim of characterising the metabolic effects of over-expressing *Ppar* δ during a high fat diet, a total dose of AAVPPAR 9.6×10^{10} vg/animal was injected in the skeletal muscles of mice. After the administration, animals were placed under a high fat diet and the experimental design detailed in Figure 2 was followed.

4.2.1. *Ppar* δ expression in the skeletal muscle

Thirteen weeks after the AAV administration, the muscular expression of *Ppar* δ was checked by real time PCR analysis. As previously described (Hancock et al., 2008), the high fat diet itself increased the muscular expression of *Ppar* δ 3-fold compared to chow-fed animals (Figure 37). However, AAVPPAR injected mice overexpressed *Ppar* δ approximately 18-fold compared to HFD-fed control mice.

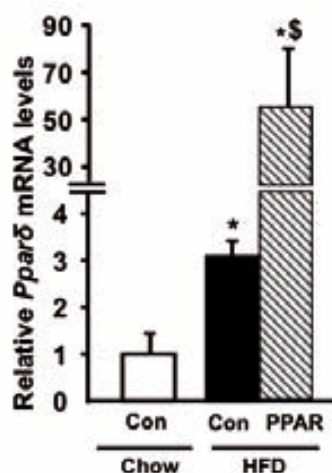


Figure 37. Expression of *Ppar* δ in the skeletal muscle. *Ppar* δ expression was analysed by quantitative Real Time PCR in *Tibialis cranialis* samples from control (Con) and AAVPPAR (PPAR) treated animals fed with a chow diet (Chow) or a high fat diet (HFD) and analysed at week 13

after vector administration. The abundance of *Ppar δ* was normalized by the expression of the housekeeping gene *36b4* as indicated in Materials and Methods. Data are means \pm SEM of minimum 4 animals per Group. * p <0.05 vs. Con Chow; § p <0.05 vs. Con HFD.

4.2.2. Body weight gain and adiposity

At week ten, chow-fed control animals presented a 20% increase in their body weight (Figure 38a). High fat fed control and AAVPPAR treated animals showed a similar increase of approximately 65% in their body weight, thus becoming obese (Figure 38a). No differences in food intake were observed between groups of mice (Figure 38b). In agreement with the body weight gain, the WAT mass of both control and AAVPPAR-treated animals, approximately increased three times compared to chow fed mice (Figure 38c). This was also consistent with a similar increase in serum leptin levels between HFD-fed control and AAVPPAR treated mice compared to chow fed animals (Figure 38d).

Thus, these results indicate that the muscular overexpression of *Ppar δ* did not change the body-weight gain after feeding a high fat diet.

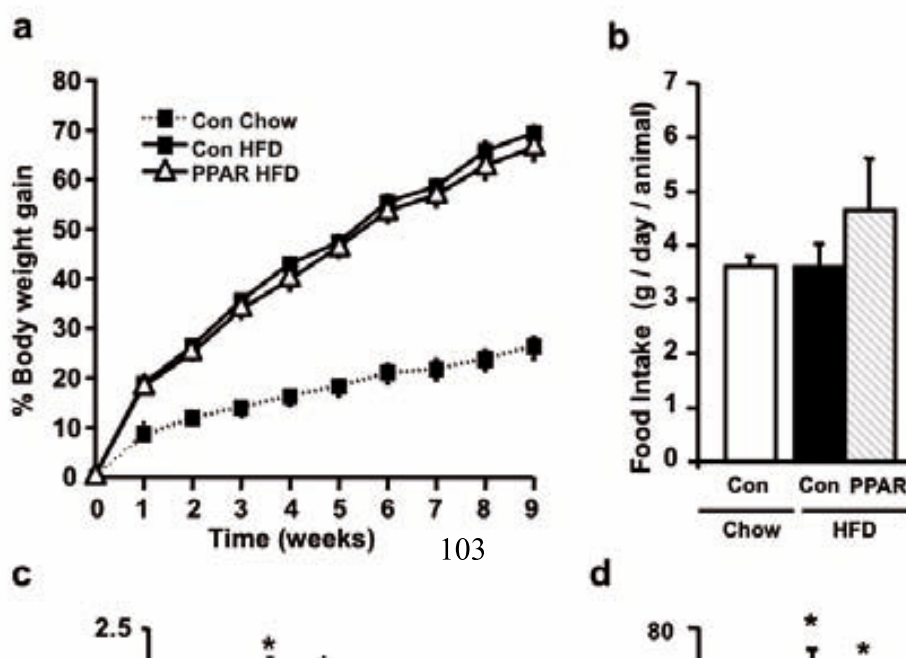


Figure 38. Body weight gain, food intake, eWAT weight and Leptin measurements. (a) Body weight gain was measured weekly in control (Con) or AAVPPAR treated animals (PPAR) under a high fat diet (HFD) or fed with a chow diet (chow) during nine weeks after the start of the high fat feeding (week 1). (b) Food intake. Food was measured weekly after week one. Results are expressed as grams of food consumed per day and animal. (c) Epididymal white adipose tissue weight was measured at week 13. (d) Circulating Leptin Levels were measured at week 13 as stated in Materials and Methods. Data are means \pm SEM of minimum 8 animals per Group. * $p < 0.05$ vs. Con Chow.

4.2.3. Hepatic triglyceride content

Control and AAVPPAR treated animals fed with a HFD presented a large increase in triglyceride accumulation compared to chow-fed control mice (Figure 39a). The high fat diet approximately increased the liver triglyceride content by a 6.5-fold in control animals compared to chow-fed mice. No differences were detected between AAVPPAR-treated mice and their control counterparts, indicating that *Ppar δ* overexpression did not prevent the appearance of liver steatosis (Figure 39b).

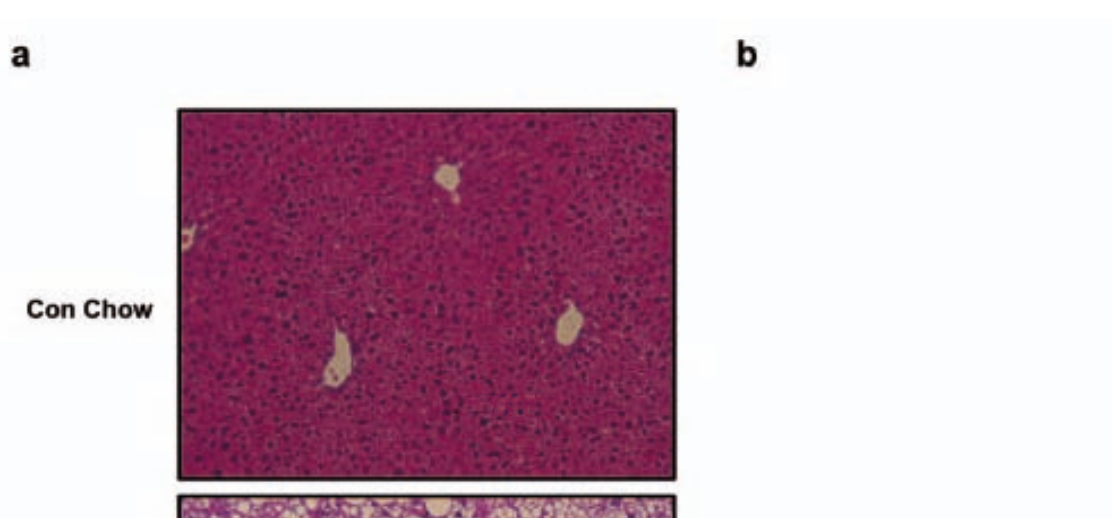


Figure 39. Liver histology and hepatic triglyceride accumulation. (a) Representative liver sections from control animals fed a chow diet (Con Chow) or a high fat diet (Con HFD) and AAVPPAR treated animals in a high fat diet (PPAR HFD) stained with Haematoxylin/Eosin are showed. Lipid accumulation inside hepatocytes is observed as an increase in the number and size of lipid droplets (100x). (b) Hepatic Triglyceride quantification. Analysis was performed as stated in Materials and Methods. Data are means \pm SEM of minimum 5 animals per group. * $p < 0.05$ vs. Con Chow.

4.2.4. Triglyceride content and fatty acid oxidation in the skeletal muscle

The lipid content was also measured in the skeletal muscles. The high fat diet increased the muscular fat accumulation by a 2.5-fold compared to muscles from chow-fed animals (Figure 40). AAVPPAR treated muscles accumulated fat to the same extent as the muscles from control animals in HFD (Figure 40). Thus, the muscular overexpression of *Ppar δ* did not prevent the high-fat diet-mediated lipid accumulation in the skeletal muscle.

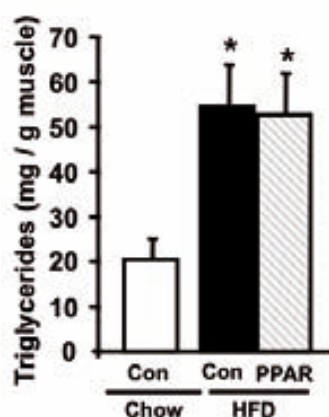


Figure 40. Skeletal muscle triglyceride content. Animals were euthanized at week 13 and *Gastrocnemius* muscle samples were obtained. The Analysis was performed as stated in materials and methods. Data are means \pm SEM of minimum 5 animals per Group. * $p < 0.05$ vs. Con Chow.

Cpt1 expression was also determined as a measure of fatty acid oxidation in skeletal muscles overexpressing *Ppar δ* . In agreement with the level of fat accumulation in the skeletal muscle, the abundance of *Cpt1* was not changed by the overexpression of *Ppar δ* compared to control muscles (Figure 41). Thus, this result suggests that muscular fatty acid oxidation was not modified by the expression of *Ppar δ* .

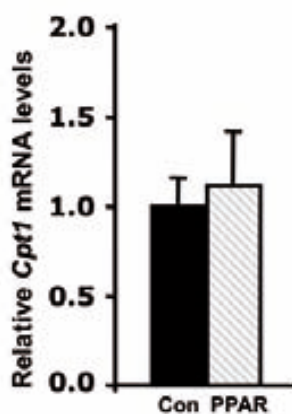


Figure 41. Expression of *Cpt1* in the skeletal muscle. *Cpt1* expression was analysed by quantitative Real Time PCR in *Tibialis cranialis* samples from High-fat fed Control (con) and AAVPPAR (PPAR)-treated mice at week 13 after AAV administration. The abundance of *Cpt1* was normalized by the expression of the housekeeping gene *36B4* as indicated in Materials and Methods. Data are means \pm SEM of minimum 4 animals per group.

4.2.5. Study of glucose homeostasis

Blood Glucose levels were determined 9 weeks after the beginning of the high fat diet. No significant changes in glycemia were found between groups (Figure 42a).

To study the insulin responsiveness in AAVPPAR treated mice, an insulin tolerance test was performed. After the exogenous insulin administration, chow-fed control animals reduced their initial glycaemia by a 50% approximately. HFD-fed control animals showed a reduction of about 30% in their initial glucose levels, indicating that they had become insulin resistant. AAVPPAR-injected animals presented a 35% reduction in their initial glycaemia, indicating that, similarly to HFD-fed control mice, they developed insulin resistance (Figure 42b).

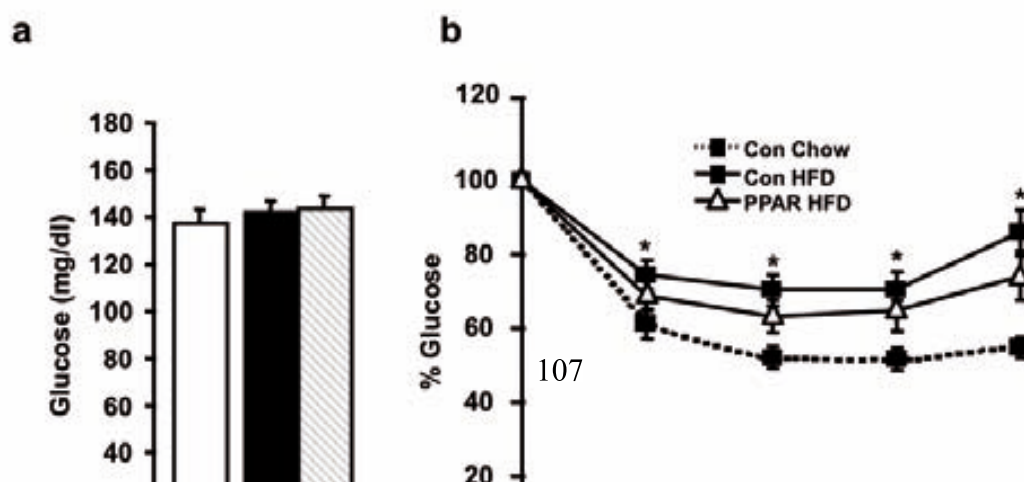


Figure 42. Glycemia and Insulin Tolerance Test. (a) Blood Glucose levels measured in control chow fed animals (Con) and AAVPPAR treated (PPAR) animals fed either with a chow diet (chow) or a High-fat diet (HFD). Measurements were performed at week 10. (b) Insulin Tolerance Test. Insulin (0.75 U/kg) was injected intraperitoneally into fed animals. Blood samples were taken from the tail vein at indicated times. Results are expressed as percentage of blood glucose values at time 0. Data are means \pm SEM of minimum 6 animals per Group. * p <0.05 vs. Con Chow.

4.2.6. Insulin signalling in the skeletal muscle

As an indicator of muscular insulin sensitivity, total and phosphorylated AKT were measured in the treated skeletal muscles of starved control and AAVPPAR mice fed a HFD, before and after insulin stimulation (Figure 43a). Subsequently, the fold increase of AKT phosphorylation between basal and stimulated conditions was calculated. As Figure 44b shows, control and AAVPPAR treated muscles presented a similar fold increase of AKT phosphorylation after insulin stimulation. Thus, this result indicates that the muscular overexpression of *Ppar δ* in adult mice did not improve the insulin signaling in HFD conditions, which was in agreement with the insulin resistance state observed in these animals.

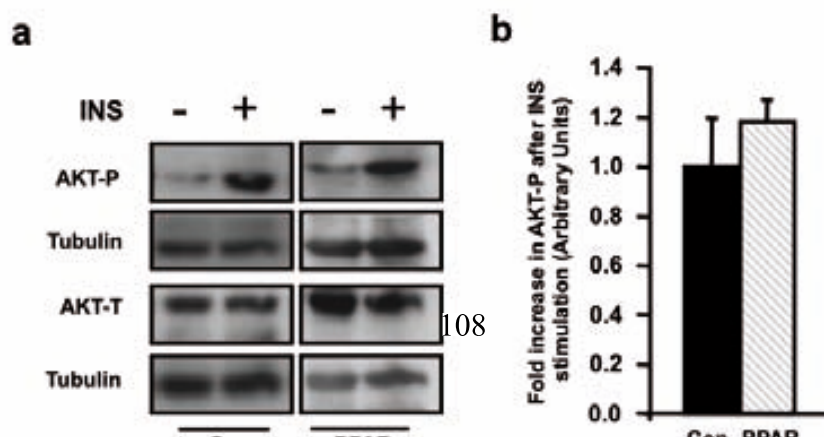


Figure 43. Analysis of the insulin signalling pathway in skeletal muscle. (a) Representative western blot analysis of phosphorylated (P)Ser473-AKT (AKT-P) and total AKT (AKT-T) from control high-fat fed (HFD), and AAVPPAR treated (HFD PPAR) animals stimulated with (+) or without (-) insulin (5 U/Kg). *Gastrocnemius* muscle protein lysates were used. (b) Band quantification by densitometric analysis. Results are expressed as means \pm SEM of the fold-increase in AKT-P after Insulin stimulation and relative to Con HFD of minimum 3 animals per group. Fold-increase was obtained by calculating the ratio between P^{Ser473}-AKT and total AKT in basal and stimulated conditions. Tubulin was used as a loading control. (n=3). These experiments were performed at week 13.

4.2.7. Determination of circulating metabolites

At week 13, serum FFAs and glycerol levels were determined. Free fatty acids presented a trend to be increased in HFD-fed control and AAVPPAR-treated mice compared to their chow-fed control counterparts (Figure 44a). Glycerol levels were approximately 2.5-fold increased in HFD-fed groups compared to animals fed a chow diet (Figure 44b).

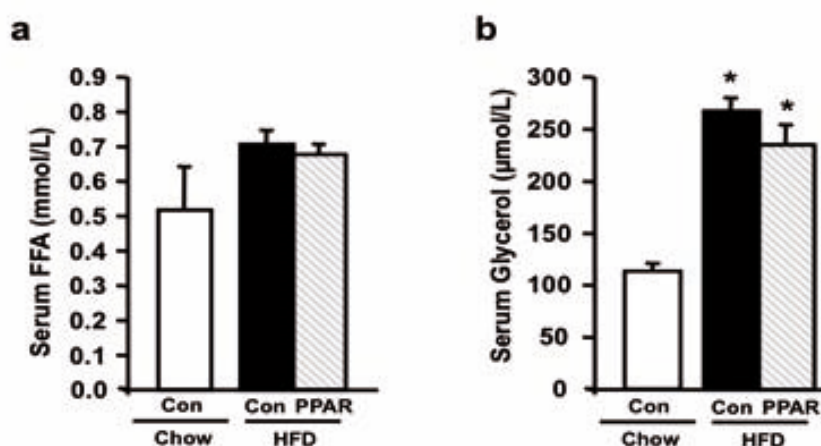


Figure 44. Serum levels of metabolites and hormones. (a) Free fatty acid and (b) Glycerol circulating levels measured in control (Con) and AAVPPAR-treated (PPAR) animals fed either with a chow diet (chow) or a High-fat diet (HFD). Measurements were performed at week 13 of the experiment as stated in Material and Methods. Data are means \pm SEM of minimum 8 animals per Group. * $p < 0.05$ vs. Con Chow.

4.3. Metabolic effects of *Ppar δ* and *Pgc1 α* overexpression in the skeletal muscle of high-fat fed mice

Results obtained by the overexpression of *Ppar* δ show that this approach did not prevent the development of obesity and insulin resistance. This may be the result of that the transgene, even though it was expressed, it may not have been active enough to produce a relevant biological effect. It has been shown that the transgenic animals overexpressing PPAR δ in the skeletal muscle that resulted in a prevention against HFD express a modified form of the protein that was constitutively active (Wang et al., 2003b). Given that the activation of the fatty acid metabolism by PPAR δ seems to be mediated through the coactivation of this transcription factor by PGC1 α , we aimed to determine whether overexpressing PPAR δ along with an overexpression of PGC1 α in the same skeletal muscle, could result in the prevention of the diabetogenic consequences of a prolonged HFD. Thus, in the last part of this study we administered both genes to the skeletal muscle of mice using a combination of AAVPPAR (9.6×10^{10} vg/mouse) and AAVPGC (1.8×10^{10} vg/mouse). Afterwards, mice were fed a high fat diet and analysed as stated in Figure 2.

4.3.1. *Ppar* δ and *Pgc1* α expression in the skeletal muscle

Thirteen weeks after the AAV administration mice were euthanized and the expression levels of *Pgc1* α and *Ppar* δ were determined in *Tibialis Cranialis* muscle. *Pgc1* α expression increased 4-fold in animals injected with AAVPGC and AAVPPAR (AAVPGC/PPAR) compared to control animals fed either with a chow or a HFD-diet (Figure 45a). These levels of expression of *Pgc1* α were similar to those observed when AAVPGC was injected alone, indicating that the infectivity of AAVPGC and the resulting expression of *Pgc1* α was not affected by the co-injection with AAVPPAR (Figure 45a). In contrast, the expression of *Ppar* δ in AAVPGC/PPAR injected muscles was approximately 150-fold increased

compared to Chow-fed control animals (Figure 45b). These levels of overexpression represent approximately a 3-fold increase compared to those achieved when AAVPPAR was injected alone, suggesting that the endogenous expression of *Ppar δ* was probably enhanced by the co-overexpression of *Ppar δ* and *Pgc1 α* .

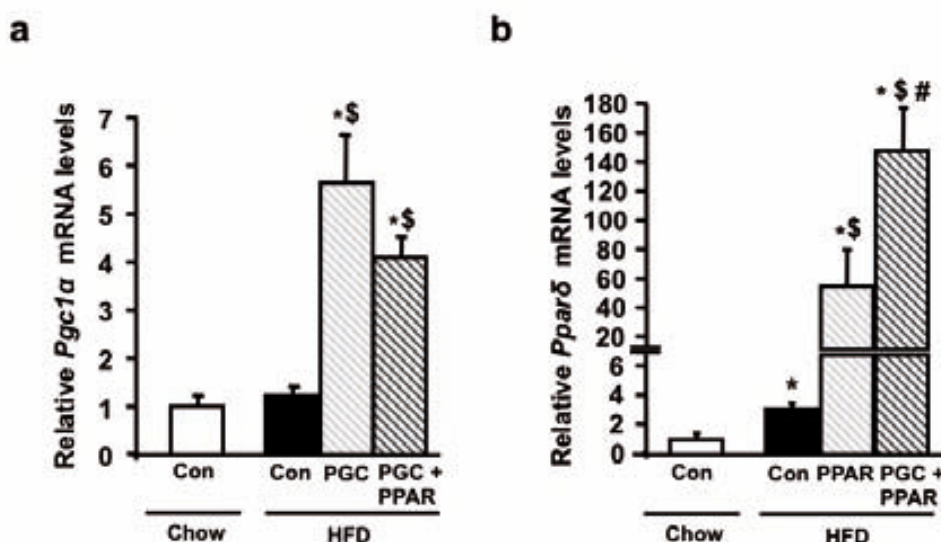


Figure 45. Muscular expression of *Pgc1 α* and *Ppar δ* . (a) *Pgc1 α* and (b) *Ppar δ* expression was analysed by Quantitative Real Time PCR of skeletal muscle samples of control (Con), AAVPGC-treated (PGC), AAVPPAR-treated (PPAR) or AAVPGC and AAVPPAR-treated (PGC+PPAR) mice fed a high-fat diet (HFD) or a chow diet (Chow) at week 13. The abundance of *Pgc1 α* and *Ppar δ* expression was normalized by the expression of the housekeeping gene *36B4* as indicated in Material and Methods. Data are means \pm SEM of minimum 4 animals per Group. * p <0.05 vs. Con Chow; \$ p <0.05 vs. Con HFD; # p <0.05 vs. PPAR.

4.3.2. Body weight gain and adiposity

After nine weeks in the HFD, the body weight gain of AAVPGC/PPAR injected animals was reduced approximately by a 10% compared to control animals fed the HFD (Figure 46a). This reduction was not due to differences in their feeding behaviour since both groups ate to the same extent (Figure 46b). In accordance to their reduction in body weight gain, WAT mass in AAVPGC/PPAR-injected animals was approximately 15% reduced compared to HFD-fed control animals (Figure 46c). However, no differences were found in circulating leptin levels between the two groups of mice (Figure 46c). Thus,

these results indicate that the muscular co-overexpression of *Ppar δ* and *Pgc1 α* during a high-fat diet led to a reduction in the body weight gain, partially contributed by a reduction of fat accumulation in WAT.

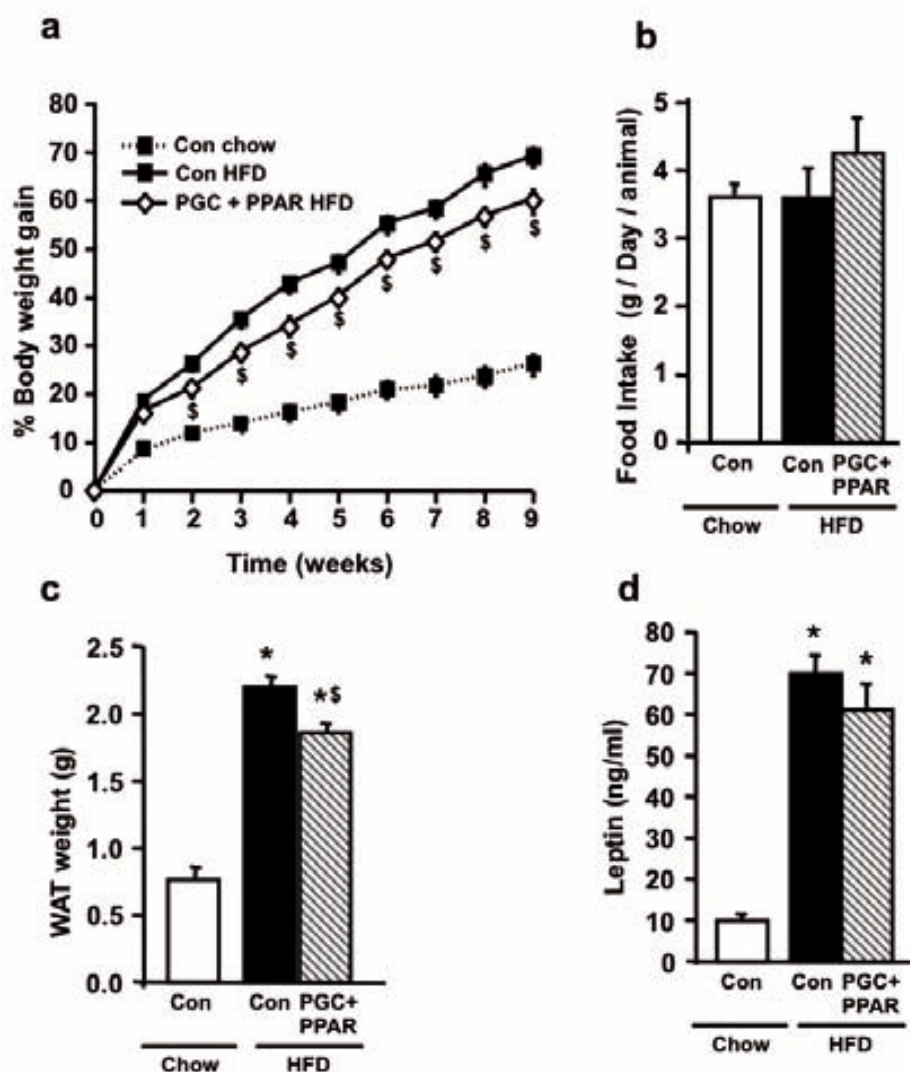


Figure 46. Body weight gain, food intake, eWAT weight and Leptin measurements. (a) Body weight gain was measured weekly in control (Con) or AAVPGC/PPAR treated animals (PGC+PPAR) under a High fat diet (HFD) or fed with a chow diet (chow) during nine weeks after the start of the high fat feeding (week 1). (b) Food intake. Food was measured weekly after week one. Results are expressed as grams of food consumed per day and animal. (c) Epididymal white adipose tissue weight was measured at week 13. (d) Circulating Leptin Levels were measured at week 13 as stated in Materials and Methods. Data are means \pm SEM of minimum 8 animals per Group. * $p < 0.05$ vs. Con Chow; § $p < 0.05$ vs. Con HFD.

4.3.3. Hepatic triglyceride content

Liver histological sections stained with Haematoxylin/Eosin showed that both control and AAVPGC/PPAR treated animals fed the HFD appeared to have

a massive accumulation of triglycerides in the liver compared to chow-fed mice (Figure 47a). Triglyceride quantification showed that both groups of animals in HFD presented the same increase in the triglycerides content in the liver. Thus, the co-overexpression of both *Ppar δ* and *Pgc1 α* in did not prevent the hepatic steatosis during prolonged high fat diets (Figure 47b).

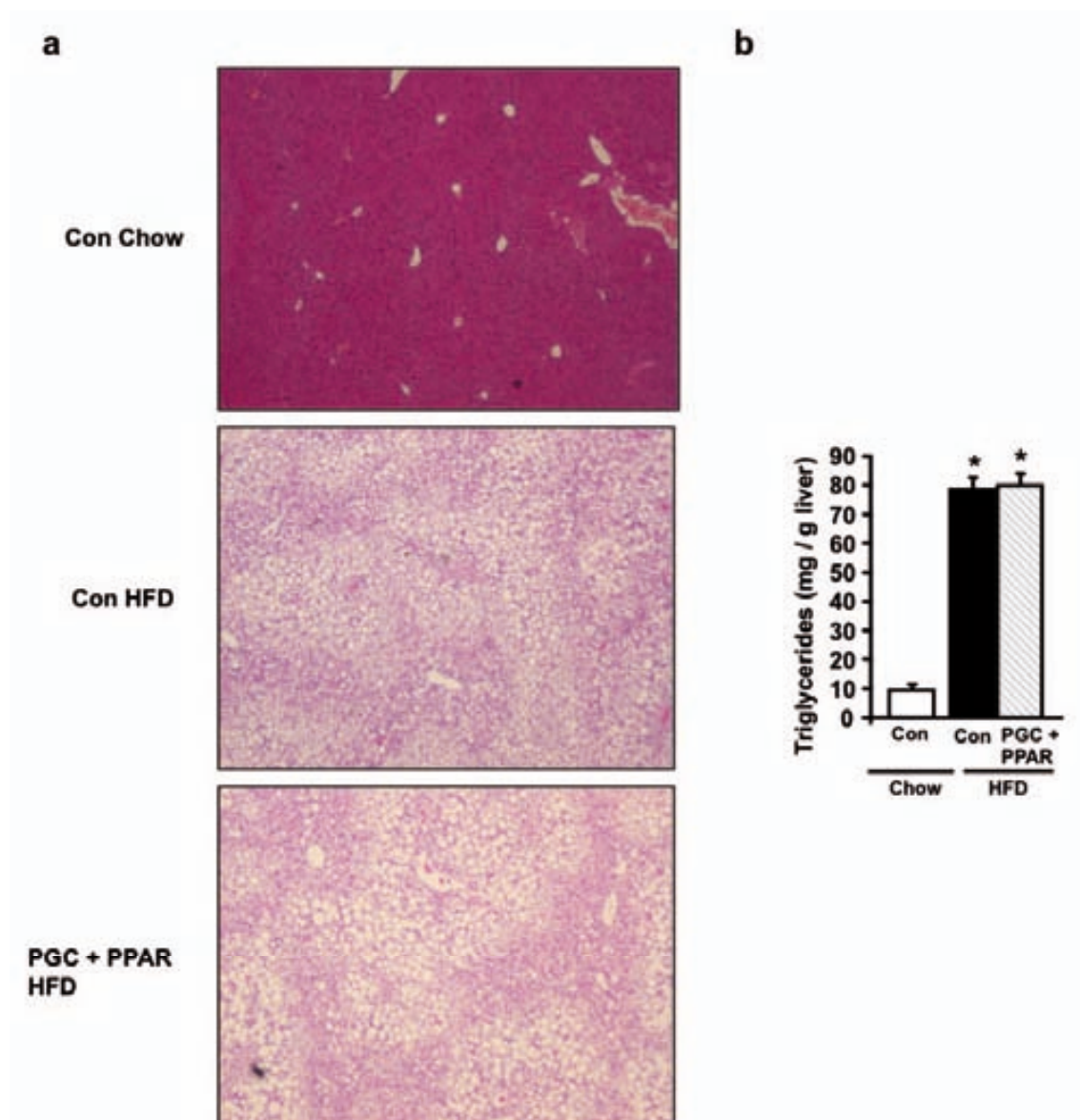


Figure 47. Liver histology and hepatic triglyceride accumulation. (a) Representative liver sections from control animals fed a chow diet (Con Chow), control animals fed a High fat diet (Con HFD) and AAVPGC/PPAR treated animals in a high fat diet (PGC + PPAR HFD) stained with Haematoxylin/Eosin are showed. Lipid accumulation inside hepatocytes is observed as an increase in the number and size of lipid droplets (40x). (b) Hepatic Triglyceride quantification.

Analysis was performed as stated in Materials and Methods. Data are means \pm SEM of minimum 5 animals per Group. * p <0.05 vs. Con Chow.

4.3.4. Triglyceride content and fatty acid oxidation in the skeletal muscle

The accumulation of triglycerides in the skeletal muscle of mice fed a HFD was highly increased compared to skeletal muscles from control animals fed a chow diet (Figure 48). Nevertheless, triglyceride accumulation in skeletal muscles from mice treated with AAVPGC/PPAR was almost normalised (Figure 48).

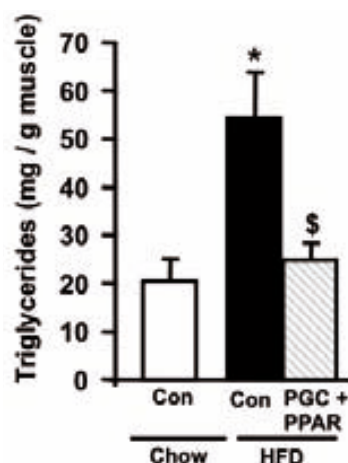


Figure 48. Skeletal muscle triglyceride content. Animals were euthanized at week 13 and *Gastrocnemius* muscle samples were obtained. The Analysis was performed as stated in Materials and Methods. Data are means \pm SEM of minimum 5 animals per Group. * p <0.05 vs. Con HFD; § p <0.05 vs. Con HFD.

The expression of *Cpt1* was studied in skeletal muscles overexpressing *Pgc1 α* and *Ppar δ* . The co-overexpression of *Pgc1 α* and *Ppar δ* led to an expression of *Cpt1* that was approximately 2.5-fold greater compared to muscles from high fat fed control animals (Figure 49), suggesting that fatty acid oxidation was increased. This level of overexpression was, at the same time, higher than that achieved when *Pgc1 α* and *Ppar δ* were overexpressed individually thus suggesting that the co-overexpression of *Pgc1 α* and *Ppar δ* in

the same skeletal muscle probably led to additive effects in the expression of *Cpt1*.

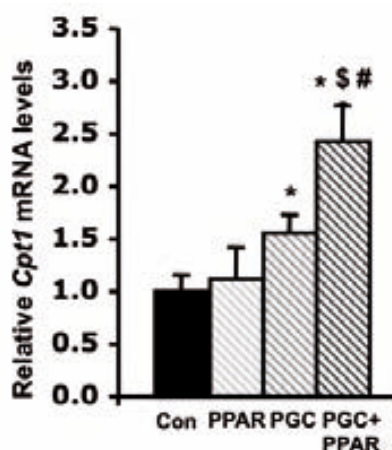


Figure 49. Expression of *Cpt1* in the skeletal muscle. *Cpt1* expression was analysed by quantitative Real Time PCR in *Tibialis cranialis* samples from High-fat fed Control (con), AAVPPAR treated (PPAR), AAVPGC treated (PGC), or AAVPGC/PPAR treated (PGC+PPAR) animals euthanized at week 13. The abundance of CPT1 was normalized by the expression of the housekeeping gene *36B4* as indicated in Materials and Methods. Data are means \pm SEM of minimum 4 animals per Group. * p <0.05 vs. Con HFD; \$ p <0.05 vs. PPAR; # p <0.05 vs. PGC.

4.3.5. Study of glucose homeostasis

After nine weeks of high fat feeding, no differences in glucose levels were detected between the different groups of animals (Figure 50a).

An insulin tolerance test was performed in AAVPGC/PPAR treated animals in order to study their insulin responsiveness. After the exogenous insulin administration, control animals fed a chow diet showed a 50% reduction in their initial glucose values (Figure 50b). As expected, glucose levels in control animals fed a HFD were only reduced by a 30%, indicating that they were insulin resistant (Figure 50b). In contrast, glycemia was reduced by a 50% in AAVPGC/PPAR injected animals, indicating that they remained insulin sensitive (Figure 50b). Thus, these results suggest that the muscular co-

overexpression of *Pgc1 α* and *Ppar δ* protected mice from high-fat diet-induced insulin resistance.

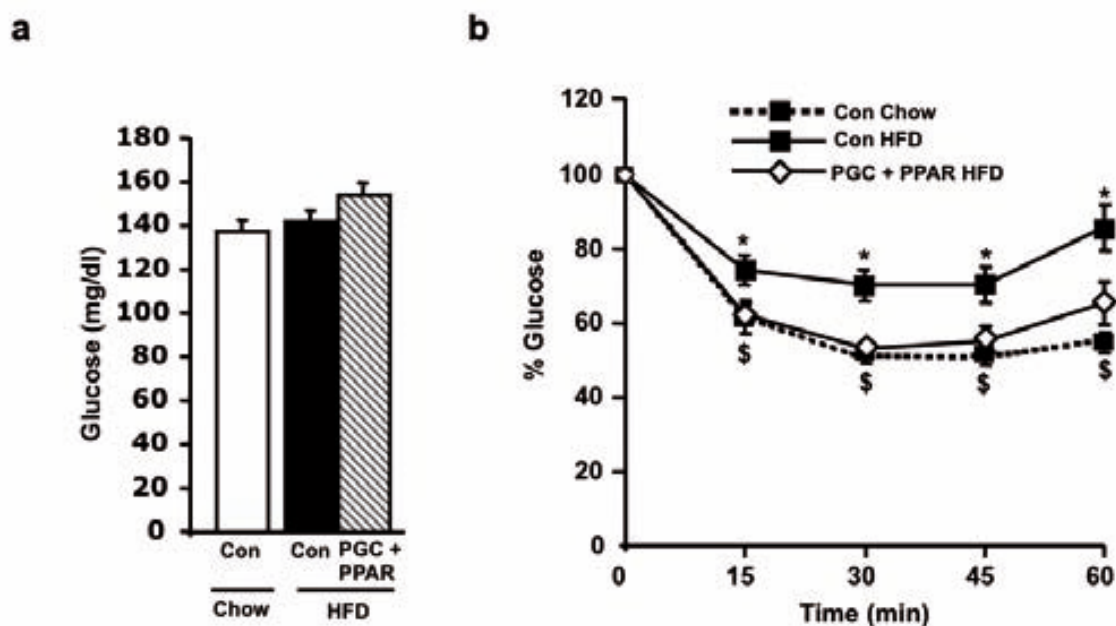


Figure 50. Glycemia and Insulin Tolerance Test. (a) Blood Glucose levels measured in control chow fed animals (Con) and AAVPGC/PPAR treated (PGC+PPAR) animals fed either with a chow diet (chow) or a High-fat diet (HFD). Measurements were performed at week 10. (b) Insulin Tolerance Test. Insulin (0.75 U/kg) was injected intraperitoneally into fed animals. Blood samples were taken from the tail vein at indicated times. Results are expressed as percentage of blood glucose values at time 0. Data are means \pm SEM of minimum 6 animals per Group. * $p < 0.05$ vs. Con Chow; $^{\$}p < 0.05$ vs. Con HFD.

4.3.6. Insulin signalling in the skeletal muscle

The fold increase in insulin-stimulated AKT-P in skeletal muscle from control and AAVPGC/PPAR was studied as a measure of muscular insulin sensitivity (Figure 51a). The skeletal muscles treated with AAVPGC/PPAR presented approximately a 50% increase in insulin-mediated AKT phosphorylation fold change compared to those from the HFD control group (Figure 51b). Thus, the muscular co-overexpression of *Pgc1 α* and *Ppar δ* in

adult mice resulted in an enhancement of the insulin signalling pathway in high fat diet conditions, suggesting that these muscles were more insulin sensitive.

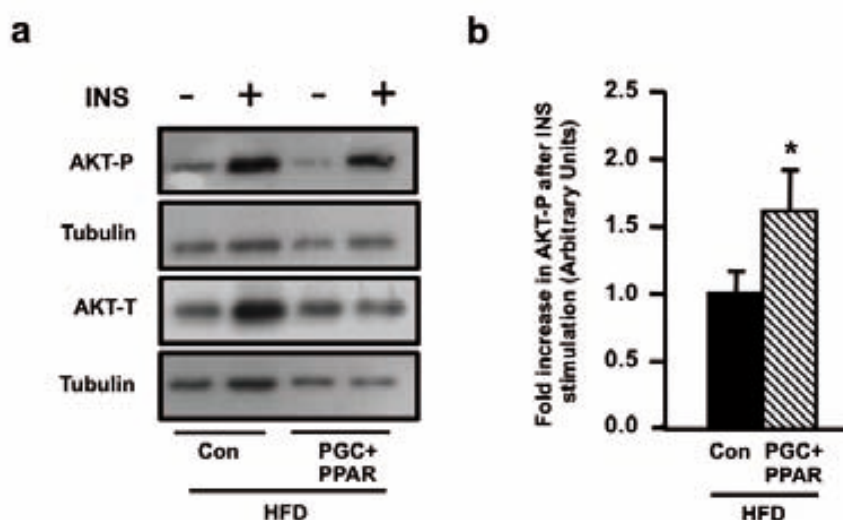


Figure 51. Analysis of the insulin signalling pathway in skeletal muscle. (a) Representative Western blot analysis of phosphorylated (P)Ser473-AKT (AKT-P) and total AKT (AKT-T) from control high-fat fed (HFD), and AAVPGC/PPAR treated (HFD PGC+PPAR) animals stimulated with (+) or without (-) insulin (5 U/Kg). *Gastrocnemius* muscle protein lysates were used. **(b)** Band quantification by densitometric analysis. Results are expressed as means \pm SEM of the fold-increase in AKT-P after Insulin stimulation and relative to Con HFD of minimum 3 animals per group. Fold-increase was obtained by calculating the ratio between P^{Ser473}-AKT and total AKT in basal and stimulated conditions. Tubulin was used as a loading control. * $p < 0.05$ vs. Con HFD. These experiments were performed at week 13.

4.3.7. Determination of circulating metabolites

In control and AAVPGC/PPAR injected animals, circulating free fatty acids presented a trend to be increased in control animals in high-fat diet compared to chow-fed control animals. Animals treated with AAVPGC/PPAR presented similar FFA levels to HFD-control mice (Figure 52a). Likewise, both control and AAVPGC/PPAR-injected animals fed a HFD presented approximately a 2.5-fold increase in circulating glycerol levels compared to chow-fed control mice (Figure 52b).

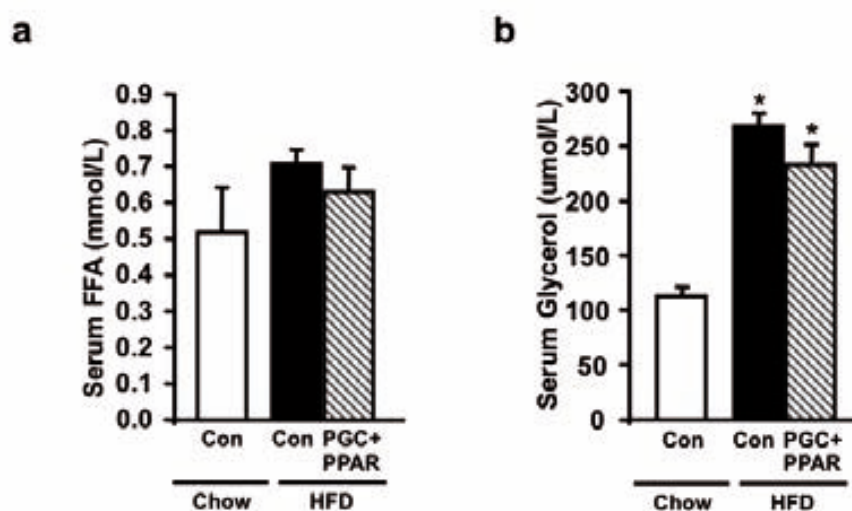


Figure 52. Serum levels of metabolites. (a) Free fatty acid and (b) Glycerol levels were measured in serum from control (Con) and AAVPGC-treated (PGC) animals fed either with a chow diet (chow) or a High-fat diet (HFD). Measurements were performed at week 13 of the experiment as stated in Material and Methods. Data are means \pm SEM of minimum 8 animals per Group. * $p < 0.05$ vs. Con Chow.

Thus, the muscular co-overexpression of *Pgc1 α* and *Ppar δ* resulted in the prevention of the development of insulin resistance induced by a high fat diet. Moreover, the body weight gain was reduced about a 10% by the expression of both genes during the diet.

Type 2 diabetes is the most common metabolic disease in the world and its prevalence is rapidly increasing (Chen et al., 2011). Although current treatments for type 2 diabetes have greatly improved the patient's quality of life, all therapies to date still present drawbacks and secondary side effects. Using any combination of the existing drugs along with changes in diet and exercise are only short-term effective, making of the insulin-treatment a must after a while. Additionally, the fact that each patient has a different sensitivity for each compound, which varies along with the development of the disease, plus the need of using two or more drugs at the same time, makes of the correct dosing very difficult and specific for each patient. Thus, the development of new effective treatments based on a better knowledge of the disease is a necessary landmark in the future research.

The recent development of gene therapy has given medicine a new tool to treat human diseases. To date, more than 1800 gene therapy clinical trials have been approved involving the treatment of various illnesses (Ginn et al., 2013). In the particular case of type 2 diabetes, no clinical trials based on gene therapy have been started to date. The polygenic nature of the disease, involving the metabolic malfunction of different tissues at the same time, makes of the choice of a candidate gene and a target tissue to manipulate difficult compared to other diseases. Thus, in order to develop a gene therapy trial for type 2 diabetes, it is important to first identify an adequate approach. Type 2 diabetes is strongly associated with obesity. The excessive accumulation of fatty acids in peripheral tissues is strongly linked to insulin resistance and reduced glucose uptake. Therefore, the development of gene therapy approaches centred on the expression of key genes to increase glucose uptake and fatty acid oxidation may probably improve insulin sensitivity and prevent the development of type 2 diabetes and obesity. With

this aim, in this study we evaluated the ability of different genes to increase glucose uptake and the oxidative capacity of the skeletal muscle in a model of high fat diet-induced diabetes.

We choose the skeletal muscle as the target organ to genetically manipulate for several reasons. Metabolically the skeletal muscle is a very important organ. It is a key participant in normal glucose homeostasis, accounting for up to 80% of glucose uptake after a meal (DeFronzo, 2004) and it is also a major tissue using fatty acid oxidation to produce energy, specially during fasting (Abdul-Ghani et al., 2010). Furthermore, insulin resistance in the skeletal muscle is a primary and key defect for the establishment of type 2 diabetes (DeFronzo et al., 2009). In the pathogenesis of insulin resistance, glucose uptake in the skeletal muscle is reduced, contributed by the reduced capacity of the skeletal muscle to phosphorylate glucose (Bonadonna et al., 1996). At the same time, there is a deregulation of the skeletal muscle oxidative function leading to the accumulation of triglycerides, contributing to the development of insulin resistance (Simoneau et al., 1999). In this regard, increases in glucose phosphorylation and oxidative capacity by the skeletal muscle have been suggested as possible strategies to ameliorate insulin resistance and type 2 diabetes (Jimenez-Chillaron et al., 1999; Zhang et al., 2010a).

Additionally, the skeletal muscle is an attractive tissue for gene therapy and gene transfer. It is easily accessible by non-invasive procedures and the resulting expression is stable due to the slow turnover of the muscle cells (Kay, 2011). To overexpress the different genes we used AAV1 vectors administrated to the skeletal muscle via intramuscular administration. This procedure has several advantages over others. It is straightforward and safe (Manno et al., 2003), vector dissemination outside the skeletal muscle is

modest (Arruda et al., 2001) and the transduction efficiency is not limited to the presence of pre-existing neutralizing antibodies (Manno et al., 2003). AAV1 vectors are among the best AAV serotypes to transduce the skeletal muscle, achieving higher levels of transgene delivery and long-term expression compared to other serotypes (Chao et al., 2000; Riviere et al., 2006). Furthermore, these vectors have been administered intramuscularly in a large number of studies using various animal models (Callejas et al., 2013; Fernandez-Sanchez et al., 2012; Mas et al., 2006) and in clinical trials, being safe and well tolerated (Buchlis et al., 2012; Flotte et al., 2011; Manno et al., 2003; Stroes et al., 2008).

During type 2 diabetes, glucose transport and phosphorylation are reduced in the skeletal muscle. However, experimental evidence suggests that the rate of intracellular glucose phosphorylation is impaired to a greater extent than glucose transport (Bonadonna et al., 1996). In our laboratory, we generated a transgenic mouse model overexpressing *Gck* in the skeletal muscle (Otaegui et al., 2000). The increase in glucose phosphorylation caused by the muscular overexpression of *Gck*, preserved glucose uptake, insulin sensitivity and prevented obesity when these animals were challenged with a high fat diet (Otaegui et al., 2003). Thus, in the first part of this study, we wondered whether increasing glucose phosphorylation in the skeletal muscle by transferring the *Gck* gene in high fat fed mice, could become a good approach towards developing a gene therapy protocol for type 2 diabetes.

We performed two separate experiments injecting two different doses of AAV*Gck* in the skeletal muscle. When injected with the lower dose, AAV*Gck*-treated animals became as obese as control animals in HFD. Accordingly, no differences were observed in WAT weight or triglyceride accumulation in liver.

However, as indicated in the insulin tolerance test, AAV*Gck*-treated animals preserved insulin sensitivity despite being fed with a high fat diet. In agreement, as high fat fed control animals needed hyperinsulinemia to maintain normal glucose levels, AAV*Gck*-treated mice presented normoglycaemia and normoinsulinemia. Additionally, the levels of muscular phosphorylated AKT were similar between groups. Since insulin is the main trigger for AKT-phosphorylation in the skeletal muscle, this suggests that the skeletal muscles expressing *Gck* remained insulin sensitive, probably contributing to the observed prevention in systemic insulin resistance. Thus, the increase in glucose phosphorylation mediated by *Gck* in the skeletal muscle probably preserved glucose uptake and insulin sensitivity in this tissue, contributing to attenuate the secretory response of pancreatic β -cells and maintaining normoinsulinemia. Normoinsulinemia and normal insulin sensitivity were also observed in transgenic animals expressing *Gck* in the skeletal muscle challenged with a HFD (Otaegui et al., 2003). However, Zucker fatty rats expressing *Gck* in the skeletal muscle driven by adenoviral vectors developed severe hyperinsulinemia, despite showing increased glucose uptake when stimulated with insulin (Jimenez-Chillaron et al., 2002). Apart from differences between the high fat diet mice model and the Zucker fatty rat that could explain the different outcomes in systemic insulin resistance, we expressed *Gck* in six different mice muscles as Jimenez-Chillaron et al. only transduced the *Gastrconemius* muscle of both rat forepaws. This suggests that the quantity of muscle mass expressing *Gck* might be important to the translation of the local muscular *Gck*-induced insulin sensitivity to systemic insulin sensitivity.

Since the expression of *Gck* in skeletal muscle proved to prevent obesity in our transgenic model, we wondered whether achieving a higher *Gck* expression could also lead to reductions in body weight gain while keeping

animals insulin sensitive during a HFD. Animals treated with the higher dose of AAV*Gck* achieved a higher expression of *Gck* during the experiment, as evidenced by the northern blot. AAV*Gck*-injected animals decreased their body weight gain by a 10% compared to HFD-fed control animals. During a high fat diet, the majority of weight gained is composed of lipids accumulating in different tissues. In agreement with the reduced body weight gain, AAV*Gck*-treated animals presented a trend to show reduced epididymal fat pad mass and a reduction in hepatic lipid accumulation. Despite that no differences in lipid muscular accumulation were detected between groups, the fact that *Cpt1* expression was increased in AAV*Gck*-treated muscles indicates that fatty acid oxidation was probably enhanced in this tissue, providing an explanation to the observed reduction in the HFD-induced body weight gain. This is in agreement with the transgenic mouse model expressing *Gck* in the skeletal muscle that was literally protected against obesity (Otaegui et al., 2003). These mice overexpressed *Ucp3* in the skeletal muscle, a protein suggested to increase fatty acid oxidation (Wang et al., 2003a). The fact that *Ucp3* and *Cpt1* are induced by the activation of AMPK, suggests a possible involvement of this protein in the activation of fatty acid metabolism by *Gck* (Li et al., 2007; Stoppani et al., 2002). Furthermore, as indicated in the insulin tolerance test, animals treated with the higher dose of AAV*Gck* kept being as insulin sensitive as chow-fed control animals. Thus, increasing the dose of AAV*Gck* resulted in a mild reduction in body weight gain, probably due to an increased fatty acid oxidation in the skeletal muscle, while preventing high fat diet-induced insulin resistance. This suggests that further increasing the dose of AAV*Gck* might result in higher reductions in body weight gain.

The skeletal muscles of type 2 diabetic patients show alterations in the capacity to metabolize fat, probably as a consequence of a reduced oxidative

capacity (Blaak, 2004; Kelley et al., 1999). The number and size of mitochondria, genes related to β -oxidation, and the activity of proteins in the respiration chain, have been found to be reduced in the skeletal muscle of type 2 diabetic individuals (Befroy et al., 2007; Morino et al., 2005; Simoneau et al., 1999). Given the key role in regulating the muscular oxidative capacity by PGC1 α as well as mitochondrial biogenesis, it has been suggested that this protein may have a role in the pathology of type 2 diabetes. Accordingly the muscular expression of PGC1 α is reduced in type 2 diabetic patients (Mootha et al., 2003; Patti et al., 2003). Thus, in the second part of this study, we checked whether increasing the oxidative capacity of the skeletal muscle by overexpressing *Pgc1 α* could prevent the deleterious effects of a high fat diet. Furthermore, increasing the oxidative capacity of AAV*Gck*-treated muscles by co-overexpressing *Pgc1 α* could result in ameliorations in body weight gain. The expression of PGC1 α has been described to increase glucose uptake by overexpressing *Glut4* in skeletal muscle cells (Michael et al., 2001). So *Pgc1 α* could further facilitate glucose uptake mediated by *Gck*. Thus, in a separate experiment, we also studied the metabolic effects of co-overexpressing *Pgc1 α* and *Gck* during a high fat diet.

AAVPGC-treated animals became as insulin resistant as control animals fed the HFD, as observed in the insulin tolerance test. The muscular insulin-induced activation of AKT in AAVPGC1 treated animals was lower than that observed in HFD control animals. This indicates that the overexpression of *Pgc1 α* reduced insulin sensitivity in the skeletal muscle of treated animals, situation that can help to develop systemic insulin resistance. AAVPGC1-treated animals presented a 10% reduction in body weight gain and WAT mass. This reduction could be explained by the observed increase in *Cpt1* expression

in the skeletal muscle, indicating that fatty acid oxidation was probably enhanced by the expression of *Pgc1 α* . However, this increase in fatty acid oxidation was not sufficient to avoid triglyceride accumulation in the skeletal muscle, suggesting that oxidation could have been over-surpassed by the income of fatty acids in this tissue. A misbalance between the fatty acid supply and oxidation in the skeletal muscle has been recently suggested to be related to muscular insulin resistance (Muoio et al., 2008). Interestingly, the specific muscular overexpression of PGC1 α in transgenic mice fed a high fat diet, resulted in the up-regulation of genes related to both fatty acid uptake and oxidation. These animals presented massive accumulation of muscular tryglicerides, lipid intermediate species and insulin resistance, suggesting increased supply of fatty acids over oxidation (Choi et al., 2008). Thus, the overexpression of *Pgc1 α* in AAVPGC-treated muscles could have also led to a similar metabolic misbalance leading to muscular insulin resistance. Furthermore, PGC1 α overexpression resulted in the increased abundance of TRB3, a negative regulator of AKT phosphorylation (Choi et al., 2008; Koo et al., 2004). Given the reduced insulin-stimulated AKT-phosphorylation in the skeletal muscles of AAVPGC-treated mice, TRB3 could have also contributed to the observed development of muscular insulin resistance.

Experiments using a transgenic model of specific muscular overexpression of PGC1 α have yielded controversial results. For instance, these animals were more prone to HFD-induced insulin resistance (Choi et al., 2008), however they showed protection against age-induced insulin resistance (Wenz et al., 2009). This suggests that PGC1 α has different effects in diet-induced versus age-associated insulin resistance. However, insulin sensitivity was restored when the same HFD-fed transgenic animals were subjected to an

exercise regime, suggesting that the beneficial effects of exercise were amplified by the expression of PGC1 α (Summermatter et al., 2013). Animal models that have reported deleterious effects in insulin sensitivity by PGC1 α , including our results, overexpressed this protein by more than 6-fold (Choi et al., 2008; Miura et al., 2003). In agreement with the expected role at promoting insulin sensitivity, the modest overexpression of PGC1 α in the *tibialis anterior* muscle of sedentary Zucker fatty rats, or in a transgenic mouse model (1.25-fold increase, and 2-fold increase respectively) was sufficient to prevent the development of insulin resistance in the skeletal muscle (Benton et al., 2010; Liang et al., 2009). Thus, the addition of an exercise protocol to AAVPGC-treated animals or a more moderate muscular overexpression of *Pgc1 α* , might lead to improved whole body insulin sensitivity. However, this needs to be determined.

An increase in the oxidative capacity of AAV*Gck*-treated muscles could ameliorate the reductions in body weight gain observed by the overexpression of *Gck*. Thus, we also studied the metabolic effects of co-overexpressing *Pgc1 α* and *Gck* during a high fat diet.

AAVPGC/*Gck* treated animals became as obese as control animals in HFD, along with similar levels of liver and WAT triglyceride content. However, in the skeletal muscles of AAVPGC/*Gck* treated animals, the expression of *Cpt1* was highly increased, along with a trend to present reduced accumulation of triglycerides. This indicates that fatty acid oxidation was probably increased in this tissue but surprisingly this did not have any effect on body weight gain. As *Gck* overexpressing animals remained insulin sensitive, those co-overexpressing *Pgc1 α* and *Gck* were as insulin resistant as control animals in HFD during the insulin tolerance test. Thus, the co-overexpression of *Pgc1 α* and *Gck* did only

not prevent insulin resistance, but abolished the insulin-sensitizing effects mediated by *Gck*. Long-chain Acyl CoAs can inhibit the activity of *Gck* (Tippett et al., 1982). It has been recently proposed that an incomplete oxidation of triglycerides, occurring when fatty acid oxidation is promoted without a coordinated increase in the TCA flux, can lead to the accumulation of harmful lipid intermediates, including LCACoAs, and insulin resistance (Muoio et al., 2006). Thus, an excessive activation of fatty acid oxidation by the co-overexpression of *Gck* and *Pgc1 α* could have led to *Gck* inhibition along with insulin resistance.

Thus, the muscular cooverexpression of *Pgc1 α* and *Gck* during a HFD abolished the reductions in body weight gain and the ameliorations in insulin resistance observed when these genes were overexpressed separately.

As a coactivator, PGC1 α binds to a large number of transcription factors including all members of the PPAR family. In the skeletal muscle, PPAR δ is considered to be the prevalent PPAR isoform and the most important one at regulating the lipid catabolism in this tissue (Evans et al., 2004; Muoio et al., 2002). Accordingly, the activation of PPAR δ in the skeletal muscle increases the expression of genes related to fatty acid metabolism, resulting in increased rates of fatty acid oxidation (Holst et al., 2003; Muoio et al., 2002; Wang et al., 2003b). The use of specific activators or transgenic models of PPAR δ , have led to ameliorations in insulin sensitivity and obesity (Oliver et al., 2001; Riserus et al., 2008; Tanaka et al., 2003; Wang et al., 2004). Thus, promoting fatty acid oxidation by the muscular overexpression of PPAR δ could be preventive of the diabetogenic consequences of a prolonged HFD. As another possible approximation, in the third part of this work, we studied the effects of

overexpressing PPAR δ in the skeletal muscle of HFD-fed mice. Furthermore, in a separate experiment, we also studied the effects of co-overexpressing PGC1 α and PPAR δ .

Despite we achieved a robust muscular overexpression of *Ppar δ* during the experiment, AAVPPAR-treated animals pretty much behaved like control HFD-fed animals. They developed obesity to the same degree as that observed in control HFD-fed animals, along with similar accumulations of triglycerides in liver, WAT and skeletal muscle. Accordingly, the muscular expression of CPT1 was the same in both groups, suggesting that the overexpression of *Ppar δ* did not change the levels of muscular fatty acid oxidation. The behaviour of AAVPPAR treated animals during the insulin tolerance test was not different from that observed in HFD-fed control animals, indicating that Insulin resistance was also not prevented by the expression of *Ppar δ* . In agreement, the levels of insulin-induced AKT phosphorylation were the same between groups, demonstrating that the muscular overexpression of *Ppar δ* did not prevent the development of insulin resistance in the skeletal muscle. Thus, the overexpression of *Ppar δ* in the skeletal muscle of HFD-fed animals remained without appreciable metabolic changes.

In order to be biologically active, PPAR δ needs to be activated by ligands which include fatty acids and their derivatives (Ehrenborg et al., 2009). Despite that a high fat diet provides a large diversity of fatty acids, our results suggest that our transgene might have not been active enough to produce a relevant observable biological effect. In contraposition with our results, the specific muscular overexpression of a constitutively activated form of PPAR δ conferred resistance to HFD-related obesity with improved metabolic profiles (Wang et

al., 2004). Other studies showing ameliorations in insulin resistance and obesity by PPAR δ used specific activators of the protein (Riserus et al., 2008; Tanaka et al., 2003). Thus, this indicates that the sole overexpression of the wild type form PPAR δ during a HFD is not enough to induce a relevant metabolic effect.

PPAR δ is a ligand-inducible transcription factor. When a ligand or an agonist binds to PPAR δ it suffers a conformational change that results in the recruitment of coactivators which allow transcription of target genes (Berger et al., 2002). PGC1 α is one of these coactivators found to interact with PPAR δ (Wang et al., 2003b). Interestingly, much of the actions of PPAR δ activation in the skeletal muscle resemble those observed by PGC1 α . For instance, the overexpression of PGC1 α in skeletal muscle (Lin et al., 2002) led to effects on muscle metabolism similar to those of overexpression of the activated form of PPAR δ (Wang et al., 2004). The muscular expression of both genes is up-regulated by exercise (Baar et al., 2002; Russell et al., 2003). The presence of PGC1 α and PPAR δ is enriched in type I oxidative muscle fibres (Lin et al., 2002; Wang et al., 2004). Both proteins share common target genes (Choi et al., 2008; Tanaka et al., 2003). This suggests that many metabolic adaptations of the skeletal muscle are orchestrated by the PGC1 α coactivation of PPAR δ . In accordance, fatty acid oxidation induced by PPAR δ activation was shown to be mediated and dependent on PGC1 α coactivation (Kleiner et al., 2009). Thus, we wondered whether the co-overexpression of both genes in the skeletal muscle, would lead to the prevention of insulin resistance related to a HFD.

The expression of *Pgc1 α* in AAVPGC/PPAR-treated muscles was similar to that obtained in AAVPGC-treated ones. However the expression of *Ppar δ* almost triplicated the one observed when AAVPPAR was used alone. Since the

dose of AAVPPAR in both experiments was the same, this indicates that the resulting expression was a consequence of the transcriptional activation of the endogenous PPAR δ gene by the co-overexpression of *Pgc1 α* and *Ppar δ* . Since PPAR δ and PGC1 α are induced under similar conditions, PPAR δ might be a possible target gene of the PPAR/PGC interaction.

The co-overexpression of *Pgc1 α* and *Ppar δ* led to 10% reduction in body weight gain during the HFD, along with a mild reduction in WAT mass. Additionally, triglyceride accumulation in the skeletal muscle of AAVPGC/PPAR-treated animals was almost normalised and comparable to chow-fed control skeletal muscles. The almost complete prevention in the accumulation of triglycerides in the skeletal muscles of AAVPGC/PPAR-treated animals was not observed when *Pgc1 α* and *Ppar δ* were overexpressed individually, suggesting a higher activation of fatty acid oxidation by the co-overexpression of both genes. In accordance, the muscular *Cpt1* expression in AAVPGC/PPAR treated animals, was higher than that achieved when *Pgc1 α* or *Ppar δ* were overexpressed individually. The expression of CPT1 induced by PPAR δ activation, along with the expression of other fatty acid oxidation genes, was potentiated by the overexpression of PGC1 α in cells, suggesting cooperative gene transcription mediated by PGC1 α coactivation of PPAR δ (Kleiner et al., 2009). Thus, the same mechanism of PGC1 α coactivation could be responsible for the enhanced *Cpt1* expression and for the increased fatty acid oxidation in the skeletal muscles of AAVPGC/PPAR treated mice. The enhancement in *Cpt1* also provides an explanation to the reduced body weight gain during the experiment.

AAVPGC/PPAR treated animals were as sensitive to insulin as chow-fed control mice during the insulin tolerance test. Accordingly, the increased insulin-induced AKT phosphorylation levels indicate that the skeletal muscles co-overexpressing *Pgc1 α* and *Ppar δ* were more insulin sensitive than those from HFD-fed control mice. The amelioration in muscular insulin resistance might be explained by the reduced accumulation of triglycerides in this tissue. However, an increase in fatty acid oxidation without a balanced increase in the TCA cycle activity can lead to incomplete triglyceride oxidation and insulin resistance. It has been recently proposed that in physiological conditions of high oxidative activity, such as during exercise, the coordinated activity of PPAR δ and PGC1 α would ensure the coupling between fatty acid oxidation and the TCA cycle (Muoio et al., 2006). This would be possible by the ability of PGC1 α to promote the expression of genes involved in the TCA cycle and genes involved in the formation of intermediates in the TCA cycle (anaplerotic genes) (Koves et al., 2005). This would couple the increases in AcetylCoA, induced by PPAR δ activation of triglyceride catabolism, to oxidation in the TCA cycle, and not to DAG or ceramide formation (Koves et al., 2005). Such mechanism would explain the observed increases in fatty acid oxidation along with preserved insulin sensitivity in the skeletal muscles of AAVPGC/PPAR treated animals, which probably contributed to the prevention of systemic insulin resistance during the diet.

Thus, the muscular co-overexpression of *Pgc1 α* and *Ppar δ* prevented the development of insulin resistance and reduced the body weight gain during a high fat diet.

In summary, we have developed a screening based on AAV-mediated gene transfer to the skeletal muscle with the aim of identifying a new gene therapy approach for type 2 diabetes. We show that the overexpression of *Pgc1 α* alone, or in combination with *Gck*, does not prevent the development of insulin resistance. Similarly, the overexpression of *Ppar δ* does not ameliorate the insulin resistance induced by a high fat diet. In contrast, the increase of muscular glucose phosphorylation by the overexpression of *Gck*, and the increase in the muscular oxidative capacity by the co-overexpression of *Pgc1 α* and *Ppar δ* , prevents the development of insulin resistance and reduces body weight gain in a model of diet-induced diabetes. Based on our results, we propose that the muscular overexpression of *Gck* or the co-overexpression of *Pgc1 α* and *Ppar δ* by using AAV vectors might have a great potential to treat type 2 diabetes. However, more studies will be needed to elucidate the feasibility of these approaches.

1. Increasing the muscular glucose phosphorylation by the overexpression of *Gck* using AAV vectors in skeletal muscles of adult mice, prevented the development of insulin resistance linked to a high fat diet.
2. Achieving a higher expression of *Gck* by increasing the dose of AAV*Gck* in the skeletal muscle, mildly reduced the body weight gain during a high fat diet while preventing insulin resistance. The reduction in body weight gain is probably attributable to an increase in muscular fatty acid oxidation.
3. The overexpression of *Pgc1 α* using AAV vectors in the skeletal muscles of adult mice did not prevent the development of insulin resistance induced by a high fat diet. Furthermore, the skeletal muscles overexpressing *Pgc1 α* were more insulin resistant under a high fat diet environment.
4. AAVPGC-treated animals presented a mild reduction in body weight gain during the high fat diet, probably contributed by an increased fatty acid oxidation in the skeletal muscle.
5. The AAV-mediated muscular co-overexpression of *Pgc1 α* and *Gck* did not prevent the development of insulin resistance and obesity during a high fat diet. Furthermore, the co-overexpression of both genes abolished the effects on body weight gain and insulin resistance seen when these genes were overexpressed alone.
6. The muscular overexpression of *Ppar δ* did not ameliorate the high fat diet-induced insulin resistance and obesity.

7. The muscular co-overexpression of *Pgc1 α* and *Ppar δ* reduced the body weight gain related to a high fat diet. This was probably caused by an increase in fatty acid oxidation in the skeletal muscles overexpressing both genes.

8. The muscular co-overexpression of *Pgc1 α* and *Ppar δ* prevented the development of insulin resistance during a high fat diet. This is probably due to an increase in the oxidative capacity of the skeletal muscles overexpressing both genes, thus normalising the muscular triglyceride accumulation and contributing to the observed increase in muscular insulin sensitivity.

9. This study represents the first search for a gene transfer approach to treat type 2 diabetes. The muscular overexpression of *Gck* or the co-overexpression of *Pgc1 α* and *Ppar δ* by AAV vectors might be potential new approaches to treat insulin resistance and type 2 diabetes.

1. MATERIALS

1.1. Bacterial Strains

The chemically competent *E.Coli DH5 α* strain (Invitrogen) was used to obtain all the plasmid preparations used in this study. Since all plasmids were carrying the ampicillin resistance cassette, the bacterial culture was grown using Luria broth's (LB, Conda, Madrid) medium supplemented with 50 μ g/ml ampicillin. When cells were grown on a solid medium, 2% agar was added to the LB medium.

1.2. Animals

8-week old C57BL/6 mice were used for all experiments (Harlan, Indianapolis, Indiana, USA). Mice were kept in a specific pathogen-free facility (SER-CBATEG) under controlled temperature and light conditions (12 hours of light and 12 hours of darkness with lights on at 8 a.m.). Mice had free access to water and to chow diet (2018S Teklad Global, Harlan Teklad, Madison, Wisconsin, USA) or a high fat diet (TD.88137, Teklad Global diets, Harlan Teklad, Madison, Wisconsin, USA).

1.3. Anaesthetics

For tissue sampling, animals were anesthetised by means of inhalational anaesthetics Isoflurano (IsoFlo[®], Abbot Animal Health, Illinois, USA) and euthanized by decapitation. Tissues were excised and kept at -80 °C until analysis.

For insulin-induced AKT-phosphorylation studies, animals were anesthetized with a solution containing 2ml of Ketamine (Imalgene 500, Merial,

Lyon; France), 0.5 ml of Xylazine (Rompun, Bayer HealthCare, Kiel, Germany) in 7.5 ml of PBS. Animals were injected intraperitoneally with 10 μ l of the solution per gram of mice body weight.

Animal care and experimental procedures were approved by the Ethics Committee in Animal and Human Experimentation of the Universitat Autònoma de Barcelona (UAB).

1.4. Antibodies

The specification of the antibodies and reagents used for the detection of proteins by immunohistochemistry and Western Blot are summarized in the following table:

Antibody	Raised in	Supplier	Code
Immunohistochemistry			
Primary Antibodies			
Anti-GFP	goat	Abcam	ab6673
Secondary Antibodies			
Anti-Goat IgG	donkey	Santa Cruz	SC-2042
Western-Blot			
Primary Antibodies			
Anti-AKT phosphorylated (Ser 473)	rabbit	Cell Signalling	9271
Anti-AKT	rabbit	Cell Signalling	9272
Anti-Tubulin	rabbit	Abcam	ab4074
Secondary Antibodies			
HRP Anti-rabbit IgG	swine	Dako Cytomation	P0217

1.5. Plasmids

The plasmids used in this study are summarized in the following table:

Name	Promoter	Gene of Interest	PolyA
pGG2- <i>Gck</i>	CMV	<i>Gck</i>	SV40
pGG2-PGC	CMV	PGC1 α	SV40
pGG2-PPAR	CMV	PPAR δ	SV40

The CMV promoter contains the human cytomegalovirus (CMV) major immediate/early promoter/enhancer. It directs ubiquitous expression.

The following table summarizes the strategies to construct the different plasmids:

Name	Source	
pGG2- <i>Gck</i>	Vector	pGG2 (Généthon, Evry, France) digested with EcoRI
	Insert	pTG-6600- <i>Gck</i> (CBATEG) digested with EcoRI
pGG2-PGC	Vector	pGG2 (Généthon, Evry, France) digested with Xho I, Not I
	Insert	pTG-6600-PGC (CBATEG) digested with Xho I, Not I
pGG2-PPAR	Vector	pGG2 (Généthon, Evry, France) digested with Xho I, Not I
	Insert	pYX-ASC-PPARd (Open biosystems, Livermore, CA, USA) digested with Sal I, Not I

The rat *Gck* cDNA was originally given by Dr.P.lynedijan (Genève university, Genève, Switzerland).

The mouse PGC1 α cDNA was originally given by Dr.B.Spieguelman (Dana-Farber Cancer Institute, Boston, MA, USA).

1.6. Probes

Rat glucokinase probe was obtained as a 1.7kb EcoRI-AvrII digestion fragment from the pGG2-Gck plasmid.

1.7. Reagents

All molecular biology reagents were obtained from the commercial manufactures Roche (Roche Diagnostics Corp., IN, USA), Invitrogen Corporation (now Life Technologies) (San Diego, CA, USA), Bio-Rad Laboratories (Hercules, CA, USA), Amersham Biosciences (Piscataway, NJ, USA), Sigma (St.Louis, MO, USA), Promega Corporation (Madison, WI, USA), BASF (Barcelona, Spain), Qiagen (Hilden, Germany), QBIOgen (now MP Biomedicals) (Irvine, CA, USA), Fermentas (St. Leon-Rot, Germany) and New England Biolabs (Ipswich, MA, USA).

2. Methods

2.1. Basic DNA techniques

2.1.1. Plasmid DNA preparation

Minipreparations of plasmid DNA were performed using the alkaline lysis protocol originally described by Birnboim and colleagues (Birnboim et al., 1979). When higher amounts of plasmid DNA were required, the EndoFree Plasmid Mega Kit (Qiagen) was used.

2.1.2. DNA digestion with restriction enzymes

Each restriction enzyme required specific reaction conditions of pH, ionic strength and temperature. Therefore, in each case, the manufacturer's instructions were followed (New England Biolabs, Roche, Promega or Fermentas). In general, DNA was digested at a concentration of 0.5 µg/µl using 1-4 units of the enzyme per µg of DNA. Digestions were carried out for 2-3 h with the specific buffer and the digestion products were analyzed in agarose gels. If DNA was to be cleaved with two or more restriction enzymes, digestions were carried out simultaneously if the buffer and temperature was compatible for all restriction enzymes. When the enzymes had different requirements, digestions were performed sequentially. After the first digestion of DNA with one enzyme, it was purified from salts and enzyme, etc. using the GeneClean® kit (QBIogene) according to the manufacturer's instructions. The DNA was eluted in 30 µl of water and the second digestion performed directly.

2.1.3. Dephosphorylation of DNA fragments

DNA can be rendered resistant to self-ligation by enzymatic removal of phosphate residues from their 5' termini with phosphatases. The Shrimp Alkaline Phosphatase (SAP, Promega) was used and dephosphorylation reactions were performed for 30 min at 37°C with the manufacturer's buffer. Upon completion, the enzyme was inactivated by heating to 65° C for 15 min.

2.1.4. Ligation of DNA fragments

The bacteriophage *T4 DNA ligase* was used for the ligation reactions following the manufacturer's instructions (New England Biolabs). The reaction was carried out in the presence of the ligation buffer with ATP for 2-3 h at 16°C.

2.1.5. DNA resolution and purification

Electrophoresis through agarose gels was the standard method used to separate, identify and purify DNA fragments. One per cent agarose gels were used to resolve DNA fragments between 0.5-7 kb. The location and relative size of DNA within the gel was determined by staining the gel with low concentrations of the fluorescent dye ethidium bromide, which intercalates between the two strands of DNA. The presence of DNA was visualized with low wavelength ultraviolet (310 nm) light using a transilluminator and a camera system (Syngene). This technique allows detection down to 5 ng of DNA. The relative sizes of DNA fragments were calculated comparing the location of the DNA band with the bands of the DNA 1kb ladder (Invitrogen). Gels were prepared by dissolving agarose in 1x TAE (Tris-acetate pH 8.3, 40mM and EDTA 1mM). Samples were loaded in 10x loading dye and electrophoresed in 1x TAE electrophoresis buffer at 80 V.

2.1.6. Transformation of competent E.Coli

Plasmid DNA can be introduced into competent bacteria by the process of transformation. Heat-shock transformation was the method of choice. Competent cells were thawed on ice at the moment of use and 1-3 μ l (1-10 ng) of the DNA ligation reaction or control DNA was added directly to the cells. Cells and DNA were mixed and incubated on ice for 30 min. After that, a heat-shock of 30 seconds in a 42°C water bath was applied after which cells were immediately put on ice for 2 minutes. Nine hundred μ l of LB was added and cells incubated for 1 hour at 37°C with moderate shaking. Following this, 100 μ l of the suspension was plated in LB plates with the appropriate antibiotic and incubated at 37°C overnight.

2.2. RNA analysis

2.2.1. Total RNA isolation

Total RNA was obtained following the commercial TriPure Isolation Reagent (Roche) protocol. This protocol is based on the method described previously. Basically, 50-100 mg of skeletal muscle samples were homogenized in 1 ml of with a Polytron® type tissue homogenizer. RNA isolation from other cell components is based on a phenol- chloroform extraction using guanidine thiocyanate as a ribonuclease inhibitor. RNA is then precipitated with isopropanol, and washed with 70% ethanol. Finally, the RNA pellet is resuspended in 30 µl of water treated with diethylpyrocarbonate (DEPC), which acts as a ribonuclease inhibitor. The final RNA concentration was determined by measurement of the absorbance at 260 nm using a Nanodrop 1000 spectrophotometer (Thermo Scientific, USA).

2.2.2. Analysis of RNA expression by Northern Blot

2.2.2.1. RNA electrophoresis in agarose/formaldehyde denaturing gels

The isolated total RNA was mixed with the appropriate volume of a 5x denaturing loading buffer (deionised formamide, MOPS/EDTA, formaldehyde, glycerol, sterile H₂O, and bromophenol blue as a colorant) and heated at 65°C for 15 minutes, after which it was immediately placed in ice to prevent renaturalization. The denaturalized RNA samples were then loaded and run for 3-4 hours at 50V in denaturing 1% agarose/MOPS gels containing 2.2 M formaldehyde. Given the conditions of the electrophoresis, the RNA keeps denaturalized, allowing the separation of the different mRNA depending on their molecular weight. Moreover, to prevent enzymatic degradation of RNA by ribonucleases, all the solutions were prepared with RNase-free water and were autoclaved and filtered.

2.2.2.2. Transference of RNA from gel to membrane

The RNA in the gel was then transferred to a positively charged nylon membrane (Roche Diagnostics, USA) by using the Turboblotter® system (Schleicher & Schuell, Keene, New Hampshire). This system uses the negative pressure applied by the capillarity of a high ionic strength buffer like SSC 10x (NaCl 1.5M, sodium citrate 0.15M, pH 7.4) through absorbent paper GB002 and GB004 (Schleicher & Schuell, Keene, New Hampshire). After at least 2 hours, RNA was covalently linked to the nylon membrane by the 120.000 µJ UV irradiation using the UV-Stratalinker 1800 (Stratagene, La Jolla, CA).

2.2.2.3. Prehybridization and hybridization of membrane

Once the RNA was fixed in the nylon membrane, it was incubated with a prehybridization/hybridization buffer (Na₂HPO₄ 0.25 mM pH 7.2, SDS 20%, EDTA 1mM, Blocking reagent 0.5%) for 2 hours at 65°C in rotational agitation. This solution blocks the parts of the membrane that have no RNA fixed in it, and therefore reduces non-specific hybridization. Afterwards, the radioactively marked probe is added to the solution, and it is incubated at 65°C overnight.

2.2.2.4. Radioactive labelling of DNA probes

The commercial kit Ready-to-Go™ DNA Labelling Beads (-dCTP32) (Amersham Biosciences) was used to label the probe following the manufacture's instructions. Briefly, 25 ng of the probe were boiled for 5 minutes in a final volume of 45 µl to denature DNA, and quickly placed in ice for 2 minutes to avoid renaturalisation. The denatured DNA solution was then added to a lyophilized mixture containing dATP, dGTP, dTTP and the Klenow

fragment of the E. coli DNA polymerase provided by the manufacturer. Next, 5 μ l of [α -³²P]-dCTP (3000 Ci/mmol; Amersham Corp., Arlington Heights, Ill, USA) was added and the mixture incubated for 15 minutes at 37 °C. This technique allows the synthesis of DNA probes uniformly labelled and with a high specific radioactivity. The non-incorporated radioactive nucleotides were separated with Sephadex G-50 gel filtration columns (Probe Quant G-50 Micro Columns, Amersham Pharmacia Biotech). This step helps to reduce the non-specific or background radioactive signal.

2.2.2.5. Membrane washes and developing

The following morning several washes of the blot were performed to rinse excessive or non-specifically bound probe. These consisted of 3 consecutive washes with progressively higher stringency: two 10-minute washes at room temperature with a low-astringency buffer solution (NaCl 300 mM, sodium citrate 30 mM, SDS 0.1%) and a final 15-minute wash at 65 °C with a high-astringency buffer solution (NaCl 15 mM, sodium citrate 1.5 mM, SDS 0.1%). Finally, the blots were exposed to a photographic film (Eastman KODAK Company, New York, USA) to obtain the visualization of the signal.

2.2.3. Analysis of RNA expression by RT-PCR

2.2.3.1. DNase treatment of RNA

Two μ g of RNA of each sample were treated with DNase (DNase I Amplification Grade, Invitrogen) following provider's instructions. After the treatment, 1 μ g of RNA was used for retro transcription to cDNA and the rest was stored at -80°C.

2.2.3.2. cDNA synthesis

One µg of total RNA was retrotranscribed to first-strand cDNA using the Transcriptor First Strand cDNA Synthesis Kit (Roche) following manufacturer's instructions. Oligo-dT oligonucleotides were used as primers for the reaction in the presence of Protector RNase inhibitor.

2.2.3.3. Quantitative PCR

RT-PCR was performed in a SmartCycler II (Cepheid, USA) using EXPRESS 2X qPCR SuperMix (Invitrogen). The sequences of the respective forward and reverse oligonucleotide primers used are summarized in the following table:

Gene	Name	Forward Primer	Reverse Primer
Gck	Glucokinase	GATGCAGAAGGAGATGGACCGT	AACGCACGTAGGTGGTAACAT
Pgc1α	Peroxisome proliferator-activated receptor gamma coactivator 1-alpha	ATACCGCAAAGAGCAGGAGAAG	CTCAAGACGAGCGAAAAGCGTCACAG
Pparδ	Peroxisome proliferator-activated receptor delta	TCCATCGTCAACAAAGACGGG	ACTTGGGCTCAATGATGTAC
Cpt1b	Carnitine palmitoyltransferase I	GCACACCAGGCAGTAGCTTT	CAGGAGTTGATTCCAGACAGGTA
36b4	Ribosomal protein, large, P0	GGCCCTGCACTCTCGCTTT	TGCCAGGACGCGCTTGT

We used the *delta-delta*-Ct method ($2^{-\Delta\Delta C_t}$) described by Livak (Livak et al., 2001) to relatively quantitate the expression of the genes of interest. Although an optimal doubling during each PCR cycle with an amplification rate of 100% is assumed, this method is widely used. With this method, C_ts (the threshold cycle or Ct indicates the fractional cycle number at which the amount of amplified target reaches a fixed threshold) for the gene of interest in both the test sample and calibrator sample are adjusted in relation to a normalizer gene Ct from the same two samples. The resulting $\Delta\Delta C_t$ value is incorporated to determine the fold difference in expression.

$$\text{Fold difference} = 2^{-\Delta\Delta C_t}$$

$$\Delta C_{t \text{ sample}} - \Delta C_{t \text{ calibrator}} = \Delta\Delta C_t$$

$$C_{t \text{ GOI}^S} - C_{t \text{ norm}^S} = \Delta C_{t \text{ sample}}$$

$$C_{t \text{ GOI}^C} - C_{t \text{ norm}^C} = \Delta C_{t \text{ calibrator}}$$

2.3. Production, purification, titration and administration of AAV vectors

2.3.1. Production of AAV vectors

AAV vectors were generated in HEK293 cells cultured in 10 roller bottles (RB) by the triple transfection method mediated by Calcium Chloride. Cells were grown to 80-90% confluence in Dulbecos Modified Eagle Medium (DMEM) (PAA laboratories, Pasching, Austria) supplemented with 10% Fetal Bovine Serum (FBS)(PAA) and 1% Penicillin/Streptomycin (PS)(PAA). Once confluence was reached, media was substituted by 200 ml per roller bottle of Iscove's Modified Dulbeco's Medium (IDDM) (PAA) supplemented with 2% FBS. After that, the transfection protocol was initiated. Five conical tubes of 250 ml (Corning, Amsterdam, The Netherlands) were used to aliquot 125 ml (25 ml in each tub) of HEBS solution (2xHEPES + Na₂HPO₄ 70mM). After that, the following solution was prepared in a separate conical tube:

- 31,25 ml CaCl 1M
- 1250 µg of pAAV rep/cap (plasmid containing the sequences for the capsid proteins and proteins necessary for virus replication)
- 1250 µg of pGG2-Genome (plasmid containing the gene of interest plus the ITRs)
- 2500 µg of pWEAD (plasmid containing Adenovirus helper functions)
- Sterile H₂O up to 125 ml

25 ml of the solution with the three plasmids was added, drop by drop, over each tube containing HEBS, under constant vortexing. The mixture was

incubated during 25-30 minutes at room temperature and, after a short vortex, 25 ml of this solution was added to each RB. RBs were then incubated during 6-8h at 37°C with a constant spinning of 0.25 rpm. After that, the medium was changed to DMEM supplemented with 10% FBS + P/S. After 4 days of incubation, cells were detached from the RB by strong hand shacking. Medium and cells were then centrifuged at 1000g during 20-30 minutes at 4°C in 1l tubes. Supernatant was discarded and the pellet (cells) resuspended with a sterile solution of TRIS 10mM ph 8 to a final volume of 30 ml. At this point cells were frozen at -80°C until purification.

2.3.2. AAV purification

AAVs from the cell suspension were purified using two successive CsCl gradients.

The cell suspension was subjected to three cycles of freeze-thaw using liquid nitrogen and a water bath at 37°C to lyse the cells and free the containing AAVs. Ten mg of RNase (Boehringer Manheim) and ten mg of DNase (Boehringer Manheim) were added to the AAV suspension and incubated at 37°C during 30 minutes. Sodium deoxycolate (Roche) was added afterwards to a final concentration of 0.5% and incubated 10 minutes more at 37°C. After this, the AAV suspension was put on ice during 10 minutes and 0.35g of CsCl per ml was added (thus reaching a final density of 1.3 g/ml). The final volume was adjusted to 20 ml.

The first gradient was prepared in 36 ml tubes specific for the SW28 ultracentrifuge rotor (Beckman Coulter). Nine ml of a solution of CsCl with a density of 1.6 g/ml was added first. After that, nine mls of a CsCl solution of 1.41 g/ml was added on top. Finally, the AAV suspension was added and the tube was levelled with CsCl 1.4 g/ml. Tubes were centrifuged 24 hours at 27000 rpm at 4°C. Aliquots of 1 ml were recovered by puncturing tubes with a

needle. In order to determine the fractions containing most of the virus a quantitative PCR was performed in each fraction, as it follows:

- 2 μ l of a 1:1000 dilution of each fraction.
- 12.5 μ l of SYBR (Roche)
- 8.5 μ l H₂O
- 1 μ l of reverse and forward primer, specific for the CMV promoter.

The PCR conditions consisted of an initial step of 94°C of during 5 min, 25 cycles of 94°C during 1 min, 52-53°C 1 min, 72°C 1 min and a final step of 10 min at 72°C.

The specific primers in the reaction were the following:

CMV (Citomegalovirus). Forward: GTTCCTAACGGTCAGTTCACAG

CMV (Citomegalovirus). Reverse: CGGGTTATTGCCATGACTGCCC

The aliquots with more amplification during the PCR were selected. The second gradient was started by adding 1-2 ml of a solution of 1.6 g/ml CsCl in thermo-sealable *ultra-clear* tubes (Beckman). The selected aliquots containing the virus were added on top and the tube was levelled with a solution of 1.41 g/ml of CsCl. Tubes were centrifuged all night at 60000 rpm using the Ty70.1 rotor (Beckman). All fractions were recovered in 0.5 ml/fraction and a second quantitative PCR (same conditions as the first) was used to select the aliquots with higher AAVs.

Selected aliquots were subjected to dialysis in 10000 Da cassettes (Slide-A-Lyzer dialysis products, Pierce, Rockford, USA) with PBS as a dialysis solution. PBS was changed after 1 and 2 hours. After that, dialysis was left all night at 4°C. The day after the virus was aliquoted and set for titration.

2.3.3. AAV titration

Viruses were titrated by quantitative slot blot hybridization. In order to perform the slot blot, first the DNA from a sample of the AAV suspension was extracted. DNA contained in 2 μ l of the AAV preparation was extracted in 78 μ l of proteinase K buffer during 1 hour at 37°C. The mix was cooled to room temperature and sterile H₂O was added up to a final volume of 120 μ l. A first extraction with 200 μ l of Phenol-Chloroform-isoamyl alcohol (25:24:1) was performed. The upper phase was subjected to a second extraction with 200 μ l of chloroform-isoamyl alcohol (24:1). After that 8 μ l of glycogen (5 mg/ml, Ambion), 20 μ l of Sodium Acetate 3 M (pH=5.2), and 450 μ l of ethanol were added to the upper phase. DNA was precipitated at -80°C during 1 hour and centrifuged at maximum speed for 20 minutes. The DNA pellet was washed with cold 70% ethanol and finally resuspended in 10 μ l of TE buffer.

Different dilutions of the extracted DNA were done in spotting solution. 5 μ l, 2.5 μ l, 1 μ l and 0.5 μ l of DNA were added to 150 μ l of spotting solution. Different dilutions of plasmid standards were performed in spotting solution so that they covered a range from 20 ng to 0.5 ng.

A Pre-cut Biodyne B membrane and pre-cut filter papers were humidified in pre-wetting solution for 30 min. The slot blot apparatus was assembled with the papers and the membrane and vacuum was applied. Standards and samples were then loaded. Vacuum was stopped when samples passed through. Slot blot was disassembled and the membrane was transferred to a hybridization tray (Perkin Elmer) containing 100 ml of hybridization solution and incubated at 65°C during 15 minutes. After that hybridization solution was removed and 30 ml of new hybridization solution containing a marked probe, specific for the

CMV promoter, was added. The membrane was incubated in this solution for 20 minutes at 65°C and washed twice with 100 ml of washing solution after the hybridization. The membrane was then placed in a seal-a-meal bag and exposed overnight with a film (Eastman KODAK company, New York, USA) in an X-ray cassette at -80°C.

2.3.4. AAV injection in the skeletal muscle

For AAV1 injection to the skeletal muscle, mice were anesthetized with an intraperitoneal injection of ketamine (100 mg/kg) (Imalgene 500®, Merial, Barcelona, Spain) and xylazine (10 mg/kg) (Rompun®, Bayer, Leverkusen, Germany). Both back hindlimbs were shaved to easily inject the *tibialis anterior*, *gastrocnemius* and *quadriceps*. 30 µl of a solution that contains the required dose of the diluted vector in Ca²⁺Mg²⁺PBS (Life Technologies) was injected using 0.5 ml insulin syringes (B.Braun, Melsungen, Germany). After the injections, mice were returned to cage.

2.4. Western Blot

2.4.1. Protein extraction

Frozen samples of *Quadriceps* or *Gastrocnemius* muscles were homogenized in 1 ml of a protein homogenization buffer with a Polytron® type tissue homogenizer and kept in ice thereafter. Extracts were centrifuged for 5 minutes at 12.000 x g at 4°C to precipitate cellular debris, and protein concentration in the supernatants was determined.

Homogenization buffer : 50 mM Tris-HCl pH=7.5, 0.27 M sucrose, 1 mM EGTA, 1 mM EDTA, 50 mM NaF, 10 mM Na β-glycerolphosphate, 5 mM Ppi, 1 % Triton X-100. Just before use, protease inhibitors were added to the buffer (one

tablet per each 10 ml of buffer, Complete Mini EDTA-free protease inhibitor cocktail tablets, Roche Diagnostics GMBH, Germany)

2.4.2. Bradford method for protein quantification

In order to quantify the protein content in a sample, the Bradford method was used. This method is based on the shift in the colour of Coomassie brilliant blue dye when complexed with proteins. This colour shift produces a change in the absorbance maximum from 495 to 595 nm. Appropriate volumes of the protein extracts were diluted to 800 µl in distilled water, to which 200 µl of the Bradford reagent (Bio-Rad Protein Assay, Bio-Rad, Germany) were added. The same reaction was performed with different amounts (0-20 µg) of bovine serum albumin (BSA) to obtain the standard curve. After adding the Bradford reagent, samples were mixed and incubated for 5 minutes before measuring their absorbance at 595 nm in a spectrophotometer.

2.4.3. Electroforesis in polyacrylamine gels (SDS-PAGE)

Protein expression was analyzed by electrophoresis of the different protein extracts in two-phase polyacrylamide gels in the presence of SDS 10 % polyacrylamide gels with SDS (Laemmli, 1970). SDS-PAGE polyacrylamide gels were made of two different gels. The upper gel was the *stacking gel*, which with its low concentration of polyacrylamide (3.9 %) allowed the proteins to stack together into a tightly packed band before entering the other gel. The bottom gel was the *resolving gel*, which was composed of 10 % polyacrylamide (acrylamide-bisacrylamide 30 %, BioRad) and allowed the separation of proteins according to their molecular weights. Protein extracts were mixed with a 1/5 volume of a Laemmli loading buffer and denaturalized at 90° C for 2 minutes, before being loaded into the SDS-PAGE gel. Electrophoresis was carried out at 50 V while samples were migrating in the stacking gel, and increased to 80 V

when samples entered the resolving gel. Pre-stained molecular weight markers were run on the same gel to facilitate band identification (Pre-stained SDS-PAGE Standards, Broad Range and Kaleidoscope, BioRad Laboratories, Hercules, CA, EEUU).

Staking Buffer (pH 6.8): 0,5 M Tris-Cl, 0.4 % W/V SDS

Resolving Buffer (pH 8.8): 1.5M Tris-Cl, 0.4 % W/V SDS

Electrophoresis Buffer: 5 mM Tris, 192 mM glycine, 0.1 % SDS (w/v).

Laemmli loading Buffer 5x: 20 mM phosphate buffer pH=7.0, 30 % V/V Glycerol, 4 % SDS, 2 % V/V 2-β-mercaptoetanol and bromophenol blue as a dye.

2.4.4. Protein transference to membranes and immunodetection

Electrotransference of proteins from the polyacrylamide gel to PVDF membranes (Hyperbond-P, Amersham Biosciences) was performed with Transblot model 2051 blotter (LKB/Pharmacia) at 100 V for 2 hours at 4° C in electrotransference buffer. After transference, membranes were stained with Ponceau dye to evaluate protein quality and loading differences between samples. Afterwards, membranes were washed to completely remove Ponceau dye and subsequently blocked with TBS-T with 5 % bovine serum albumin (BSA) or with 5 % W/V dry skimmed milk, depending on each antibody's preferences, for 2 hours in agitation at room temperature. Later, membranes were incubated with appropriate primary antibodies, summarized in *Section 1.4.*, diluted in TBS-T-BSA overnight at 4° C in agitation. Membranes were then washed with TBS-T (3 washes of 10 minutes each) and incubated for half an hour at room temperature with the corresponding peroxidase-conjugated secondary antibodies, summarized in *Section 1.4.*, diluted at 1:10000 in TBS-T-BSA. Finally, the membranes were washed again with TBS-T and TBS (one 5-minute wash). Immunodetection was performed by using ECL Plus® Western

Blotting analysis system (Amersham Biosciences Europe GmbH, Freiburg, Germany), following manufacturer's instructions. Then, the ECL-treated membrane was exposed to a photographic film to visualize the signal. The pixel intensity of the bands obtained was determined with the GeneSnap software for the Gene Genius Bio Imaging System (Syngene, Cambridge, UK).

Electrotransference buffer: 25 mM Tris, 150 mM glycine, 20 % V/V methanol

TBS buffer: 25 mM Tris-HCl, 137 mM NaCl

TBS-T: 25 mM Tris-HCl, 137 mM NaCl 0.05 % Tween20

2.5. Histological Analysis

2.5.1. Haematoxylin/eosin staining

Liver samples were fixed for 12-24 h in formalin, embedded in paraffin and sectioned. Sections were deparaffinised and stained with haematoxylin, rinsed in water and stained again with eosin. Samples were then dehydrated and mounted.

2.5.2. Immunohistochemistry

For immunohistochemical detection, sections were deparaffinised and incubated overnight at 4° C with specific antibodies for each protein (see list, *Section 1.4.*), washed with PBS three times for 5 minutes each wash and incubated with the corresponding secondary antibodies (see list, *Section 1.4.*). Antibodies were revealed with ABC Complex (Vector Laboratories Ltd., UK), which employs 3'3'-diaminobenzidine (DAB) as the substrate chromogen. Sections were counterstained in Mayer's haematoxylin. Images were visualized using a Nikon Eclipse E800 microscope (Nikon, Tokyo, Japan) connected to a videocamera.

2.6. *In vivo* techniques

2.6.1. Food intake determination

Food intake was obtained by calculating the difference between the amount of food initially added to the cage of mice and the amount of food remaining on the cage one week later. Since each cage could house up to five mice, the number of mice housed in each particular cage divided the result. Results were expressed as grams/day/animal.

2.6.2. Insulin tolerance test

The insulin tolerance test is used to evaluate the sensitivity of mice to an insulin load. Those animals which experience reduced insulin hypoglycemic response are considered to be insulin resistant. After removal of food, basal glucose levels of awake mice were determined. Subsequently, mice were intraperitoneally injected with a dose of 0.75 units of insulin per kg of body weight (Humulina Regular®, Eli Lilly, Indianapolis, IN). Blood samples were taken from mice tail vein at 15, 30, 45 and 60, min after the insulin challenge. Blood glucose levels were measured with a Glucometer Elite™ (Bayer, Leverkusen, Germany). Data was represented as % of basal glycaemia.

2.6.3. Insulin induced AKT-phosphorylation studies in the skeletal muscle

To study insulin signalling in the skeletal muscle, overnight starved animals were anaesthetized by an intraperitoneal injection of 100 mg/kg body weight of ketamine (Imalgene®, Merial, Lyon, France) and 10 mg/kg body weight of xylazine (Rompun® Bayer, Leverkusen, Germany). Once anaesthetized, a tourniquet was applied to the right leg to avoid excessive bleeding after tissue excision. After that, *quadriceps*, *gastrocnemius* and *tibialis anterior* muscles were excised and frozen into liquid nitrogen. Immediately, mice were injected with an intraperitoneal injection of 5 U of insulin per gram of

body weight. Fifteen minutes after insulin stimulation, *tibialis*, *gastrocnemius* and *quadriceps* from the left leg were excised and frozen. Protein extracts of different samples were obtained to carry on Western Blot analysis.

2.6.4. Measurement of serum parameters

Serum samples were obtained from blood samples collected by decapitation of mice under inhaled anaesthesia. Blood was collected in non-heparinized tubes and let to coagulate for 30 minutes at 4°C. To obtain the serum, samples were centrifuged at 6000xg for 20 minutes in a refrigerated centrifuge. Serums were separated, aliquoted, and kept at -80°C until further use.

2.6.4.1. Glucose

Blood glucose levels are measured with a Glucometer Elite™ (Bayer, Leverkusen, Germany) of blood obtained by cutting off the tip of the animals' tail.

2.6.4.2. Insulin

Circulating insulin levels were determined by radioimmunoassay in 100 µl serum samples using Insulin-CT RIA Kit (MP, Biochemichals, Orengerburg, NY, USA) following the manufacturer's instructions. Samples from high fat fed animals were diluted 1:4 to ensure that they were in the range of detection. The insulin detection level of the kit is 5.5 µUI/ml, with a measurable range in concentration from 5.5 µUI/ml to 310 µUI/ml.

2.6.4.3. Free fatty acids

Non-esterified serum free fatty acid levels were determined spectrophotometrically using the commercial product NEFA C (Wako Chemicals, Neuss, Germany) and the autoanalyzer PENTRA 400 (ABX Diagnostics, Montpellier, France). The method is based on the enzymatic reaction of acil-CoA synthetase and acil-Co oxidase.

2.6.4.4. Triglycerides

Serum triglyceride levels were determined spectrophotometrically using the commercial product GPO-PAP (Roche Diagnostics, Basel, Switzerland) and the autoanalyzer PENTRA 400. The method is based on the enzymatic GPO-PAP reaction described by Fossati *et al.* (Fossati *et al.*, 1982) in which quinoneimina (PAP) chromogen is obtained from p-clorophenol and 4-aminoantipirine reaction catalyzed by glycerol kinase, glycerol-3-phosphate oxidase (GPO) and peroxidase.

2.6.4.5. Leptin

Serum leptin levels were determined using the *Mouse Leptin ELISA Kit* (Crystal Chemical, Chicago, IL, USA), following the manufacturer's instructions.

2.6.4.6. Skeletal muscle triglyceride content

To determine the amount of liver and skeletal muscle triglycerides content, we used the method described by Carr and colleagues (Carr *et al.*, 1993), based on the chloroform:methanol (2:1) extraction described previously by Folch (Folch *et al.*, 1957). To extract triglycerides, frozen samples of approximately 100 mg were weighted and homogenized in 15 ml chloroform:methanol (2:1). Lipid and aqueous phases were then separated by adding 3 ml of H₂SO₄ 0.05 % and keeping them overnight at 4° C. Once the phases were separated, the aqueous superior phase was eliminated using a

Pasteur pipet and 1 ml of the inferior lipid phase was recuperated in a glass tube. 1 ml of a chloroform and Triton X-100 at 1 % solution was added to the glass tube and it was incubated at 90° C in a bath, to evaporate the chloroform. By the use of the chloroform and Triton X-100 mix, any remaining aqueous particle was eliminated from the lipid phase. After the evaporation, chloroform was rinsed to the walls of the tube to concentrate the sample and, it was warmed again at 90° C to evaporate the chloroform. Once the sediment was completely dry and concentrated, it was resuspended by the addition of 500 µl of H₂O miliQ at 37° C. The amount of triglycerides was finally determined using the commercial product GPO-PAP (Roche Diagnostics, Basel, Switzerland) and the autoanalyzer PENTRA 400.

2.7. Statistical analysis

All values are expressed as the mean ± SEM (standard error of the media). Differences between groups were compared by Student *t* test and ANOVA. Statistical significance was considered if $p < 0.05$.

Abdul-Ghani, M.A., and DeFronzo, R.A., 2010. Pathogenesis of insulin resistance in skeletal muscle. *J Biomed Biotechnol* 2010, 476279.

Adams, J.M., 2nd, Pratipanawatr, T., Berria, R., Wang, E., DeFronzo, R.A., Sullards, M.C., and Mandarino, L.J., 2004. Ceramide content is increased in skeletal muscle from obese insulin-resistant humans. *Diabetes* 53, 25-31.

Alvarez, E., Roncero, I., Chowen, J.A., Vazquez, P., and Blazquez, E., 2002. Evidence that glucokinase regulatory protein is expressed and interacts with glucokinase in rat brain. *J Neurochem* 80, 45-53.

Arner, P., 2005. Human fat cell lipolysis: biochemistry, regulation and clinical role. *Best Pract Res Clin Endocrinol Metab* 19, 471-82.

Arruda, V.R., Fields, P.A., Milner, R., Wainwright, L., De Miguel, M.P., Donovan, P.J., Herzog, R.W., Nichols, T.C., Biegel, J.A., Razavi, M., Dake, M., Huff, D., Flake, A.W., Couto, L., Kay, M.A., and High, K.A., 2001. Lack of germline transmission of vector sequences following systemic administration of recombinant AAV-2 vector in males. *Mol Ther* 4, 586-92.

Arruda, V.R., Schuettrumpf, J., Herzog, R.W., Nichols, T.C., Robinson, N., Lotfi, Y., Mingozi, F., Xiao, W., Couto, L.B., and High, K.A., 2004. Safety and efficacy of factor IX gene transfer to skeletal muscle in murine and canine hemophilia B models by adeno-associated viral vector serotype 1. *Blood* 103, 85-92.

Avignon, A., Yamada, K., Zhou, X., Spencer, B., Cardona, O., Saba-Siddique, S., Galloway, L., Standaert, M.L., and Farese, R.V., 1996. Chronic activation of protein kinase C in soleus muscles and other tissues of insulin-resistant type II diabetic Goto-Kakizaki (GK), obese/aged, and obese/Zucker rats. A mechanism for inhibiting glycogen synthesis. *Diabetes* 45, 1396-404.

Ayuso, E., Mingozi, F., and Bosch, F., 2010a. Production, purification and characterization of adeno-associated vectors. *Curr Gene Ther* 10, 423-36.

Ayuso, E., Mingozi, F., Montane, J., Leon, X., Anguela, X.M., Haurigot, V., Edmonson, S.A., Africa, L., Zhou, S., High, K.A., Bosch, F., and Wright, J.F., 2010b. High AAV vector purity results in serotype- and tissue-independent enhancement of transduction efficiency. *Gene Ther* 17, 503-10.

Baar, K., Wende, A.R., Jones, T.E., Marison, M., Nolte, L.A., Chen, M., Kelly, D.P., and Holloszy, J.O., 2002. Adaptations of skeletal muscle to exercise: rapid increase in the transcriptional coactivator PGC-1. *FASEB J* 16, 1879-86.

Bantle, J.P., Wylie-Rosett, J., Albright, A.L., Apovian, C.M., Clark, N.G., Franz, M.J., Hoogwerf, B.J., Lichtenstein, A.H., Mayer-Davis, E., Mooradian, A.D., and Wheeler, M.L., 2008. Nutrition recommendations and interventions for diabetes: a position statement of the American Diabetes Association. *Diabetes Care* 31 Suppl 1, S61-78.

- Bassel-Duby, R., and Olson, E.N., 2006. Signaling pathways in skeletal muscle remodeling. *Annu Rev Biochem* 75, 19-37.
- Befroy, D.E., Petersen, K.F., Dufour, S., Mason, G.F., de Graaf, R.A., Rothman, D.L., and Shulman, G.I., 2007. Impaired mitochondrial substrate oxidation in muscle of insulin-resistant offspring of type 2 diabetic patients. *Diabetes* 56, 1376-81.
- Benton, C.R., Holloway, G.P., Han, X.X., Yoshida, Y., Snook, L.A., Lally, J., Glatz, J.F., Luiken, J.J., Chabowski, A., and Bonen, A., 2010. Increased levels of peroxisome proliferator-activated receptor gamma, coactivator 1 alpha (PGC-1 alpha) improve lipid utilisation, insulin signalling and glucose transport in skeletal muscle of lean and insulin-resistant obese Zucker rats. *Diabetologia* 53, 2008-19.
- Benton, C.R., Nickerson, J.G., Lally, J., Han, X.X., Holloway, G.P., Glatz, J.F., Luiken, J.J., Graham, T.E., Heikkila, J.J., and Bonen, A., 2008. Modest PGC-1alpha overexpression in muscle in vivo is sufficient to increase insulin sensitivity and palmitate oxidation in subsarcolemmal, not intermyofibrillar, mitochondria. *J Biol Chem* 283, 4228-40.
- Berger, J., and Moller, D.E., 2002. The mechanisms of action of PPARs. *Annu Rev Med* 53, 409-35.
- Bevilacqua, S., Buzzigoli, G., Bonadonna, R., Brandi, L.S., Oleggini, M., Boni, C., Geloni, M., and Ferrannini, E., 1990. Operation of Randle's cycle in patients with NIDDM. *Diabetes* 39, 383-9.
- Bezire, V., Spriet, L.L., Campbell, S., Sabet, N., Gerrits, M., Bonen, A., and Harper, M.E., 2005. Constitutive UCP3 overexpression at physiological levels increases mouse skeletal muscle capacity for fatty acid transport and oxidation. *FASEB J* 19, 977-9.
- Birnboim, H.C., and Doly, J., 1979. A rapid alkaline extraction procedure for screening recombinant plasmid DNA. *Nucleic Acids Res* 7, 1513-23.
- Blaak, E.E., 2004. Basic disturbances in skeletal muscle fatty acid metabolism in obesity and type 2 diabetes mellitus. *Proc Nutr Soc* 63, 323-30.
- Bonadonna, R.C., Del Prato, S., Bonora, E., Saccomani, M.P., Gulli, G., Natali, A., Frascerra, S., Pecori, N., Ferrannini, E., Bier, D., Cobelli, C., and DeFronzo, R.A., 1996. Roles of glucose transport and glucose phosphorylation in muscle insulin resistance of NIDDM. *Diabetes* 45, 915-25.
- Bonnard, C., Durand, A., Peyrol, S., Chansaume, E., Chauvin, M.A., Morio, B., Vidal, H., and Rieusset, J., 2008. Mitochondrial dysfunction results from oxidative stress in the skeletal muscle of diet-induced insulin-resistant mice. *J Clin Invest* 118, 789-800.
- Boyko, E.J., Fujimoto, W.Y., Leonetti, D.L., and Newell-Morris, L., 2000. Visceral adiposity and risk of type 2 diabetes: a prospective study among Japanese Americans. *Diabetes Care* 23, 465-71.

- Bruce, C.R., Hoy, A.J., Turner, N., Watt, M.J., Allen, T.L., Carpenter, K., Cooney, G.J., Febbraio, M.A., and Kraegen, E.W., 2009. Overexpression of carnitine palmitoyltransferase-1 in skeletal muscle is sufficient to enhance fatty acid oxidation and improve high-fat diet-induced insulin resistance. *Diabetes* 58, 550-8.
- Buchlis, G., Podsakoff, G.M., Radu, A., Hawk, S.M., Flake, A.W., Mingozzi, F., and High, K.A., 2012. Factor IX expression in skeletal muscle of a severe hemophilia B patient 10 years after AAV-mediated gene transfer. *Blood* 119, 3038-41.
- Buning, H., Perabo, L., Coutelle, O., Quadt-Humme, S., and Hallek, M., 2008. Recent developments in adeno-associated virus vector technology. *J Gene Med* 10, 717-33.
- Callejas, D., Mann, C.J., Ayuso, E., Lage, R., Grifoll, I., Roca, C., Andaluz, A., Ruiz-de Gopegui, R., Montane, J., Munoz, S., Ferre, T., Haurigot, V., Zhou, S., Ruberte, J., Mingozzi, F., High, K.A., Garcia, F., and Bosch, F., 2013. Treatment of diabetes and long-term survival after insulin and glucokinase gene therapy. *Diabetes* 62, 1718-29.
- Carr, T.P., Andresen, C.J., and Rudel, L.L., 1993. Enzymatic determination of triglyceride, free cholesterol, and total cholesterol in tissue lipid extracts. *Clin Biochem* 26, 39-42.
- Chan, J.C., Malik, V., Jia, W., Kadowaki, T., Yajnik, C.S., Yoon, K.H., and Hu, F.B., 2009. Diabetes in Asia: epidemiology, risk factors, and pathophysiology. *JAMA* 301, 2129-40.
- Chang, P.Y., Jensen, J., Printz, R.L., Granner, D.K., Ivy, J.L., and Moller, D.E., 1996. Overexpression of hexokinase II in transgenic mice. Evidence that increased phosphorylation augments muscle glucose uptake. *J Biol Chem* 271, 14834-9.
- Chao, H., Liu, Y., Rabinowitz, J., Li, C., Samulski, R.J., and Walsh, C.E., 2000. Several log increase in therapeutic transgene delivery by distinct adeno-associated viral serotype vectors. *Mol Ther* 2, 619-23.
- Chen, L., Magliano, D.J., and Zimmet, P.Z., 2011. The worldwide epidemiology of type 2 diabetes mellitus-present and future perspectives. *Nat Rev Endocrinol*.
- Cheng, L., Ding, G., Qin, Q., Huang, Y., Lewis, W., He, N., Evans, R.M., Schneider, M.D., Brako, F.A., Xiao, Y., Chen, Y.E., and Yang, Q., 2004a. Cardiomyocyte-restricted peroxisome proliferator-activated receptor-delta deletion perturbs myocardial fatty acid oxidation and leads to cardiomyopathy. *Nat Med* 10, 1245-50.
- Cheng, L., Ding, G., Qin, Q., Xiao, Y., Woods, D., Chen, Y.E., and Yang, Q., 2004b. Peroxisome proliferator-activated receptor delta activates fatty acid oxidation in cultured neonatal and adult cardiomyocytes. *Biochem Biophys Res Commun* 313, 277-86.

Chinsomboon, J., Ruas, J., Gupta, R.K., Thom, R., Shoag, J., Rowe, G.C., Sawada, N., Raghuram, S., and Arany, Z., 2009. The transcriptional coactivator PGC-1 α mediates exercise-induced angiogenesis in skeletal muscle. *Proc Natl Acad Sci U S A* 106, 21401-6.

Choi, C.S., Befroy, D.E., Codella, R., Kim, S., Reznick, R.M., Hwang, Y.J., Liu, Z.X., Lee, H.Y., Distefano, A., Samuel, V.T., Zhang, D., Cline, G.W., Handschin, C., Lin, J., Petersen, K.F., Spiegelman, B.M., and Shulman, G.I., 2008. Paradoxical effects of increased expression of PGC-1 α on muscle mitochondrial function and insulin-stimulated muscle glucose metabolism. *Proc Natl Acad Sci U S A* 105, 19926-31.

Choi, C.S., Fillmore, J.J., Kim, J.K., Liu, Z.X., Kim, S., Collier, E.F., Kulkarni, A., Distefano, A., Hwang, Y.J., Kahn, M., Chen, Y., Yu, C., Moore, I.K., Reznick, R.M., Higashimori, T., and Shulman, G.I., 2007a. Overexpression of uncoupling protein 3 in skeletal muscle protects against fat-induced insulin resistance. *J Clin Invest* 117, 1995-2003.

Choi, C.S., Savage, D.B., Abu-Elheiga, L., Liu, Z.X., Kim, S., Kulkarni, A., Distefano, A., Hwang, Y.J., Reznick, R.M., Codella, R., Zhang, D., Cline, G.W., Wakil, S.J., and Shulman, G.I., 2007b. Continuous fat oxidation in acetyl-CoA carboxylase 2 knockout mice increases total energy expenditure, reduces fat mass, and improves insulin sensitivity. *Proc Natl Acad Sci U S A* 104, 16480-5.

Cimini, A., Bernardo, A., Cifone, M.G., Di Marzio, L., and Di Loreto, S., 2003. TNF α downregulates PPAR δ expression in oligodendrocyte progenitor cells: implications for demyelinating diseases. *Glia* 41, 3-14.

Coura Rdos, S., and Nardi, N.B., 2007. The state of the art of adeno-associated virus-based vectors in gene therapy. *Virol J* 4, 99.

Daoudi, M., Hennuyer, N., Borland, M.G., Touche, V., Duhem, C., Gross, B., Caiazzo, R., Kerr-Conte, J., Pattou, F., Peters, J.M., Staels, B., and Lestavel, S., 2011. PPAR β / δ activation induces enteroendocrine L cell GLP-1 production. *Gastroenterology* 140, 1564-74.

Davidson, B.L., and McCray, P.B., Jr., 2011. Current prospects for RNA interference-based therapies. *Nat Rev Genet* 12, 329-40.

DeFronzo, R.A., 2004. Pathogenesis of type 2 diabetes mellitus. *Med Clin North Am* 88, 787-835, ix.

DeFronzo, R.A., 2009. Banting Lecture. From the triumvirate to the ominous octet: a new paradigm for the treatment of type 2 diabetes mellitus. *Diabetes* 58, 773-95.

DeFronzo, R.A., and Tripathy, D., 2009. Skeletal muscle insulin resistance is the primary defect in type 2 diabetes. *Diabetes Care* 32 Suppl 2, S157-63.

Echtay, K.S., 2007. Mitochondrial uncoupling proteins--what is their physiological role? *Free Radic Biol Med* 43, 1351-71.

Ehrenborg, E., and Krook, A., 2009. Regulation of skeletal muscle physiology and metabolism by peroxisome proliferator-activated receptor delta. *Pharmacol Rev* 61, 373-93.

Evans, R.M., Barish, G.D., and Wang, Y.X., 2004. PPARs and the complex journey to obesity. *Nat Med* 10, 355-61.

Fanelli, M., Filippi, E., Sentinelli, F., Romeo, S., Fallarino, M., Buzzetti, R., Leonetti, F., and Baroni, M.G., 2005. The Gly482Ser missense mutation of the peroxisome proliferator-activated receptor gamma coactivator-1 alpha (PGC-1 alpha) gene associates with reduced insulin sensitivity in normal and glucose-intolerant obese subjects. *Dis Markers* 21, 175-80.

Feige, J.N., Gelman, L., Michalik, L., Desvergne, B., and Wahli, W., 2006. From molecular action to physiological outputs: peroxisome proliferator-activated receptors are nuclear receptors at the crossroads of key cellular functions. *Prog Lipid Res* 45, 120-59.

Fernandez-Sanchez, L., Lax, P., Isiegas, C., Ayuso, E., Ruiz, J.M., de la Villa, P., Bosch, F., de la Rosa, E.J., and Cuenca, N., 2012. Proinsulin slows retinal degeneration and vision loss in the P23H rat model of retinitis pigmentosa. *Hum Gene Ther* 23, 1290-300.

Finck, B.N., and Kelly, D.P., 2006. PGC-1 coactivators: inducible regulators of energy metabolism in health and disease. *J Clin Invest* 116, 615-22.

Flotte, T.R., Trapnell, B.C., Humphries, M., Carey, B., Calcedo, R., Rouhani, F., Campbell-Thompson, M., Yachnis, A.T., Sandhaus, R.A., McElvaney, N.G., Mueller, C., Messina, L.M., Wilson, J.M., Brantly, M., Knop, D.R., Ye, G.J., and Chulay, J.D., 2011. Phase 2 clinical trial of a recombinant adeno-associated viral vector expressing alpha1-antitrypsin: interim results. *Hum Gene Ther* 22, 1239-47.

Folch, J., Lees, M., and Sloane Stanley, G.H., 1957. A simple method for the isolation and purification of total lipides from animal tissues. *J Biol Chem* 226, 497-509.

Fossati, P., and Prencipe, L., 1982. Serum triglycerides determined colorimetrically with an enzyme that produces hydrogen peroxide. *Clin Chem* 28, 2077-80.

Fueger, P.T., Bracy, D.P., Malabanan, C.M., Pencek, R.R., Granner, D.K., and Wasserman, D.H., 2004. Hexokinase II overexpression improves exercise-stimulated but not insulin-stimulated muscle glucose uptake in high-fat-fed C57BL/6J mice. *Diabetes* 53, 306-14.

Garcia-Roves, P.M., Huss, J., and Holloszy, J.O., 2006. Role of calcineurin in exercise-induced mitochondrial biogenesis. *Am J Physiol Endocrinol Metab* 290, E1172-9.

Ginn, S.L., Alexander, I.E., Edelstein, M.L., Abedi, M.R., and Wixon, J., 2013. Gene therapy clinical trials worldwide to 2012 - an update. *J Gene Med* 15, 65-77.

Girroir, E.E., Hollingshead, H.E., He, P., Zhu, B., Perdew, G.H., and Peters, J.M., 2008. Quantitative expression patterns of peroxisome proliferator-activated receptor-beta/delta (PPARbeta/delta) protein in mice. *Biochem Biophys Res Commun* 371, 456-61.

Goetzel, R.Z., Hawkins, K., Ozminkowski, R.J., and Wang, S., 2003. The health and productivity cost burden of the "top 10" physical and mental health conditions affecting six large U.S. employers in 1999. *J Occup Environ Med* 45, 5-14.

Goto, M., Terada, S., Kato, M., Katoh, M., Yokozeki, T., Tabata, I., and Shimokawa, T., 2000. cDNA Cloning and mRNA analysis of PGC-1 in epitrochlearis muscle in swimming-exercised rats. *Biochem Biophys Res Commun* 274, 350-4.

Guilherme, A., Virbasius, J.V., Puri, V., and Czech, M.P., 2008. Adipocyte dysfunctions linking obesity to insulin resistance and type 2 diabetes. *Nat Rev Mol Cell Biol* 9, 367-77.

Hajduch, E., Balendran, A., Batty, I.H., Litherland, G.J., Blair, A.S., Downes, C.P., and Hundal, H.S., 2001. Ceramide impairs the insulin-dependent membrane recruitment of protein kinase B leading to a loss in downstream signalling in L6 skeletal muscle cells. *Diabetologia* 44, 173-83.

Hales, C.N., and Barker, D.J., 1992. Type 2 (non-insulin-dependent) diabetes mellitus: the thrifty phenotype hypothesis. *Diabetologia* 35, 595-601.

Hancock, C.R., Han, D.H., Chen, M., Terada, S., Yasuda, T., Wright, D.C., and Holloszy, J.O., 2008. High-fat diets cause insulin resistance despite an increase in muscle mitochondria. *Proc Natl Acad Sci U S A* 105, 7815-20.

Handelsman, Y., 2011. Role of bile acid sequestrants in the treatment of type 2 diabetes. *Diabetes Care* 34 Suppl 2, S244-50.

Handschin, C., Choi, C.S., Chin, S., Kim, S., Kawamori, D., Kurpad, A.J., Neubauer, N., Hu, J., Mootha, V.K., Kim, Y.B., Kulkarni, R.N., Shulman, G.I., and Spiegelman, B.M., 2007. Abnormal glucose homeostasis in skeletal muscle-specific PGC-1alpha knockout mice reveals skeletal muscle-pancreatic beta cell crosstalk. *J Clin Invest* 117, 3463-74.

Handschin, C., Rhee, J., Lin, J., Tarr, P.T., and Spiegelman, B.M., 2003. An autoregulatory loop controls peroxisome proliferator-activated receptor gamma coactivator 1 alpha expression in muscle. *Proc Natl Acad Sci U S A* 100, 7111-6.

Hara, K., Tobe, K., Okada, T., Kadowaki, H., Akanuma, Y., Ito, C., Kimura, S., and Kadowaki, T., 2002. A genetic variation in the PGC-1 gene could confer insulin resistance and susceptibility to Type II diabetes. *Diabetologia* 45, 740-3.

He, L., Kim, T., Long, Q., Liu, J., Wang, P., Zhou, Y., Ding, Y., Prasain, J., Wood, P.A., and Yang, Q., 2012. Carnitine palmitoyltransferase-1b deficiency aggravates pressure overload-induced cardiac hypertrophy caused by lipotoxicity. *Circulation* 126, 1705-16.

Holst, D., Luquet, S., Nogueira, V., Kristiansen, K., Leverve, X., and Grimaldi, P.A., 2003. Nutritional regulation and role of peroxisome proliferator-activated receptor delta in fatty acid catabolism in skeletal muscle. *Biochim Biophys Acta* 1633, 43-50.

Hossain, P., Kavar, B., and El Nahas, M., 2007. Obesity and diabetes in the developing world--a growing challenge. *N Engl J Med* 356, 213-5.

Hu, F.B., Manson, J.E., Stampfer, M.J., Colditz, G., Liu, S., Solomon, C.G., and Willett, W.C., 2001. Diet, lifestyle, and the risk of type 2 diabetes mellitus in women. *N Engl J Med* 345, 790-7.

Huss, J.M., and Kelly, D.P., 2004. Nuclear receptor signaling and cardiac energetics. *Circ Res* 95, 568-78.

Imamura, M., and Maeda, S., 2011. Genetics of type 2 diabetes: the GWAS era and future perspectives [Review]. *Endocr J* 58, 723-39.

Inzucchi, S.E., Bergenstal, R.M., Buse, J.B., Diamant, M., Ferrannini, E., Nauck, M., Peters, A.L., Tsapas, A., Wender, R., and Matthews, D.R., 2012. Management of Hyperglycemia in Type 2 Diabetes: A Patient-Centered Approach: Position Statement of the American Diabetes Association (ADA) and the European Association for the Study of Diabetes (EASD). *Diabetes Care* 35, 1364-79.

Itani, S.I., Pories, W.J., Macdonald, K.G., and Dohm, G.L., 2001. Increased protein kinase C theta in skeletal muscle of diabetic patients. *Metabolism* 50, 553-7.

Itani, S.I., Ruderman, N.B., Schmieder, F., and Boden, G., 2002. Lipid-induced insulin resistance in human muscle is associated with changes in diacylglycerol, protein kinase C, and I κ B α . *Diabetes* 51, 2005-11.

Itani, S.I., Zhou, Q., Pories, W.J., MacDonald, K.G., and Dohm, G.L., 2000. Involvement of protein kinase C in human skeletal muscle insulin resistance and obesity. *Diabetes* 49, 1353-8.

Ilyedjian, P.B., 2009. Molecular physiology of mammalian glucokinase. *Cell Mol Life Sci* 66, 27-42.

Jimenez-Chillaron, J.C., Newgard, C.B., and Gomez-Foix, A.M., 1999. Increased glucose disposal induced by adenovirus-mediated transfer of glucokinase to skeletal muscle in vivo. *FASEB J* 13, 2153-60.

Jimenez-Chillaron, J.C., Telemaque-Potts, S., Gomez-Valades, A.G., Anderson, P., Newgard, C.B., and Gomez-Foix, A.M., 2002. Glucokinase gene transfer to skeletal muscle of diabetic Zucker fatty rats improves insulin-sensitive glucose uptake. *Metabolism* 51, 121-6.

- Jove, M., Salla, J., Planavila, A., Cabrero, A., Michalik, L., Wahli, W., Laguna, J.C., and Vazquez-Carrera, M., 2004. Impaired expression of NADH dehydrogenase subunit 1 and PPARgamma coactivator-1 in skeletal muscle of ZDF rats: restoration by troglitazone. *J Lipid Res* 45, 113-23.
- Kahn, S.E., Hull, R.L., and Utzschneider, K.M., 2006. Mechanisms linking obesity to insulin resistance and type 2 diabetes. *Nature* 444, 840-6.
- Kay, M.A., 2011. State-of-the-art gene-based therapies: the road ahead. *Nat Rev Genet* 12, 316-28.
- Kay, M.A., Glorioso, J.C., and Naldini, L., 2001. Viral vectors for gene therapy: the art of turning infectious agents into vehicles of therapeutics. *Nat Med* 7, 33-40.
- Kelley, D.E., 2005. Skeletal muscle fat oxidation: timing and flexibility are everything. *J Clin Invest* 115, 1699-702.
- Kelley, D.E., Goodpaster, B., Wing, R.R., and Simoneau, J.A., 1999. Skeletal muscle fatty acid metabolism in association with insulin resistance, obesity, and weight loss. *Am J Physiol* 277, E1130-41.
- Kelley, D.E., Mokan, M., Simoneau, J.A., and Mandarino, L.J., 1993. Interaction between glucose and free fatty acid metabolism in human skeletal muscle. *J Clin Invest* 92, 91-8.
- Kelly, D.P., and Scarpulla, R.C., 2004. Transcriptional regulatory circuits controlling mitochondrial biogenesis and function. *Genes Dev* 18, 357-68.
- Kelly, T., Yang, W., Chen, C.S., Reynolds, K., and He, J., 2008. Global burden of obesity in 2005 and projections to 2030. *Int J Obes (Lond)* 32, 1431-7.
- Kersten, S., Seydoux, J., Peters, J.M., Gonzalez, F.J., Desvergne, B., and Wahli, W., 1999. Peroxisome proliferator-activated receptor alpha mediates the adaptive response to fasting. *J Clin Invest* 103, 1489-98.
- Klein, S., Fontana, L., Young, V.L., Coggan, A.R., Kilo, C., Patterson, B.W., and Mohammed, B.S., 2004a. Absence of an effect of liposuction on insulin action and risk factors for coronary heart disease. *N Engl J Med* 350, 2549-57.
- Klein, S., Sheard, N.F., Pi-Sunyer, X., Daly, A., Wylie-Rosett, J., Kulkarni, K., and Clark, N.G., 2004b. Weight management through lifestyle modification for the prevention and management of type 2 diabetes: rationale and strategies: a statement of the American Diabetes Association, the North American Association for the Study of Obesity, and the American Society for Clinical Nutrition. *Diabetes Care* 27, 2067-73.

- Kleiner, S., Nguyen-Tran, V., Bare, O., Huang, X., Spiegelman, B., and Wu, Z., 2009. PPAR δ agonism activates fatty acid oxidation via PGC-1 α but does not increase mitochondrial gene expression and function. *J Biol Chem* 284, 18624-33.
- Knowler, W.C., Bennett, P.H., Hamman, R.F., and Miller, M., 1978. Diabetes incidence and prevalence in Pima Indians: a 19-fold greater incidence than in Rochester, Minnesota. *Am J Epidemiol* 108, 497-505.
- Koo, S.H., Satoh, H., Herzig, S., Lee, C.H., Hedrick, S., Kulkarni, R., Evans, R.M., Olefsky, J., and Montminy, M., 2004. PGC-1 promotes insulin resistance in liver through PPAR α -dependent induction of TRB-3. *Nat Med* 10, 530-4.
- Koves, T.R., Li, P., An, J., Akimoto, T., Slentz, D., Ilkayeva, O., Dohm, G.L., Yan, Z., Newgard, C.B., and Muoio, D.M., 2005. Peroxisome proliferator-activated receptor-gamma co-activator 1 α -mediated metabolic remodeling of skeletal myocytes mimics exercise training and reverses lipid-induced mitochondrial inefficiency. *J Biol Chem* 280, 33588-98.
- Krssak, M., Falk Petersen, K., Dresner, A., DiPietro, L., Vogel, S.M., Rothman, D.L., Roden, M., and Shulman, G.I., 1999. Intramyocellular lipid concentrations are correlated with insulin sensitivity in humans: a ^1H NMR spectroscopy study. *Diabetologia* 42, 113-6.
- Laemmli, U.K., 1970. Cleavage of structural proteins during the assembly of the head of bacteriophage T4. *Nature* 227, 680-5.
- Lebovitz, H.E., and Banerji, M.A., 2005. Point: visceral adiposity is causally related to insulin resistance. *Diabetes Care* 28, 2322-5.
- Lee, C.H., Chawla, A., Urbiztondo, N., Liao, D., Boisvert, W.A., Evans, R.M., and Curtiss, L.K., 2003. Transcriptional repression of atherogenic inflammation: modulation by PPAR δ . *Science* 302, 453-7.
- Lehman, J.J., Barger, P.M., Kovacs, A., Saffitz, J.E., Medeiros, D.M., and Kelly, D.P., 2000. Peroxisome proliferator-activated receptor gamma coactivator-1 promotes cardiac mitochondrial biogenesis. *J Clin Invest* 106, 847-56.
- Lemieux, S., Prud'homme, D., Nadeau, A., Tremblay, A., Bouchard, C., and Despres, J.P., 1996. Seven-year changes in body fat and visceral adipose tissue in women. Association with indexes of plasma glucose-insulin homeostasis. *Diabetes Care* 19, 983-91.
- Leone, T.C., Lehman, J.J., Finck, B.N., Schaeffer, P.J., Wende, A.R., Boudina, S., Courtois, M., Wozniak, D.F., Sambandam, N., Bernal-Mizrachi, C., Chen, Z., Holloszy, J.O., Medeiros, D.M., Schmidt, R.E., Saffitz, J.E., Abel, E.D., Semenkovich, C.F., and Kelly, D.P., 2005. PGC-1 α deficiency causes multi-system energy metabolic derangements: muscle dysfunction, abnormal weight control and hepatic steatosis. *PLoS Biol* 3, e101.

- Lewis, J.D., Ferrara, A., Peng, T., Hedderson, M., Bilker, W.B., Quesenberry, C.P., Jr., Vaughn, D.J., Nessel, L., Selby, J., and Strom, B.L., 2011. Risk of bladder cancer among diabetic patients treated with pioglitazone: interim report of a longitudinal cohort study. *Diabetes Care* 34, 916-22.
- Li, L., Wu, L., Wang, C., Liu, L., and Zhao, Y., 2007. Adiponectin modulates carnitine palmitoyltransferase-1 through AMPK signaling cascade in rat cardiomyocytes. *Regul Pept* 139, 72-9.
- Liang, H., Balas, B., Tantiwong, P., Dube, J., Goodpaster, B.H., O'Doherty, R.M., DeFronzo, R.A., Richardson, A., Musi, N., and Ward, W.F., 2009. Whole body overexpression of PGC-1alpha has opposite effects on hepatic and muscle insulin sensitivity. *Am J Physiol Endocrinol Metab* 296, E945-54.
- Lin, J., Wu, H., Tarr, P.T., Zhang, C.Y., Wu, Z., Boss, O., Michael, L.F., Puigserver, P., Isotani, E., Olson, E.N., Lowell, B.B., Bassel-Duby, R., and Spiegelman, B.M., 2002. Transcriptional co-activator PGC-1 alpha drives the formation of slow-twitch muscle fibres. *Nature* 418, 797-801.
- Ling, C., Poulsen, P., Carlsson, E., Ridderstrale, M., Almgren, P., Wojtaszewski, J., Beck-Nielsen, H., Groop, L., and Vaag, A., 2004. Multiple environmental and genetic factors influence skeletal muscle PGC-1alpha and PGC-1beta gene expression in twins. *J Clin Invest* 114, 1518-26.
- Lira, V.A., Benton, C.R., Yan, Z., and Bonen, A., 2010. PGC-1alpha regulation by exercise training and its influences on muscle function and insulin sensitivity. *Am J Physiol Endocrinol Metab* 299, E145-61.
- Livak, K.J., and Schmittgen, T.D., 2001. Analysis of relative gene expression data using real-time quantitative PCR and the 2^{-Delta Delta C(T)} Method. *Methods* 25, 402-8.
- Livingston, R.C., Bachman-Carter, K., Frank, C., and Mason, W.B., 1993. Diabetes mellitus in Tohon O'odham pregnancies. *Diabetes Care* 16, 318-21.
- Long, Y.C., Glund, S., Garcia-Roves, P.M., and Zierath, J.R., 2007. Calcineurin regulates skeletal muscle metabolism via coordinated changes in gene expression. *J Biol Chem* 282, 1607-14.
- Long, Y.C., and Zierath, J.R., 2006. AMP-activated protein kinase signaling in metabolic regulation. *J Clin Invest* 116, 1776-83.
- Lowell, B.B., and Shulman, G.I., 2005. Mitochondrial dysfunction and type 2 diabetes. *Science* 307, 384-7.
- Luquet, S., Lopez-Soriano, J., Holst, D., Fredenrich, A., Melki, J., Rassoulzadegan, M., and Grimaldi, P.A., 2003. Peroxisome proliferator-activated receptor delta controls muscle development and oxidative capability. *FASEB J* 17, 2299-301.

Lutgers, H.L., Gerrits, E.G., Sluiter, W.J., Ubink-Veltmaat, L.J., Landman, G.W., Links, T.P., Gans, R.O., Smit, A.J., andBilo, H.J., 2009. Life expectancy in a large cohort of type 2 diabetes patients treated in primary care (ZODIAC-10). *PLoS One* 4, e6817.

Mahoney, D.J., Parise, G., Melov, S., Safdar, A., andTarnopolsky, M.A., 2005. Analysis of global mRNA expression in human skeletal muscle during recovery from endurance exercise. *FASEB J* 19, 1498-500.

Mann, C.J., Ayuso, E., Anguela, X.M., andBosch, F., 2010. Skeletal muscle metabolism in the pathology and treatment of type 1 diabetes. *Curr Pharm Des* 16, 1002-20.

Manno, C.S., Chew, A.J., Hutchison, S., Larson, P.J., Herzog, R.W., Arruda, V.R., Tai, S.J., Ragni, M.V., Thompson, A., Ozelo, M., Couto, L.B., Leonard, D.G., Johnson, F.A., McClelland, A., Scallan, C., Skarsgard, E., Flake, A.W., Kay, M.A., High, K.A., andGlader, B., 2003. AAV-mediated factor IX gene transfer to skeletal muscle in patients with severe hemophilia B. *Blood* 101, 2963-72.

Marette, A., Richardson, J.M., Ramlal, T., Balon, T.W., Vranic, M., Pessin, J.E., andKlip, A., 1992. Abundance, localization, and insulin-induced translocation of glucose transporters in red and white muscle. *Am J Physiol* 263, C443-52.

Marliss, E.B., Aoki, T.T., Unger, R.H., Soeldner, J.S., andCahill, G.F., Jr., 1970. Glucagon levels and metabolic effects in fasting man. *J Clin Invest* 49, 2256-70.

Mas, A., Montane, J., Anguela, X.M., Munoz, S., Douar, A.M., Riu, E., Otaegui, P., andBosch, F., 2006. Reversal of type 1 diabetes by engineering a glucose sensor in skeletal muscle. *Diabetes* 55, 1546-53.

Matschinsky, F.M., Magnuson, M.A., Zelent, D., Jetton, T.L., Doliba, N., Han, Y., Taub, R., andGrimsby, J., 2006. The network of glucokinase-expressing cells in glucose homeostasis and the potential of glucokinase activators for diabetes therapy. *Diabetes* 55, 1-12.

McCarthy, M.I., 2010. Genomics, type 2 diabetes, and obesity. *N Engl J Med* 363, 2339-50.

McCarty, M.F., 2005. Up-regulation of PPARgamma coactivator-1alpha as a strategy for preventing and reversing insulin resistance and obesity. *Med Hypotheses* 64, 399-407.

McGarry, J.D., andDobbins, R.L., 1999. Fatty acids, lipotoxicity and insulin secretion. *Diabetologia* 42, 128-38.

Michael, L.F., Wu, Z., Cheatham, R.B., Puigserver, P., Adelmant, G., Lehman, J.J., Kelly, D.P., andSpiegelman, B.M., 2001. Restoration of insulin-sensitive glucose transporter (GLUT4) gene expression in muscle cells by the transcriptional coactivator PGC-1. *Proc Natl Acad Sci U S A* 98, 3820-5.

- Michalik, L., Desvergne, B., Tan, N.S., Basu-Modak, S., Escher, P., Rieusset, J., Peters, J.M., Kaya, G., Gonzalez, F.J., Zakany, J., Metzger, D., Chambon, P., Duboule, D., and Wahli, W., 2001. Impaired skin wound healing in peroxisome proliferator-activated receptor (PPAR)alpha and PPARbeta mutant mice. *J Cell Biol* 154, 799-814.
- Millet, L., Vidal, H., Andreelli, F., Larrouy, D., Riou, J.P., Ricquier, D., Laville, M., and Langin, D., 1997. Increased uncoupling protein-2 and -3 mRNA expression during fasting in obese and lean humans. *J Clin Invest* 100, 2665-70.
- Mingozzi, F., and High, K.A., 2011. Therapeutic in vivo gene transfer for genetic disease using AAV: progress and challenges. *Nat Rev Genet* 12, 341-55.
- Miura, S., Kai, Y., Ono, M., and Ezaki, O., 2003. Overexpression of peroxisome proliferator-activated receptor gamma coactivator-1alpha down-regulates GLUT4 mRNA in skeletal muscles. *J Biol Chem* 278, 31385-90.
- Mohan, V., 2004. Why are Indians more prone to diabetes? *J Assoc Physicians India* 52, 468-74.
- Mole, P.A., Oscai, L.B., and Holloszy, J.O., 1971. Adaptation of muscle to exercise. Increase in levels of palmitoyl Coa synthetase, carnitine palmitoyltransferase, and palmitoyl Coa dehydrogenase, and in the capacity to oxidize fatty acids. *J Clin Invest* 50, 2323-30.
- Mootha, V.K., Lindgren, C.M., Eriksson, K.F., Subramanian, A., Sihag, S., Lehar, J., Puigserver, P., Carlsson, E., Ridderstrale, M., Laurila, E., Houstis, N., Daly, M.J., Patterson, N., Mesirov, J.P., Golub, T.R., Tamayo, P., Spiegelman, B., Lander, E.S., Hirschhorn, J.N., Altshuler, D., and Groop, L.C., 2003. PGC-1alpha-responsive genes involved in oxidative phosphorylation are coordinately downregulated in human diabetes. *Nat Genet* 34, 267-73.
- Morino, K., Petersen, K.F., Dufour, S., Befroy, D., Frattini, J., Shatzkes, N., Neschen, S., White, M.F., Bilz, S., Sono, S., Pypaert, M., and Shulman, G.I., 2005. Reduced mitochondrial density and increased IRS-1 serine phosphorylation in muscle of insulin-resistant offspring of type 2 diabetic parents. *J Clin Invest* 115, 3587-93.
- Motala, A.A., Omar, M.A., and Pirie, F.J., 2003. Diabetes in Africa. Epidemiology of type 1 and type 2 diabetes in Africa. *J Cardiovasc Risk* 10, 77-83.
- Muoio, D.M., MacLean, P.S., Lang, D.B., Li, S., Houmard, J.A., Way, J.M., Winegar, D.A., Corton, J.C., Dohm, G.L., and Kraus, W.E., 2002. Fatty acid homeostasis and induction of lipid regulatory genes in skeletal muscles of peroxisome proliferator-activated receptor (PPAR) alpha knock-out mice. Evidence for compensatory regulation by PPAR delta. *J Biol Chem* 277, 26089-97.
- Muoio, D.M., and Newgard, C.B., 2006. Obesity-related derangements in metabolic regulation. *Annu Rev Biochem* 75, 367-401.

Muoio, D.M., and Newgard, C.B., 2008. Mechanisms of disease: molecular and metabolic mechanisms of insulin resistance and beta-cell failure in type 2 diabetes. *Nat Rev Mol Cell Biol* 9, 193-205.

Nissen, S.E., and Wolski, K., 2010. Rosiglitazone revisited: an updated meta-analysis of risk for myocardial infarction and cardiovascular mortality. *Arch Intern Med* 170, 1191-1201.

O'Dea, K., 1984. Marked improvement in carbohydrate and lipid metabolism in diabetic Australian aborigines after temporary reversion to traditional lifestyle. *Diabetes* 33, 596-603.

Oliver, W.R., Jr., Shenk, J.L., Snaith, M.R., Russell, C.S., Plunket, K.D., Bodkin, N.L., Lewis, M.C., Winegar, D.A., Sznaidman, M.L., Lambert, M.H., Xu, H.E., Sternbach, D.D., Kliewer, S.A., Hansen, B.C., and Willson, T.M., 2001. A selective peroxisome proliferator-activated receptor delta agonist promotes reverse cholesterol transport. *Proc Natl Acad Sci U S A* 98, 5306-11.

Olson, A.L., and Pessin, J.E., 1996. Structure, function, and regulation of the mammalian facilitative glucose transporter gene family. *Annu Rev Nutr* 16, 235-56.

Otaegui, P.J., Ferre, T., Pujol, A., Riu, E., Jimenez, R., and Bosch, F., 2000. Expression of glucokinase in skeletal muscle: a new approach to counteract diabetic hyperglycemia. *Hum Gene Ther* 11, 1543-52.

Otaegui, P.J., Ferre, T., Riu, E., and Bosch, F., 2003. Prevention of obesity and insulin resistance by glucokinase expression in skeletal muscle of transgenic mice. *FASEB J* 17, 2097-9.

Patti, M.E., Butte, A.J., Crunkhorn, S., Cusi, K., Berria, R., Kashyap, S., Miyazaki, Y., Kohane, I., Costello, M., Saccone, R., Landaker, E.J., Goldfine, A.B., Mun, E., DeFronzo, R., Finlayson, J., Kahn, C.R., and Mandarino, L.J., 2003. Coordinated reduction of genes of oxidative metabolism in humans with insulin resistance and diabetes: Potential role of PGC1 and NRF1. *Proc Natl Acad Sci U S A* 100, 8466-71.

Pendergrass, M., Koval, J., Vogt, C., Yki-Jarvinen, H., Izzo, P., Pipek, R., Ardehali, H., Printz, R., Granner, D., DeFronzo, R.A., and Mandarino, L.J., 1998. Insulin-induced hexokinase II expression is reduced in obesity and NIDDM. *Diabetes* 47, 387-94.

Perseghin, G., Scifo, P., De Cobelli, F., Pagliato, E., Battezzati, A., Arcelloni, C., Vanzulli, A., Testolin, G., Pozza, G., Del Maschio, A., and Luzi, L., 1999. Intramyocellular triglyceride content is a determinant of in vivo insulin resistance in humans: a ¹H-¹³C nuclear magnetic resonance spectroscopy assessment in offspring of type 2 diabetic parents. *Diabetes* 48, 1600-6.

Pette, D., Peuker, H., and Staron, R.S., 1999. The impact of biochemical methods for single muscle fibre analysis. *Acta Physiol Scand* 166, 261-77.

Pinhas-Hamiel, O., andZeitler, P., 2005. The global spread of type 2 diabetes mellitus in children and adolescents. *J Pediatr* 146, 693-700.

Poitout, V., andRobertson, R.P., 2008. Glucolipototoxicity: fuel excess and beta-cell dysfunction. *Endocr Rev* 29, 351-66.

Pouliot, M.C., Despres, J.P., Nadeau, A., Moorjani, S., Prud'Homme, D., Lupien, P.J., Tremblay, A., andBouchard, C., 1992. Visceral obesity in men. Associations with glucose tolerance, plasma insulin, and lipoprotein levels. *Diabetes* 41, 826-34.

Printz, R.L., Magnuson, M.A., andGranner, D.K., 1993. Mammalian glucokinase. *Annu Rev Nutr* 13, 463-96.

Puigserver, P., Wu, Z., Park, C.W., Graves, R., Wright, M., andSpiegelman, B.M., 1998. A cold-inducible coactivator of nuclear receptors linked to adaptive thermogenesis. *Cell* 92, 829-39.

Rakhshandehroo, M., Knoch, B., Muller, M., andKersten, S., 2010. Peroxisome proliferator-activated receptor alpha target genes. *PPAR Res* 2010.

Ratner, R., Nauck, M., Kapitza, C., Asnaghi, V., Boldrin, M., andBalena, R., 2010. Safety and tolerability of high doses of taspoglutide, a once-weekly human GLP-1 analogue, in diabetic patients treated with metformin: a randomized double-blind placebo-controlled study. *Diabet Med* 27, 556-62.

Ren, J.M., Semenkovich, C.F., Gulve, E.A., Gao, J., andHolloszy, J.O., 1994. Exercise induces rapid increases in GLUT4 expression, glucose transport capacity, and insulin-stimulated glycogen storage in muscle. *J Biol Chem* 269, 14396-401.

Rhodes, C.J., 2005. Type 2 diabetes-a matter of beta-cell life and death? *Science* 307, 380-4.

Riserus, U., Sprecher, D., Johnson, T., Olson, E., Hirschberg, S., Liu, A., Fang, Z., Hegde, P., Richards, D., Sarov-Blat, L., Strum, J.C., Basu, S., Cheeseman, J., Fielding, B.A., Humphreys, S.M., Danoff, T., Moore, N.R., Murgatroyd, P., O'Rahilly, S., Sutton, P., Willson, T., Hassall, D., Frayn, K.N., andKarpe, F., 2008. Activation of peroxisome proliferator-activated receptor (PPAR)delta promotes reversal of multiple metabolic abnormalities, reduces oxidative stress, and increases fatty acid oxidation in moderately obese men. *Diabetes* 57, 332-9.

Ritov, V.B., Menshikova, E.V., He, J., Ferrell, R.E., Goodpaster, B.H., andKelley, D.E., 2005. Deficiency of subsarcolemmal mitochondria in obesity and type 2 diabetes. *Diabetes* 54, 8-14.

Riviere, C., Danos, O., andDouar, A.M., 2006. Long-term expression and repeated administration of AAV type 1, 2 and 5 vectors in skeletal muscle of immunocompetent adult mice. *Gene Ther* 13, 1300-8.

Robinson, M.K., 2009. Surgical treatment of obesity--weighing the facts. *N Engl J Med* 361, 520-1.

Russell, A.P., Feilchenfeldt, J., Schreiber, S., Praz, M., Crettenand, A., Gobelet, C., Meier, C.A., Bell, D.R., Kralli, A., Giacobino, J.P., and Deriaz, O., 2003. Endurance training in humans leads to fiber type-specific increases in levels of peroxisome proliferator-activated receptor-gamma coactivator-1 and peroxisome proliferator-activated receptor-alpha in skeletal muscle. *Diabetes* 52, 2874-81.

Ryder, J.W., Bassel-Duby, R., Olson, E.N., and Zierath, J.R., 2003. Skeletal muscle reprogramming by activation of calcineurin improves insulin action on metabolic pathways. *J Biol Chem* 278, 44298-304.

Salvado, L., Serrano-Marco, L., Barroso, E., Palomer, X., and Vazquez-Carrera, M., 2012. Targeting PPARbeta/delta for the treatment of type 2 diabetes mellitus. *Expert Opin Ther Targets* 16, 209-23.

Scarpulla, R.C., 2008. Transcriptional paradigms in mammalian mitochondrial biogenesis and function. *Physiol Rev* 88, 611-38.

Schafer, S.A., Machicao, F., Fritsche, A., Haring, H.U., and Kantartzis, K., 2011. New type 2 diabetes risk genes provide new insights in insulin secretion mechanisms. *Diabetes Res Clin Pract* 93 Suppl 1, S9-24.

Schiaffino, S., 2010. Fibre types in skeletal muscle: a personal account. *Acta Physiol (Oxf)* 199, 451-63.

Schrauwen, P., and Hesselink, M.K., 2004. The role of uncoupling protein 3 in fatty acid metabolism: protection against lipotoxicity? *Proc Nutr Soc* 63, 287-92.

Schrauwen, P., Hesselink, M.K., Vaartjes, I., Kornips, E., Saris, W.H., Giacobino, J.P., and Russell, A., 2002. Effect of acute exercise on uncoupling protein 3 is a fat metabolism-mediated effect. *Am J Physiol Endocrinol Metab* 282, E11-7.

Schuler, M., Ali, F., Chambon, C., Duteil, D., Bornert, J.M., Tardivel, A., Desvergne, B., Wahli, W., Chambon, P., and Metzger, D., 2006. PGC1alpha expression is controlled in skeletal muscles by PPARbeta, whose ablation results in fiber-type switching, obesity, and type 2 diabetes. *Cell Metab* 4, 407-14.

Scott, W., Stevens, J., and Binder-Macleod, S.A., 2001. Human skeletal muscle fiber type classifications. *Phys Ther* 81, 1810-6.

Shaw, J.E., Sicree, R.A., and Zimmet, P.Z., 2010. Global estimates of the prevalence of diabetes for 2010 and 2030. *Diabetes Res Clin Pract* 87, 4-14.

Shiota, C., Coffey, J., Grimsby, J., Grippo, J.F., and Magnuson, M.A., 1999. Nuclear import of hepatic glucokinase depends upon glucokinase regulatory protein, whereas export is due to a nuclear export signal sequence in glucokinase. *J Biol Chem* 274, 37125-30.

Simoneau, J.A., Veerkamp, J.H., Turcotte, L.P., and Kelley, D.E., 1999. Markers of capacity to utilize fatty acids in human skeletal muscle: relation to insulin resistance and obesity and effects of weight loss. *FASEB J* 13, 2051-60.

Springer, S.C., Silverstein, J., Copeland, K., Moore, K.R., Prazar, G.E., Raymer, T., Shiffman, R.N., Thaker, V.V., Anderson, M., Spann, S.J., and Flinn, S.K., 2013. Management of type 2 diabetes mellitus in children and adolescents. *Pediatrics* 131, e648-64.

Staels, B., Maes, M., and Zambon, A., 2008. Fibrates and future PPARalpha agonists in the treatment of cardiovascular disease. *Nat Clin Pract Cardiovasc Med* 5, 542-53.

Stoppani, J., Hildebrandt, A.L., Sakamoto, K., Cameron-Smith, D., Goodyear, L.J., and Neuffer, P.D., 2002. AMP-activated protein kinase activates transcription of the UCP3 and HKII genes in rat skeletal muscle. *Am J Physiol Endocrinol Metab* 283, E1239-48.

Storer, A.C., and Cornish-Bowden, A., 1976. Kinetics of rat liver glucokinase. Co-operative interactions with glucose at physiologically significant concentrations. *Biochem J* 159, 7-14.

Stroes, E.S., Nierman, M.C., Meulenberg, J.J., Franssen, R., Twisk, J., Henny, C.P., Maas, M.M., Zwinderman, A.H., Ross, C., Aronica, E., High, K.A., Levi, M.M., Hayden, M.R., Kastelein, J.J., and Kuivenhoven, J.A., 2008. Intramuscular administration of AAV1-lipoprotein lipase S447X lowers triglycerides in lipoprotein lipase-deficient patients. *Arterioscler Thromb Vasc Biol* 28, 2303-4.

Stumvoll, M., Goldstein, B.J., and van Haeflten, T.W., 2005. Type 2 diabetes: principles of pathogenesis and therapy. *Lancet* 365, 1333-46.

Summermatter, S., Shui, G., Maag, D., Santos, G., Wenk, M.R., and Handschin, C., 2013. PGC-1alpha improves glucose homeostasis in skeletal muscle in an activity-dependent manner. *Diabetes* 62, 85-95.

Suwa, M., Egashira, T., Nakano, H., Sasaki, H., and Kumagai, S., 2006. Metformin increases the PGC-1alpha protein and oxidative enzyme activities possibly via AMPK phosphorylation in skeletal muscle in vivo. *J Appl Physiol* 101, 1685-92.

Suwa, M., Nakano, H., and Kumagai, S., 2003. Effects of chronic AICAR treatment on fiber composition, enzyme activity, UCP3, and PGC-1 in rat muscles. *J Appl Physiol* 95, 960-8.

Szendroedi, J., Schmid, A.I., Chmelik, M., Toth, C., Brehm, A., Krssak, M., Nowotny, P., Wolzt, M., Waldhausl, W., and Roden, M., 2007. Muscle mitochondrial ATP synthesis and glucose transport/phosphorylation in type 2 diabetes. *PLoS Med* 4, e154.

Tahrani, A.A., Bailey, C.J., Del Prato, S., and Barnett, A.H., 2011. Management of type 2 diabetes: new and future developments in treatment. *Lancet* 378, 182-97.

Tahrani, A.A., Piya, M.K., Kennedy, A., and Barnett, A.H., 2010. Glycaemic control in type 2 diabetes: targets and new therapies. *Pharmacol Ther* 125, 328-61.

Tanaka, T., Yamamoto, J., Iwasaki, S., Asaba, H., Hamura, H., Ikeda, Y., Watanabe, M., Magoori, K., Ioka, R.X., Tachibana, K., Watanabe, Y., Uchiyama, Y., Sumi, K., Iguchi, H., Ito, S., Doi, T., Hamakubo, T., Naito, M., Auwerx, J., Yanagisawa, M., Kodama, T., and Sakai, J., 2003. Activation of peroxisome proliferator-activated receptor delta induces fatty acid beta-oxidation in skeletal muscle and attenuates metabolic syndrome. *Proc Natl Acad Sci U S A* 100, 15924-9.

Taniguchi, C.M., Emanuelli, B., and Kahn, C.R., 2006. Critical nodes in signalling pathways: insights into insulin action. *Nat Rev Mol Cell Biol* 7, 85-96.

Thyfault, J.P., Cree, M.G., Zheng, D., Zwetsloot, J.J., Tapscott, E.B., Koves, T.R., Ilkayeva, O., Wolfe, R.R., Muoio, D.M., and Dohm, G.L., 2007. Contraction of insulin-resistant muscle normalizes insulin action in association with increased mitochondrial activity and fatty acid catabolism. *Am J Physiol Cell Physiol* 292, C729-39.

Timmers, S., Schrauwen, P., and de Vogel, J., 2008. Muscular diacylglycerol metabolism and insulin resistance. *Physiol Behav* 94, 242-51.

Tippett, P.S., and Neet, K.E., 1982. Specific inhibition of glucokinase by long chain acyl coenzymes A below the critical micelle concentration. *J Biol Chem* 257, 12839-45.

Tonks, K.T., Ng, Y., Miller, S., Coster, A.C., Samocho-Bonet, D., Iseli, T.J., Xu, A., Patrick, E., Yang, J.Y., Junutula, J.R., Modrusan, Z., Kolumam, G., Stockli, J., Chisholm, D.J., James, D.E., and Greenfield, J.R., 2013. Impaired Akt phosphorylation in insulin-resistant human muscle is accompanied by selective and heterogeneous downstream defects. *Diabetologia* 56, 875-85.

Ukropcova, B., McNeil, M., Sereda, O., de Jonge, L., Xie, H., Bray, G.A., and Smith, S.R., 2005. Dynamic changes in fat oxidation in human primary myocytes mirror metabolic characteristics of the donor. *J Clin Invest* 115, 1934-41.

Urnov, F.D., Rebar, E.J., Holmes, M.C., Zhang, H.S., and Gregory, P.D., 2010. Genome editing with engineered zinc finger nucleases. *Nat Rev Genet* 11, 636-46.

Verma, I.M., and Weitzman, M.D., 2005. Gene therapy: twenty-first century medicine. *Annu Rev Biochem* 74, 711-38.

- Vogt, C., Ardehali, H., Iozzo, P., Yki-Jarvinen, H., Koval, J., Maezono, K., Pendergrass, M., Printz, R., Granner, D., DeFronzo, R., and Mandarino, L., 2000. Regulation of hexokinase II expression in human skeletal muscle in vivo. *Metabolism* 49, 814-8.
- Wang, S., Subramaniam, A., Cawthorne, M.A., and Clapham, J.C., 2003a. Increased fatty acid oxidation in transgenic mice overexpressing UCP3 in skeletal muscle. *Diabetes Obes Metab* 5, 295-301.
- Wang, Y.X., Lee, C.H., Tjep, S., Yu, R.T., Ham, J., Kang, H., and Evans, R.M., 2003b. Peroxisome-proliferator-activated receptor delta activates fat metabolism to prevent obesity. *Cell* 113, 159-70.
- Wang, Y.X., Zhang, C.L., Yu, R.T., Cho, H.K., Nelson, M.C., Bayuga-Ocampo, C.R., Ham, J., Kang, H., and Evans, R.M., 2004. Regulation of muscle fiber type and running endurance by PPARdelta. *PLoS Biol* 2, e294.
- Wenz, T., Rossi, S.G., Rotundo, R.L., Spiegelman, B.M., and Moraes, C.T., 2009. Increased muscle PGC-1alpha expression protects from sarcopenia and metabolic disease during aging. *Proc Natl Acad Sci U S A* 106, 20405-10.
- Wilson, J.E., 2003. Isozymes of mammalian hexokinase: structure, subcellular localization and metabolic function. *J Exp Biol* 206, 2049-57.
- Winzell, M.S., and Ahren, B., 2004. The high-fat diet-fed mouse: a model for studying mechanisms and treatment of impaired glucose tolerance and type 2 diabetes. *Diabetes* 53 Suppl 3, S215-9.
- Wu, H., Kanatous, S.B., Thurmond, F.A., Gallardo, T., Isotani, E., Bassel-Duby, R., and Williams, R.S., 2002. Regulation of mitochondrial biogenesis in skeletal muscle by CaMK. *Science* 296, 349-52.
- Wu, Z., Puigserver, P., Andersson, U., Zhang, C., Adelmant, G., Mootha, V., Troy, A., Cinti, S., Lowell, B., Scarpulla, R.C., and Spiegelman, B.M., 1999. Mechanisms controlling mitochondrial biogenesis and respiration through the thermogenic coactivator PGC-1. *Cell* 98, 115-24.
- Yoon, J.C., Puigserver, P., Chen, G., Donovan, J., Wu, Z., Rhee, J., Adelmant, G., Stafford, J., Kahn, C.R., Granner, D.K., Newgard, C.B., and Spiegelman, B.M., 2001. Control of hepatic gluconeogenesis through the transcriptional coactivator PGC-1. *Nature* 413, 131-8.
- Yu, C., Chen, Y., Cline, G.W., Zhang, D., Zong, H., Wang, Y., Bergeron, R., Kim, J.K., Cushman, S.W., Cooney, G.J., Atcheson, B., White, M.F., Kraegen, E.W., and Shulman, G.I., 2002. Mechanism by which fatty acids inhibit insulin activation of insulin receptor substrate-1 (IRS-1)-associated phosphatidylinositol 3-kinase activity in muscle. *J Biol Chem* 277, 50230-6.

Zhang, L., Keung, W., Samokhvalov, V., Wang, W., and Lopaschuk, G.D., 2010a. Role of fatty acid uptake and fatty acid beta-oxidation in mediating insulin resistance in heart and skeletal muscle. *Biochim Biophys Acta* 1801, 1-22.

Zhang, P., Zhang, X., Brown, J., Vistisen, D., Sicree, R., Shaw, J., and Nichols, G., 2010b. Global healthcare expenditure on diabetes for 2010 and 2030. *Diabetes Res Clin Pract* 87, 293-301.

Zierath, J.R., He, L., Guma, A., Odegaard Wahlstrom, E., Klip, A., and Wallberg-Henriksson, H., 1996. Insulin action on glucose transport and plasma membrane GLUT4 content in skeletal muscle from patients with NIDDM. *Diabetologia* 39, 1180-9.

Zong, H., Ren, J.M., Young, L.H., Pypaert, M., Mu, J., Birnbaum, M.J., and Shulman, G.I., 2002. AMP kinase is required for mitochondrial biogenesis in skeletal muscle in response to chronic energy deprivation. *Proc Natl Acad Sci U S A* 99, 15983-7.